UNIVERSITI SAINS MALAYSIA

Laporan Akhir Projek Penyelidikan Jangka Pendek

Carbon Dioxide Removal Mechanism using Calcium Oxide In A Fluidized Reactor

by

Assoc. Prof. Zainal Alimuddin Bin Zainal Alauddin

Prof. Horizon Walker Gitano-Briggs

Prof. Mohd Zulkifly Bin Abdullah

Mr. Mohd Mahadzir Bin Mohammud @ Mahmood

2011

Maklumat Project (Project's Details)

Maklumat Asas

Kod : U0429

No. Rujukan : 2009/126

Jenis : Universiti Penyelidikan

Tajuk : Carbon Dioxide Removal Mechanism Using Calcium Oxide In A Fluidized Reactor

Pusat Tanggungjawab : PUSAT PENGAJIAN KEJURUTERAAN MEKANIK

Pelantar : PELANTAR PENYELIDIKAN SAINS FUNDAMENTAL

Kelas RU : Individual

Status : AKTIF

Tempoh Projek (TTBBHH) : 002400

Tarikh Mula : 15 / 3 / 2009

Tarikh Hingga - Asal : 14 / 3 / 2011

Tarikh Tamat : 14 / 3 / 2011

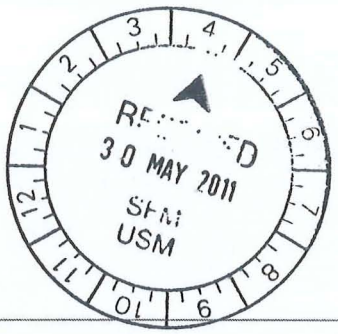

Maklumat Penyelidik

Ketua Penyelidik : PROF MADYA ZAINAL ALIMUDDIN BIN ZAINAL ALAUDDIN

Penyelidik Bersama : PROFESOR HORIZON WALKER GITANO-BRIGGS
MOHD MAHADZIR BIN MOHAMMUD @ MAHMOOD (USM)
PROFESOR MOHD ZULKIFLY BIN ABDULLAH

Maklumat Kewangan

No. Akaun : 1001 / PMEKANIK / 811122

Penaja : USM (RU)

Kategori Penaja : USM

Peruntukan Diluluskan : RM 100000

Pecahan Mengikut Tahun (Jumlah : RM 100000)

Tahun 2009 : RM 46840

Tahun 2010 : RM 53160

Peruntukan yang Telah Diterima : RM 100000

Pecahan Mengikut Tahun

Tahun 2009 : RM 46840

Tahun 2010 : RM 53160

Pecahan Vot :

Vot	Butiran Vot	Asal (RM)	Tambahan (RM)	Jumlah (RM)
11000	Gaji Dan Upahan	36000	0	36000
21000	Perbelanjaan Perjalanan Dan Sara Hidup	13000	0	13000
24000	Sewaan	4320	0	4320
26000	Bekalan Bahan Mentah Dan Bahan Untuk Penyelenggaraan	3000	0	3000
27000	Bekalan Dan Bahan-bahan Lain	42000	0	42000

29000	Perkhidmatan Iktisas Dan Perkhidmatan Lain Yang Dibeli Dan Hospitaliti	1680	0	1680
Jumlah Keseluruhan (RM)		100000	0	100000

UNIVERSITI SAINS MALAYSIA

UNIVERSITY RESEARCH GRANT
FINAL REPORT
Geran Penyelidikan Universiti
Laporan Akhir

A.	**PARTICULARS OF RESEARCH** / *MAKLUMAT PENYELIDIKAN:*
(i)	**Title of Research:** *Tajuk Penyelidikan:* CARBON DIOXIDE REMOVAL MECHANISM USING CALCIUM OXIDE IN A FLUIDIZED REACTOR
(ii)	**Account Number:** *Nombor Akaun: 811122*
B.	**PERSONAL PARTICULARS OF RESEARCHER** / *MAKLUMAT PENYELIDIK:*
(i)	**Name of Research Leader:** *Nama Ketua Penyelidik:* DR ZAINAL ALIMUDDIN BIN ZAINAL ALAUDDIN
	Name of Co-Researcher *Nama Penyelidik Bersama:* MOHD ZULKIFLY BIN ABDULLAH HORIZON GITANO WALKER MOHD MAHADZIR BIN MOHAMMUD @ MAHMOOD
(ii)	**School/Institute/Centre/Unit :** *Pusat Pengajian /Institut/Pusat/Unit :* PUSAT PENGAJIAN KEJURUTERAAN MEKANIK
C.	**Research Platform (Please tick (/) the appropriate box):** *Pelantar Penyelidikan (Sila tanda (/) kotak berkenaan):*

☐	**A. Life Sciences** *Sains Hayat*
☐	**B. Fundamental** *Fundamental*
√	**C. Engineering & Technology** *Kejuruteraan & Teknologi*
☐	**D. Social Transformation** *Transformasi Sosial*
☐	**E. Information & Communications Technology (ICT)** *Teknologi Maklumat & Komunikasi*
☐	**F. Clinical Sciences** *Sains Klinikal*
☐	**G. Biomedical & Health Sciences** *Bioperubatan Sains Kesihatan*

D. **Duration of this research :**
Tempoh masa penyelidikan ini :

***Duration :** .....2 TAHUN.....
Tempoh :

From : 15 MAC 2009 **To** : 14 MAC 2011
Dari: *Ke :*

E. ABSTRACT OF RESEARCH

(An abstract of between 100 and 200 words must be prepared in **Bahasa Malaysia and in English**. This abstract will be included in the Annual Report of the Research and Innovation Section at a later date as a means of presenting the project findings of the researcher/s to the University and the community at large)

Abstrak Penyelidikan
(Perlu disediakan di antara 100 - 200 perkataan di dalam **Bahasa Malaysia dan juga Bahasa Inggeris**.
Abstrak ini akan dimuatkan dalam Laporan Tahunan Bahagian Penyelidikan & Inovasi sebagai satu cara untuk menyampaikan dapatan projek tuan/puan kepada pihak Universiti & masyarakat luar).

Biomass gasification is a possible alternative to utilized biomass resources to compliment the depleting fossil fuel. Producer gas, a product of biomass gasification process can be used to generate power and electricity via internal combustion engine. However, the 20% carbon dioxide (CO_2) gas content in the producer gas reduces its heating values as CO_2 acts as a diluent. The used of limestone consisting mainly of the mineral calcite (calcium oxide, CaO) as calcium based sorbent to absorb CO_2 in the producer gas can make biomass technology more viable.

The reactor was developed and the behavior of CaO-sand mixtures in a cold model experiment was studied. The effect of the CaO-sand mixtures, the CaO particle sizes, the volume flow rate and the pressure of air intake were investigated experimentally. The hot model experimental was then conducted to investigate CO_2 absorption at the optimum condition obtained from the cold model experiment. The simulated gas consisting of 20% CO_2 and 80% N_2 was introduced in the reactor within temperatures of 650-750°C. The CaO percentages of 50 and 40 in sand were found to have a good fluidization at all air pressures (2 - 6 bar). In addition to that, the 1000 micron particle size of the CaO–sand mixture and the volume flow rate of air between 15 – 55 $Lmin^{-1}$ were also found to give best fluidization. In the hot model experiment, the best CO_2 absorption occurred at 50% CaO mixture with simulated gas pressure of 3 bar and the volume flow rate of 45 $Lmin^{-1}$ at 650-750°C in a small bubbling fluidized bed reactor (SBFBR).

F. **SUMMARY OF RESEARCH FINDINGS**
Ringkasan dapatan Projek Penyelidikan

This project concerns with experimental and simulation studies to investigate the absorption mechanism for CO2 using CaO-sand mixture in a fluidized bed reactor. The reactor was able to absorb the CO2 and results in increasing the quality of the producer gas.

The CO_2 absorption experimental in the reactor for the simulated producer gas and compressed producer gas showed good results. After 15-20 min operation, the CO_2 concentration in the simulated producer gas decreased approximately by 53%, Hydrogen and Carbon Monoxide increased approximately by 24% and 12%, respectively. For the compressed producer gas, the Carbon Dioxide concentration decreased approximately by 69%, Hydrogen and Carbon Monoxide increased approximately by 13% and 19%, respectively. The heating values of the compressed producer gas increased from 4.51 to 5.9 $MJN^{-1}m^{-3}$ (before and after reactor).

G. **COMPREHENSIVE TECHNICAL REPORT**
Laporan Teknikal Lengkap
Applicants are required to prepare a comprehensive technical report explaining the project.
(This report must be attached separately)
Sila sediakan laporan teknikal lengkap yang menerangkan keseluruhan projek ini.
[Laporan ini mesti dikepilkan]

LAMPIRAN A

List the key words that reflect your research:
Senaraikan kata kunci yang mencerminkan penyelidikan anda:

English	Bahasa Malaysia
Biomass gasification	Penggasan biojisim
CO2 removal	Pembuangan CO2
Fluidized bed reactor	Reaktor lapisan terbendalir

H. a) **Results/Benefits of this research**
Hasil Penyelidikan

No. *Bil:*	Category/Number: *Kategori/ Bilangan:*	Promised	Achieved
1.	**Research Publications (Specify target journals)** *Penerbitan Penyelidikan (Nyatakan sasaran jurnal)*	4	3
2.	**Human Capital Development**		
	a. Ph. D Students	1	1
	b. Masters Students		
	c. Undergraduates (Final Year Project)		
	d. Research Officers		
	e. Research Assisstants		
	f. Other: Please specify		
3.	**Patents** *Paten*		
4.	**Specific / Potential Applications** *Spesifik/Potensi aplikasin*		
5.	**Networking & Linkages** *Jaringan & Jalinan*		
6.	**Possible External Research Grants to be Acquired** *Jangkaan Geran Penyelidikan Luar Diperoleh*		

- Kindly provide copies/evidence for Category 1 to 6.

LAMPIRAN B

b) **Equipment used for this research.**
Peralatan yang telah digunakan dalam penyelidikan ini.

Items *Perkara*	Approved Equipment	Approved Requested Equipment	Location
Specialized Equipment Peralatan khusus	-	-	
Facility Kemudahan	-	-	
Infrastructure Infrastruktur	-	-	

- Please attach appendix if necessary.

I. **BUDGET** / *BAJET*

Total Approved Budget	: RM 100,000.00
Total Additional Budget	: RM
Grand Total of Approved Budget	: RM 100,000.00

Yearly Budget Distributed

Year 1	: RM 46,840.00
Year 2	: RM 53,160.00
Year 3	: RM

Additional Budget Approved

Year 1	: RM
Year 2	: RM
Year 3	: RM

Total Expenditure	: RM 83,291.30
Balance	: RM 16,708.70

- **Please attach final account statement from Treasury** LAMPIRAN C

Signature of Researcher
Tandatangan Penyelidik

6/5/11

Date
Tarikh

H. **COMMENTS OF PTJ'S RESEARCH COMMITTEE**
KOMEN JAWATANKUASA PENYELIDIKAN PERINGKAT PTJ

General Comments:
Ulasan Umum:

The research has resulted in several journal papers.

PROF. MANI MARAN A/L RATNAM
B.Eng. (UM), Ph.D. (Wales, UK)
Timbalan Dekan
(Penyelidikan & Pengajian Siswazah)
Pusat Pengajian Kejuruteraan Mekanik
Kampus Kejuruteraan
Universiti Sains Malaysia

Signature and Stamp of Chairperson of PTJ's Evaluation Committee
Tandatangan dan Cop Pengerusi Jawatankuasa Penilaian PTJ

Date : 18/05/11
Tarikh :

Signature and Stamp of Dean/ Director of PTJ
Tandatangan dan Cop Dekan/ Pengarah PTJ

Date :
Tarikh :

Prof. Madya Dr. Zaidi Mohd Ripin
Dekan
Pusat Pengajian Kejuruteraan Mekanik
Kampus Kejuruteraan
Universiti Sains Malaysia

LAMPIRAN A

LAPORAN TEKNIKAL LENGKAP

CARBON DIOXIDE REMOVAL MECHANISM USING CALCIUM OXIDE IN A FLUIDIZED BED REACTOR

CHAPTER 1: INTRODUCTION

1.1 FUEL SCENARIO IN MALAYSIA

Fuel is the most important subject in our life. Fuels have been used predominantly in power plants and to generate work in internal combustion engines. Today, fossil fuels dwindle, too expensive cause adverse effect on the environment due to emissions from combustion devices and increase greenhouse gas emissions. Malaysia is one of the countries in the world facing these problems.

Malaysia is currently known as a significant producer of oil and the second largest exporter of liquefied natural gas (LNG) in the world behind Qatar in 2009 (Energy Information Administration Report, (2010). In 2008, Malaysia had proven oil reserves of 4.0 billion barrels. Although the oil reserves is large, it is decreasing from a peak of 4.3 billion barrels in 1996. Total oil and crude oil productions in Malaysia show is reducing but increasing in consumption. These unparallel situations will cause the countries oil reserves to be exhausted in the next 15 years unless new explorations show positive results. Figure 1.1 shows oil production, crude oil production and petroleum consumption in Malaysia.

Growing demand for fossil fuels and petroleum in Malaysia to become a developed nation by 2020 will result in higher energy costs and greater dependence on imported oil given the current crude oil capacity. This can have a potentially negative impact on the nation's economic growth as rising commodity prices are closely tied to inflation rates. That is why in the modern world, especially Malaysia has tried to utilize alternative and renewable sources of energy.

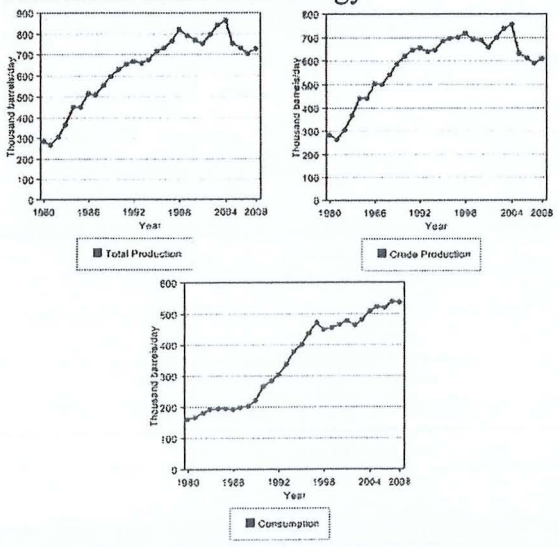

Figure 1.1- Malaysia oil production, crude oil production and petroleum consumption from 1980-2008. (EIA, 2010)

Renewable energy offers the opportunity to lower fossil fuel consumption. Energy derived from solar, wind, wave, tidal, hydroelectric, geothermal, and biomass sources are considered renewable. Because most forms of renewable energy are derived either

directly or indirectly from the sun, there is an abundant supply of renewable energy available, unlike fossil fuels. The use of renewable energy also provides environmental, economic, political benefits and they are also not depleted in time. One of the fuels from renewable energy is biomass sources.

1.2 BIOMASS

Biomass is the most abundant resources and available in almost all parts of the world. It has the potential to be one of the best options for providing on demand renewable fuel that can be utilized in various energy conversion technologies and also has the advantage of being carbon sink without contribution to the net production of CO_2. Biomass is defined as an organic material existing in all plants and animals such as forest and mill residues, wood wastes, agricultural crops and wastes, animal wastes and municipal solid wastes.

Malaysia has abundant biomass waste from its oil palm, wood and agro-industries. According to Malaysia Energy Centre (2008), Malaysia produced more than 70 million tones per year of biomass wastes worth RM 23 million annually. Over the next 20 years, the palm oil industry is expected to expand by 40%, hence the value of residues from oil palm and wood is estimated to be about RM 500 million by 2020. Of these residues the fibres, shells, empty fruit bunch and wood waste provide the greatest potential for commercial operations. At present, biomass fuels account for about 16% of the energy consumption in the country and biomass-based power generation capacity in the country stands at 138 MW, of which 100 MW is used in palm oil industries.

There are two main processes of biomass technologies for converting biomass sources into useful forms of energy: thermo-chemical and bio-chemical/biological (McKendry, 2002b). In thermo-chemical conversion, there are four processes: combustion, pyrolysis, gasification and liquefaction. In this research study only the thermo-chemical in particular gasification process will be focused. Figure 2.2 shows the thermo-chemical process, intermediate energy carriers and the final energy products resulting from thermo-chemical conversion.

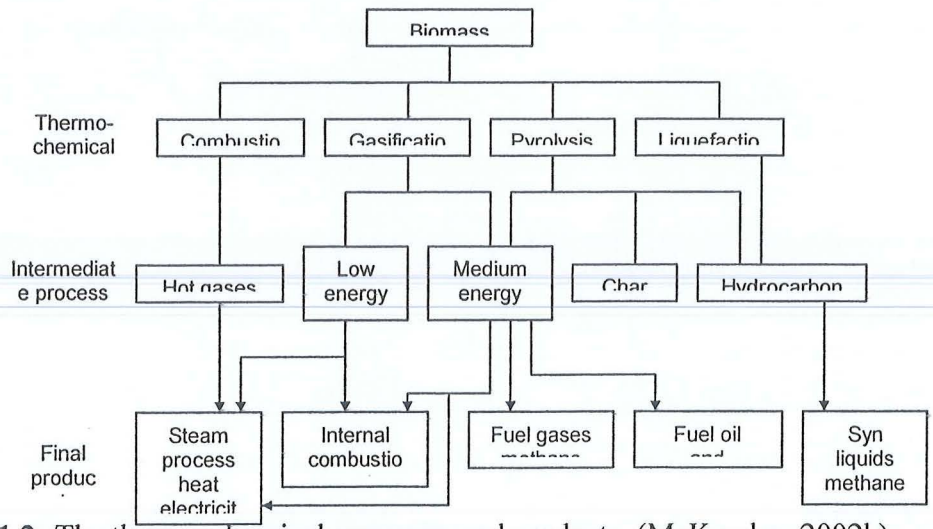

Figure 1.2: The thermo-chemical processes and products. (McKendry, 2002b)

Biomass gasification is a technology to produce low to medium energy fuel gas (Klass, 1998) for internal combustion engines or coupled to turbines to generate power. Gasification is defined as the thermal conversion of carbonaceous feedstocks such as biomass and coal into producer gas or synthesis gas (syngas - composed primarily of Hydrogen and Carbon Monoxide) using air, oxygen and steam to react with the solid fuel at high temperature, typically in the range of 800-900^{O}C. Only inert ashes by products are produced at the end of the process. According to Rezaiyan (2005) and McKendry (2002b), the producer gas produced has low calorific value (LCV) or heating value around 4-6 MJ/*N*m^3.

1.3 PROBLEMS STATEMENT

The need of doing research on the biomass sources is due to the escalating price and depleting of fossil fuels in the future. This is the first problem why the renewable sources of energy must be studied. Takuyuki Yoshioka et al. (2005) reported that around 2050, the depletion of fossil fuels is expected to worsen and alternative fuels have to be discovered. According to International Energy Agency (2004), about 80% of the primary energy production of the world comes from combustion of oil, coal and natural gas. Mukherjee (2004) also wrote that the search for alternative energy sources for sustaining the energy requirement by human being must be done because the depletion of fossil fuels is occurring at a faster rate due in increasing gap between the demand and production of fossil fuels.

The second problem is because of the burning of the fossil fuels in the IC engines. When burnt, all fossil fuels will emit carbon dioxide (CO_2) which contributes to the greenhouse gas effect into the atmosphere. According to Magnus et al. (2006), the CO_2 concentration in the atmosphere is 30% higher than it was before the industrialization era and the annual emissions are still increasing. To overcome this problem, the renewable energy sources such as biomass can be used as a fuel. Burning biomass contributes no net carbon dioxide (CO_2) to the atmosphere because replanting harvested biomass ensures that CO_2 is absorbed and returned for a cycle of new growth.

The third problem why the biomass must be studied as a fuel is because the unused wastes are a lot and managing them is difficult and expensive without added value.

Hydrogen in producer gas produced from biomass can be used as a clean fuel in the internal combustion engines to produce power and energy. However, according to Munoz et al. (2000), Sridhar et al. (2001), Zainal et al. (2002), Dogru et al. (2002), Adnan et al. (2002) and Uma et al. (2004) the percentage of hydrogen gas found in the producer gas is small approximately 6-20% by volume when using a downdraft biomass gasifier. So to increase the percentage of the hydrogen gas, the new technology has to be studied and developed. For instance the producer gas from biomass gasification system contain high amount of carbon dioxide 15-20% (Sridhar et al. 2001 and Dogru et al. 2002) there by reduces its heating values as CO_2 acts as diluents. Removing the carbon dioxide from the producer gas will improved its heating value. The heating value or the calorific value of the producer gas will be expected to increase from 4 MJ/*N*m^3 to about 6 MJ/*N*m^3. This will not just improved its heating value but inadvertently improve the amount of the combustible gas such as hydrogen, carbon monoxide and methane. This is the fourth problem identified in the research.

1.4 RESEARCH OBJECTIVES

The goal of the work presented in this thesis is to develop a bubbling fluidized bed reactor to absorb CO_2 in the producer gas using Calcium Oxide (CaO) mixed with sand as absorbent reagent for improving the quality of the producer gas. The sub-objectives are:

To simulate the hydrodynamic characteristic of a bubbling fluidized bed CO_2 absorption reactor.

To design and develop a bubbling fluidized bed CO_2 absorption reactor.

To conduct cold study to characterize the hydrodynamic behavior of the system using CaO – sand mixtures material.

To characterize the bubbling fluidized bed CO_2 absorption reactor using carbonation – calcinations process with the ceramic heater band.

To test and analyze the bubbling fluidized bed CO_2 absorption reactor with the synthesis gas and actual compressed producer gas using ceramic heater band.

1.5 RESEARCH SCOPES

The scopes of the research can be divided into four stages. Figure 1.3 shows the flow diagram designed to achieve the objectives within the scopes.

Study on calcium oxide as absorbent of carbon dioxide gas, focusing on calcination and carbonation processes.

Study on the computational fluid dynamics software such as Fluent to simulate the hydrodynamic phenomena of CaO in the bubbling fluidized bed CO_2 absorption reactor.

Study on the development of the bubbling fluidized bed CO_2 absorption reactor based on the principles of bubbling fluidization.

Study on the biomass material such as furniture wood and the process of gasification, focusing on the small downdraft gasifier.

CHAPTER 2: LITERATURE REVIEWS

INTRODUCTION

In this chapter, literature reviews have been done on types of gasifies and chemical conversion of biomass material via the gasification process into gaseous fuel. Furthermore, the combustible components of the gas are elaborated. The processes of increasing the percentages of hydrogen gas from other researchers are presented. The absorption process of carbon dioxide (CO_2) and simulation method done by other researchers are also discussed.

BIOMASS GASIFICATION

Biomass is non-fossil, energy-containing forms of carbon and includes all land and water based vegetation. It is the only indigenous renewable energy resource that is capable of displacing large amounts of solids, liquid and gaseous fossil fuels. Biomass can be used for generating electric power and industrial processing. One of the methods used to convert biomass into useful form of energy is called gasification producing the combustible gas, which can be used in internal combustion engines. The combustible gases typically consist of Hydrogen (H), Carbon Monoxide (CO) and Methane (CH_4) is commonly name as "Producer gas". Beside the combustible components, there are also incombustible components in the producer gas such as Carbon Dioxide (CO_2) and Nitrogen (N_2). According to Zhang et al. (2004), biomass when burnt or gasified will produces dirty raw gas mixture or producer gas composed of Hydrogen (H_2), Carbon Monoxide (CO), Carbon Dioxide (CO_2), Water (H_2O), Methane (CH_4) and various light hydrocarbons along with undesirable dust (ash and char), tar, Ammonia (NH_3), alkali (mostly potassium) and some other trace contaminants.

2.2.1 Types of gasifier

The gasification process occurs in a reactor called gasifier. There are basically two types of gasifiers, fixed bed and fluidized bed. The fixed bed gasifier has been the traditional process used for gasification and operated at high temperature around 1000°C. It can be classified as downdraft, updraft and cross flow, depending on the direction of the flow [McKendry, 2002c].

2.2.2 Fixed bed gasifier

2.2.2.1 Downdraft Gasifier

In a downdraft gasifier, biomass feed and air move in the same direction or co-current. The product gases leave the gasifier after passing through the hot zone, enabling partial cracking of the tars form during gasification and leave a producer gas with low tar content. The overall energy efficiency of the downdraft gasifier is low because the gases leave the gasifier unit at a high temperature of 900-1000°C and due to the high heat content carried over by the hot gas. Figure 2.1 shows a diagram of downdraft gasifier.

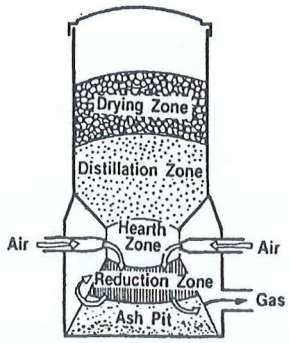

Figure 2.1: Diagram of downdraft gasification (Skov, 1974)

2.2.2.2 Updraft Gasifier

In a updraft gasifier, biomass feed is introduced at the top and the air flow from the bottom of the unit via a grate in a counter current flow. The solid char formed higher up the gasifier above the combustion zone. Updraft gasifier is simple in design and can handle biomass with high moisture content. Figure 2.2 shows a diagram of an updraft gasifier.

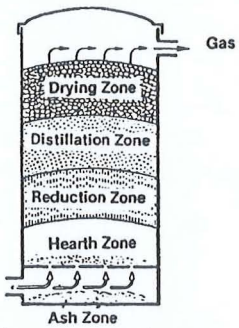

Figure 2.2: Diagram of updraft gasification (Skov, 1974)

2.2.2.3 Cross flow

In this gasifier the feed moves downwards while the air is introduced from the side. The gas is drawn from the opposite side of the unit at the same level. A hot gasification zone forms around the entrance of the air, with the pyrolysis and drying zones being formed higher up in the vessel. Ash is removed at the bottom and the temperature of the gas leaving the unit is 800-900°C. This gives low overall energy efficiency for the process and a gas with high tar content. Figure 2.3 shows the diagram of cross flow gasifier.

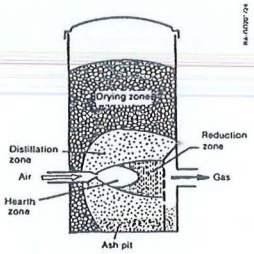

Figure 2.3: Diagram of Cross flow gasification (Skov, 1974)

2.2.3 Fluidized bed gasifier

The fluidized bed gasification has been used extensively for coal gasification for many years. It is favored by many designers for gasifier using smaller feedstock sizes. In the gasification zone of the fluidized bed, the uniform temperature distribution achieved. There are two main types of fluidized bed gasifier can be classified: bubbling fluidized bed and circulating fluidized bed.

2.2.3.1 Bubbling Fluidized Bed Gasifier (BFB)

The gasifier consists of a vessel with a grate at the bottom through which air is introduced. Above the grate is the fluidized bed of fine grained materials into which the prepared biomass feed is introduced. The BFB utilizes minimum fluidization velocity of sand and fine grained bed material to achieve fluidization state. The sand acts as a heat transfer medium. The ash entrained out the gasifier collected in a cyclone separator. For biomass material with high moisture content and low heating value, BFB is recommended. The detail concept of the BFB will be discussed in chapter 3.2 and the diagram of the bubbling fluidized bed is shown in Figure 2.4 (a).

2.2.3.2 Circulating Fluidized Bed Gasifier (CFB)

Circulating fluidized bed is suitable for waste fuels with a high percentage of non-combustibles (heating value 5 - 35 MJ/kg). It operates at a temperature around 800-900^{0}C. Crushed coal along with sorbent (limestone) is fed to the lower furnace where it is kept suspended and burnt in an upward flow of combustion air. The sorbent is fed to facilitate capture of sulfur from the coal in the bed itself resulting in consequent low sulfur emission. Due to high gas velocities, the fuel ash and un-burnt fuel are carried out of the combustor with the flue gases. These are then collected by a recycling cyclone separator and returned to the lower part of the gasifier. Figure 2.4 (b) shows a diagram of a circulating fluidized bed.

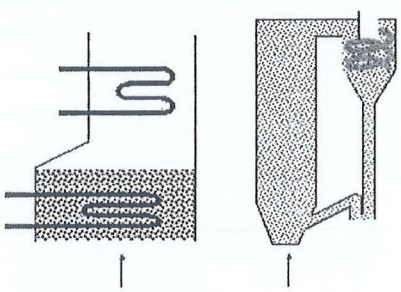

Figure 2.4: Diagram of a) bubbling bed. b) circulating bed

2.2.4 Biomass Gasification

Wood is one example of the biomass source. It is composed of cellulose, hemicellulose, and lignins (Lee S.,1996). It is defined as lignocellulosic material. The structures of hemicellulose and lignins are very complicated, which contributes to the complexity of the thermo-chemical conversion reactions. Consider wood with a chemistry formula $CH_{1.44}\ O_{0.66.}$ Ideal gasification reaction with oxygen can be written as follow:

$CH_{1.44}\ O_{0.66} + 0.17O_2 \rightarrow CO + 0.72H_2$ (2.1)

This ideal gasification reaction is an endothermic process, which means the reaction in the system absorbs energy from the surroundings in the form of heat. Oxygen is partially supplied to gasify the wood and produce carbon monoxide and hydrogen gases. According to Reed (1985), the surplus oxygen reacts with about a third of the CO and H_2 ideally produced. The equation 2.2 is the theoretical global gasification reaction with CO_2 and H_2O as additional products.

$CH_{1.44}\ O_{0.66} + 0.45O_2 \rightarrow 0.7CO + 0.3CO_2 + 0.55H_2 + 0.2H_2O$ (2.2)

Biomass materials will undergo three stages of mass loss in the gasification process. The stages are drying, pyrolysis and gasification. Inherent moisture in the biomass is removed in the drying stage. The temperature rises and the biomass particle begin to decompose and release volatiles. When this happen it is call pyrolysis stage. In the last stage, where there is insufficient oxygen supplied, partial oxidation takes place. Under this condition, partial oxidation of the residues and volatiles occur. This results in generation of partially oxidized products and combustible gases such as hydrogen, carbon monoxide and methane. These stages occur rapidly.

The amount of water depends on wood species and most species can absorb about 30% water (U.S. Departments of Agriculture, 2007). According to McKendry (2001), moisture content of wood more then 30% makes ignition difficult and will reduced heating value of the producer gas due to the need to evaporate additional moisture before combustion occur. So to improve heating value of the producer gas, moisture contents in the wood must be kept below 30%.

2.2.5 Producer Gas Compositions from Downdraft Gasifier

The producer gas consists of combustible and incombustible gases. Theoretically, the compositions of producer gas-air mixture are 15-20% H_2, 10-15% CO, 9-15% CO_2, 3-5% CH_4 and 40-50% N_2 by volume (Reed and Das, 1988).

Gunderson and Darren (2000) reported that hydrogen gas could be obtained from biomass and many compounds such as water and fossil fuels. To obtain hydrogen from biomass, pyrolysis or gasification must be applied, which typically produces a gas containing 20% hydrogen by volume, which can be further steam reformed to make higher quality gas.

Munoz et al. (2000) stated that producer gas contained 14% hydrogen (H_2), 22% carbon oxide (CO), 13% carbon dioxide (CO_2), 3% methane (CH_4) and rest, nitrogen (N_2) have been determined from wood residues using a downdraft fixed bed gasifier. In their research, they used two fuels, producer gas and gasoline to measure the performance of a spark ignition engine. The results obtained show that not so much loss of power in using producer gas compared with gasoline. The hydrocarbon and CO also reduced but CO_2 increased when using producer gas.

Sridhar et al. (2001) also stated that the producer gas can be fuelled into a spark ignition engine converted from diesel engine. They used open top downdraft gasifier system to convert biomass, causurina species wood into producer gas. The composition of the product gas was 19% H_2, 19% CO, 12% CO_2, 2% CH_4, 2% H_2O and rest, N_2. They found that the performance of the engine at higher compression engine has been smooth and the

cylinder pressure-crank angle trace has shown smooth pressure variations during the entire combustion process without any sign of abnormal pressure raise.
Zainal et al. (2002) reported that the gas composition found in their experiment of a downdraft biomass gasifier using furniture wood and wood chips was 14.05% H_2, 24.04% CO, 14.66% CO_2, 2.02% CH_4, 1.69% O and 43.62% N_2.
Dogru et al. (2002) also investigated gasification potential of hazelnut shells using downdraft gasifier. They obtained gas composition 11.11%-14.77% H_2, 8.56%-18.56% CO, 9.52%-16.33% CO_2, 1.4%-2.47% CH_4, 53.33-59.67% N_2.
Adnan et al. (2002) investigated hydrogen production from sewage sludge by applying downdraft gasification technique. They conducted the experiment using a pilot scale throated downdraft gasifier and concluded that the combustible gases from sewage sludge have a high percentage from 8.98% to 11.4% of hydrogen gas within 20.09% – 23.83% of combustible gases. This amount of gases is enough to derive internal combustion engine.
Uma et al. (2004) reported biomass gasification is one such process where producer gas could be obtained and used for power generation purposes. Biomass gasifier-based systems capable of producing power from few kilowatts up to several hundred kilowatts have been successfully developed. They investigated emission characteristics of a diesel engine in diesel alone and producer gas at different load conditions. The producer gas was produced by a downdraft gasifier system. The gas composition was 14% H_2, 19% CO, 10% CO_2, 1.9% CH_4, and remaining is N_2 have been used to run a diesel engine. CO emissions from producer gas were higher than the diesel alone at all operated load conditions, but NO_x and SO_2 emissions were decreased.
Combustible gas compositions obtained from producer gas produced from biomass gasification stated by researchers has only approximately 24% by volume maximum. Table 1 shows summary of gas composition of the producer gas from other researchers.

Table 1: Gas compositions in producer gas reported by other researchers.

	~% Vol.				
	H_2	CO	$C0_2$	CH_4	N_2
Munoz et al. (2000)	14	22	13	3	48
Sridhar et al. (2001)	19	19	12	2	48
Zainal et al. (2002),	15	24	15	2	44
Dogru et al.(2002)	15	19	16	2	48
Uma et al. (2004)	14	19	10	2	55

To increase the combustible compositions percentages in the producer gas, some methods have to be studied. The applications done by other researchers to increase the combustible gas in the producer gas is elaborated in section 2.3.

2.2.6 Producer Gas Energy Content

Producer gas must have energy content greater than 4 MJ/Nm^3 for most application to run diesel engine. The energy content can be calculated from the energy content of the components using low and high heating values for each gas as show in equation 2.4.

$$HV_{pg} = \sum (\%vol.)_g (HV)_g \qquad (2.3)$$

Where HV: heating value (MJ/Nm^3)
pg : producer gas
g : gas

According to McKendry (2001) the energy of producer gas can be classified into three types, low (4-6 MJ/Nm^3), medium (10-16 MJ/Nm^3) and high heating values (40 MJ/Nm^3). The low heating value used air as agent for gasifying, the medium heating value used steam or oxygen and the high heating value used hydrogen as a gasifying agent. In table 2 shown the comparisons of the heating value of the producer gas obtained from other researchers.

Table 2: Comparisons of heating value of producer gas with other researchers.

Researchers	Heating Value (MJ/NM^3)
Graham et. al (1981)	6.39
Walawender et. al (1985)	5.51
Xu et. al (1988)	5.5
Hoi (1992)	4.97
Jorapur et. al (1995)	5.04
Zainal (1996)	5.34
Sridhar et. al (2001)	4.67
Dogru et. al (2002)	5.15
Uma et. al (2004)	4.60

2.3 METHODS TO INCREASE PRODUCER GAS QUALITY

There are few applications that have been done to enrich quality of the producer gas especially hydrogen gas composition. Chang et al. (2004) reported that oxygen-rich air gasification methods in a bubbling fluidized bed can be used to increase the hydrogen content. The results showed higher reactor temperature favored hydrogen production to 38% vol. but too high temperature lowered gas heating value. Introduction of steam to biomass gasification is favorable for improving gas quality however excessive steam would lower gasification temperature and so the grade product gas quality.

Other researchers such as Delgado et al. (1996), Aznar et al. (1998), Gil et al. (1999), Rapagna et al. (2000), Courson et al. (2000), Schuster et al. (2001) and Mathieu et al. (2002) also wrote that using fluidized-bed, steam-gasification processes (with or without oxygen added) is capable of producing a medium heating value gas with a 30-60 % hydrogen content.

Hofbauer et al. (2000) reported that they have succeeded design a gasifier to produce a high grade synthesis gas from solid fuels. A bubbling fluidized bed gasifier was

developed and used steam as gasification agent, produced little heat loss and nearly nitrogen free product gas with high calorific value of 13 MJ/Nm^3. The experimental result showed that it is possible to produce a product gas with 40-60% hydrogen content.

Markus et al. (2004) demonstrated two difference types of gasifier plants in Austria. The first plant used fast internal circulating fluidized bed and the second used twin fire downdraft fixed bed gasifier. Results showed that composition of hydrogen gas in producer gas is high in the first plant about 35-45% vol. compared with the second plant only 16-18% by vol.

Hydrogen content in the product gas also can be increased by using a catalytic active bed material and was tested in a 100kW dual fluidized bed biomass steam gasifier (Pfeifer, 2004 and Rauch, 2004). The catalyst has been modified from olivine enriched with nickel using nickel nitrate. The result showed that Ni-olivine catalyst was very effective in reducing of tars above temperature 750°C and leads to increase the hydrogen gas content to 45%.

Zhang (2005), stated that the air blown gasification of biomass in fluidized bed reactors produces relatively low concentration of hydrogen about 8% only. To increase the hydrogen content in the producer gas, steam reforming of tars and light hydrocarbons and reacting steam with carbon monoxide via the water gas shift reaction must be used. In their experiment, they found that the hydrogen content in producer gas from the air blown gasification of biomass in fluidized bed reactors upgraded from 5.8-8.8% to as high 27-29%.

Another possibility to enhance combustible gas composition in producer gas is to remove carbon dioxide (CO_2) from the gas directly in the gasification reactor by chemical absorption process. Carbon dioxide (CO_2) content in the producer gas reduces its heating values as CO_2 acts as diluents. Removing carbon dioxide from the gas will inadvertently increase its heating value. Heating value or calorific value of the producer gas will be expected to increase from 4-5 MJ/Nm^3 to about 8-10 MJ/Nm^3. By removing carbon dioxide from the producer gas, will also improve hydrogen % content. The most well known sorbent is calcium oxide (CaO) with forms calcium carbonate ($CaCO_3$) when react with carbon dioxide.

Lin et al. (2002) wrote that the key for reaction to succeed in their new innovative hydrogen production method was water reduction by hydrocarbons and CO_2 absorption reaction. They developed an innovative method called HyPr-PING (hydrogen production by reaction-integrated novel gasification) to produce hydrogen from hydrocarbon sources such as coal, heavy oil, biomass, plastic and organic waste. Calcium hydroxide ($Ca(OH)_2$) was used as CO_2 sorbent and sodium carbonate (Na_2CO_3) with sodium hydroxide (NaOH) were used as catalysts. In their experiment, the Japanese bituminous Taiheiyo coal was mixed with 0.6g CO_2 sorbent, water and 0.05g catalyst to form slurry. The slurry was introduced into a 10 cm^3 micro-autoclave and heated at a rate of 100K/min. Then it was kept at 200°C temperature for approximately 10 min. Results showed that hydrogen content from the Japanese bituminous Taiheiyo coal was 80% of the product gas.

Hanaoka et al. (2005) also used CO_2 sorbent in their research to produce hydrogen gas from woody biomass by steam gasification. They investigated the effect of reaction parameters such as the molar ratio of CaO as CO_2 sorbent to carbon (Ca/C), reaction pressure and temperature on hydrogen yield. The $Ca(OH)_2$ powder (average particle size

0.01mm) was used as a CO_2 sorbent. During heating up to a reaction temperatures above 600°C the $Ca(OH)_2$ powder will change into CaO because of dehydration from $Ca(OH)_2$ that occurs at about 400°C. The Japanese oak (0.106-0.25mm) without bark was used as a woody biomass, $Ca(OH)_2$ and distilled water were charged in Tammann tube and placed in autoclave. It was then heated up to the desired temperature. Results showed that in the absence of CaO, the product gas contained CO_2 but when in presence of CaO (Ca/C = 1, 2, 4) no CO_2 was detected in the produced gas. The maximum yield of H_2 was obtained at Ca/C = 2 and low pressure as 0.6MPa. The H_2 yield also increased with increasing reaction temperature at 600°C, 650°C and 700°C.

Weil et al. (2006) conducted a study on simulation of hydrogen production from waste gasification coupled with cement manufacturing. They wrote that CO_2, which is formed in the gasification stage, can be removed by adding a solid sorbent such as CaO into the gasifier. Temperature in the gasifier for CO_2 absorption should be lower than 700°C. Simulation result showed that hydrogen content in the product gas reaches nearly 78% when the temperature was below 600°C due to CO_2 capture, but with increasing temperature above 600°C the H_2 content decreased to 62% because CO_2 increased. This effect can be explained by the temperature dependent carbonation reaction which decomposes $CaCO_3$ to CaO and CO_2 at high temperatures.

Mahishi and Goswami (2007) wrote of the development of a novel technique to enhance hydrogen yield of conventional biomass steam gasification by integrating gasification and absorption reactions. Pine bark has been used as biomass resource in the presence of calcium oxide at different temperatures in the range 500-700 ^{O}C. Results showed that that at 600 ^{O}C, hydrogen yield increased by 48.6% for the sorbent enhanced case. It was also observed that hydrogen yield at 500 ^{O}C and 600 ^{O}C was more than conventional hydrogen yield at 700 ^{O}C. They also stated that absorption of CO_2 by calcium oxide depends on equilibrium temperature corresponding to partial pressure of CO_2.

According to Florin and Harris (2008) on steam gasification of biomass without CO_2 capture, H_2 concentrations in the product gas achieved are only 40–50%. To increase the H_2 concentration, an in situ CO_2 sorbent was used. Results showed that when steam gasification is coupled with CO_2 capture, H_2 content increased to approximately 80%.

Guoxin and Hao (2009), have proposed hydrogen rich fuel gas production by gasification of wet biomass accompanied by CO_2 absorption. They have conducted experiment to investigate the effect of moisture content on hydrogen production and CO_2 absorption by CaO. For experiment with wet biomass, hydrogen yield was increased by 51.5% while CO_2 content was decreased by 28.4% compared to dry biomass.

With all these applications mention above, composition of the producer gas especially hydrogen from biomass gasification can be increased. In this thesis, the author will focus on the used of calcium oxide to absorb CO_2 content in the producer gas. In the last few years, the numbers of CO_2 sorbents have been intensively investigated in biomass technology fields (Guoxin and Hao, 2009; Florin and Harrin, 2008; Mahishi and Goswami, 2007; Hanoaka et al., 2005) because of their low cost, abundance and availability. Although researches on the CO_2 absorption have been widely studied, however the focused is only the used of calcium oxide, CaO in a reactor or combustor (Nikulshina et al., 2009; Manovic et al., 2009; Grase et al., 2008; Chen, 2007; Abanades et al., 2005; Grase and Abanades, 2007; Salvador et al., 2003 and Abanedes, 2002). Work done by the researchers so far have not used CaO-sand mixture as bed material for

carbonation-calcinations process to absorb and release CO_2 of the compressed producer gas from downdraft biomass gasifier. So this is the areas that will be covered in this study.

2.4 CARBON DIOXIDE (CO_2) ABSORBER

In producer gas concentration of carbon dioxide is about 16% volume. To enhance the producer gas quality, one possibility is to remove carbon dioxide by chemical absorption process and calcium oxide (CaO) is the most well known sorbent that can do it.

The background of CO_2 absorbent goes back to 1867, when DuMotay and Marechal first patented used of lime to aid the gasification of carbon by steam (Squires, 1967). A century later, the CO_2 acceptor gasification process reached a demonstration phase using the carbonation and calcination of CaO from limestone to separate CO_2 from coal gasification gases (Curran et al., 1967).

2.4.1 Calcium Oxide (CaO)

Calcium oxide or quicklime is a white crystalline solid with a melting point of 2572°C. It does not occur in nature and has to be produced from calcium carbonate ($CaCO_3$) by energy intensive conversion. This is accomplished by heating the $CaCO_3$ to above 825°C where a process called calcination or lime-burning, to liberate molecules of carbon dioxide (CO_2) and leaving CaO. This process is reversible, since once the CaO has cooled, it immediately begins to absorb carbon dioxide from the air until it is completely converted back to calcium carbonate. This process is called carbonation. Equation 2.4 shows the reaction of $CaCO_3$ to CaO.

$$CaCO_3(s) \xleftrightarrow{825^\circ C} CaO(s) + CO_2(g) \qquad (2.4)$$

2.4.2 Calcination

Calcination reaction is endothermic

$$CaCO_3 \rightarrow CaO + CO_2 \qquad \Delta H = +182.1 \quad \text{kJ mol}^{-1} \qquad (2.5)$$

which means that the forward reaction is favoured by higher temperatures. The reaction will proceed only if partial pressure of CO_2 in the gas is above the solid surface and is less than the decomposition pressure of $CaCO_3$. The latter pressure is determined by equilibrium thermodynamic considerations. A typical expression for equilibrium decomposition pressure P_{eq} quoted by Kramlich et al. (1989) is:

$$P_{eq} = 4.137x10^7 \exp\left(-\frac{20474}{T}\right) \quad \text{atm} \qquad (2.6)$$

Figure 2.5 shows the decomposition pressure of carbon dioxide over calcium carbonate by three researchers.

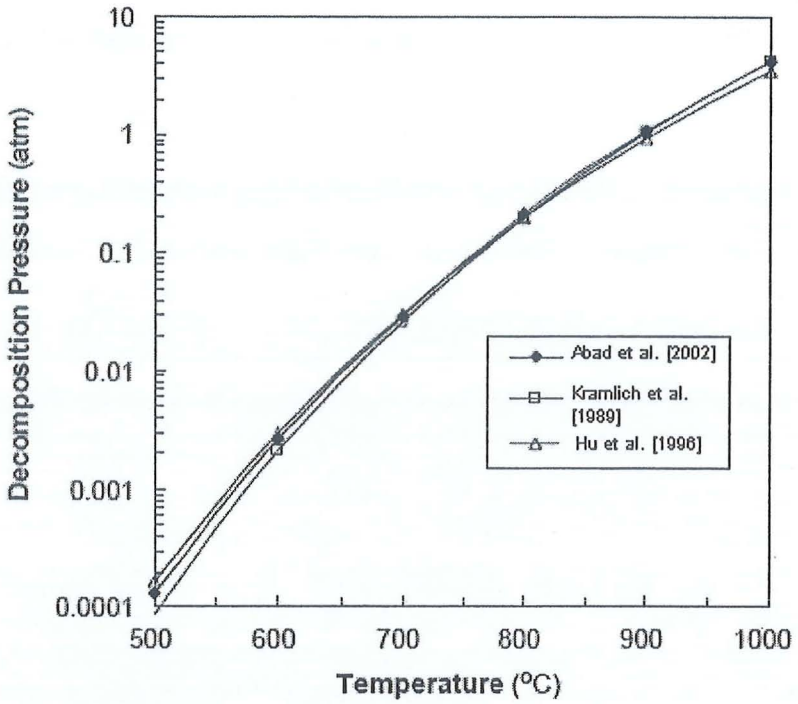

Figure 2.5: Decomposition pressure of carbon dioxide over calcium carbonate by three researchers (Stanmore and Gilot, 2005)

2.4.3 Carbonation

Carbonation is the reverse of calcination process, and is therefore exothermic.

$$CaO + CO_2 \rightarrow CaCO_3 \qquad \Delta H = -182.1 \text{ kJ mol}^{-1} \qquad (2.7)$$

Conditions for carbonation process must balance between high temperature which favour the speed of reaction and low temperature which favour equilibrium conversion.

Earlier study of carbonation reaction was carried out by Bhatia and Perlmutter (1983). Using a thermo-balance, they calcined a limestone under atmospheric pressure containing 0, 10 and 20% CO_2. As concentration of CO_2 increased, the pore sizes became larger and their size distribution less spread. The crystallinity of the lime was greater for the sample prepared in pure nitrogen. At temperatures between 550 and 725 °C, they identified an initiation period, followed by a growth period in carbonation, and finally a leveling off. Carbonation levels of over 70% could be obtained in a period of about 1 min for 81 and 137 μm particles. The rate of reaction was sensitive to temperature and increased as the temperature reduced.

Abanades and Alvarez (2003) examined the work on carbonation carried out by Bhatia and Perlmutter, and concluded that the findings were consistent with their own. The carbonation was carried out for 20 min at 650 °C under different partial pressures of CO_2. They claim that for all conditions, complete carbonation was achieved in a matter of minutes.

2.5 CFD MODELING ON BUBBLING FLUIDIZED BED

Numerical modeling techniques or computer fluid dynamics (CFD) offers a powerful tool to simulate fluid flow in bubbling fluidized bed. Fluid flow in bubbling fluidized bed are complicated, so with CFD, hydrodynamics characteristics can be studied. According to Anderson et al. (1995), the mass conservation equation, the momentum equation and the energy conservation equation are numerically solved in CFD.

Numerical studies for bubbling fluidized bed reactors have been intensively done for lab-scale or pilot-scale plants in the industries (Barea and Leckner, 2010; Park et al. 2008; Zheng, 2008 and Velden et al. 2008). However there are few numerical studies for Calcium Oxide as bed materials in bubbling fluidized bed reactor.

Vuthalurua et al. (2009) studied fluidization behaviour of solid–liquid flow in a conical reactor occupied with limestone particles. Three dimensional, unsteady state simulations using the Granular Eulerian multiphase approach were performed. Six different geometries of conical fluidized limestone reactor (FLR) have been created using Gambit and exported to Fluent in order to study the bed expansion behaviour in liquid/solid flow. The fluidization dynamics with changed variables in vessel dimensions, particle loading (limestone) and fluid flow (water flow rate) were done. They also validated the model with lab-scale FLR (Cone 1) experimental. Results showed that fluidized bed height increases with increase in inflow rates of water through the bed for the simulation as well as the experimental cases. They concluded that CFD is a powerful tool to investigate the behaviour of fluidization of limestone within the conical FLRs.

Behjat et al (2009) had developed and validated CFD models to investigate hydrodynamic phenomena of their reactor. The results were compared to experimental data obtained from the literature. It shows that with two solid phases used, particles with smaller diameters have lower volume fraction at the bottom of the bed and higher volume fraction at the top of the bed. The bed expansion was larger when a bimodal particle mixture was applied compared with the case of mono-dispersed particles.

Commercial simulation software FLUENT was also been used by Cooper and Coronella (2005) to investigate relative effects on bubbling of particle mixing and segregation in a bubbling fluidized bed reactor. They reproduce important hydrodynamic aspects of a binary fluidized bed, by modeling three phases using the Eulerian interpenetrating fluids model. The simulations predict realistic bubbles, bubbling rates, bubble wakes and bed expansion. For all operating conditions investigated, the simulated bed was well mixed axially. Gas velocity, maximum packing fraction, and solids composition did not affect the extent of mixing. However, small pockets of transient localized segregation were predicted throughout the bed.

Many researchers have done numerical study using CFD software such as Fluent. It is known as state of the art in modeling fluid flow. However, CFD simulation to investigate hydrodynamic characteristics based on Calcium Oxide is less. In this thesis CFD software Fluent will be used to study hydrodynamic characteristics of various materials in the bubbling fluidized be to reduce limestone lost and maximize efficiency.

CHAPTER 3: DESIGN AND DEVELOPMENT OF BUBBLING FLUIDIZED BED CO_2 ABSORPTION REACTOR

INTRODUCTION

The carbon dioxide, CO_2 absorption reactor or bubbling fluidized bed CO_2 absorption reactor (BFBR) is the main device of this research study. The function of the reactor is to absorb CO_2 gas composition in the producer gas from biomass product. The reactor provides a very high heating rate with closely controlled moderate temperature to enable the rapid thermal decomposition of the producer gas. The design of the reactor is carried out based on the amount of calcium oxide will be used, the fluidization and heat transfer consideration. The finalized reactor design is then fabricated and tested in the present of heat. This is because the temperature operation of the reactor has to be around 500°C to 1000°C, so the heating performance must be verified.

3.2 BUBBLING FLUIDIZED BED CONCEPT

Bubbling fluidized bed is a preferable configuration that well fit to the development criteria of the CO_2 absorption reactor. Geldart [1984] has described the fluid like behavior of the fluidized bed,

Lighter objects float on top of the bed (objects less dense than the bulk density of the bed),

The surface stays horizontal even in tilted beds,

The solids can flow through an opening in the vessel just like a liquid,

The beds have a "static" pressure head due to gravity, given by ρgh,

Levels between two similar fluidized beds equalize their static pressure heads.

The bubbling fluidized bed is dominated by rising of gas voids called bubbles. In dense phase, the upward gas enters the fluidized bed as a small bubble through the holes on gas distributor when above the minimum fluidizing velocity (u_{mf}). A complex and heterogeneous fluidisation structure is thus formed by the traversed of gas voids or bubbles. The rising bubbles cause the motion of the particulate phase. This is the main solids mixing in bubbling fluidized beds.

The gas bubbles coalesce and grow as they rise along the bed. Small gas bubbles coalesce with other and then leave the bed as larger bubbles. A condition called slugging will occur if a deep fluidized bed with small reactor diameter and sufficiently high velocity were used. In this condition , the particles rain down from the piston-like gas void when it reaches the bed surface and finally disintegrates while another slug forms and progress to the bed surface. According to Zhang and Yu [2002], the condition of slugging is usually undesirable because it will increase the problems of entrainment and lowers the performance potential of the reactor.

3.3 PARTICLES CONCERN

The selections of the solid particles that will be used in the reactor are important for the absorption reaction to occur. The different size of solid particles may behave similarly or differently in the bubbling fluidized bed.

There are four groups of solid particles according to Geldart [1973]. Group C is the finest particles, followed by group A and B, then group D is the coarsest particles. Figure 3.1 shown the detail of groups for each solid particle.

Group	Particle sizes	Examples	
C	≈ 20-30 μm (0.02-0.03 mm)	Flour or cement	Finest
A	≈ 30-100 μm (0.03-0.10 mm)	Fine biomass powder	↑
B	≈ 100-600 μm (0.04-0.50 mm)	Sand	↓
D	> 600 μm (> 0.60 mm)	Crushed limestones or coffee beams	Coarsest

Figure 3.1: The detail of Geldart groups for each solid particle

In this research study, only three sizes of particle such as group A, B and D have been determined to be used in the CO_2 absorption reactor. The Geldart group C is too extremely fine particle and fluidize under very difficult conditions.

3.4 ESTIMATION OF DESIGN PARAMETERS

As mention early, the finalized design is carried out based on the amount of calcium oxide will be used, the fluidization and heat transfer consideration. Another consideration of the design is based on the 90 mm inner diameter of the existing ceramic heater band has in the bio-energy lab.

The design initially started based on the power requirement of 4.5 kW small diesel engines. This diesel engine is located at the bio energy lab. By taking the normal efficiency of the diesel engine as 30%, the thermal input required to run the diesel engine was 15 kW from equation (3.1).

$$\eta_{diesel} = \frac{P_{out}}{P_{in}} \tag{3.1}$$

$$P_{in} = \frac{P_{out}}{\eta_{diesel}}$$

$$= \frac{4.5x10^3}{0.3}$$

$$= 15kW$$

Where,

η_{diesel} : Efficiency of diesel engine (%)

P_{in} : Thermal power input of diesel engine (kW)

P_{out} : Thermal power output of diesel engine (kW)

The diesel engine can be operated with two fuels called dual fuel mode. According to Uma et al [2004] the replacement fuel in dual fuel mode can be done with producer gas in range of 70% to 90%. Assuming 70% of producer gas was fueled into diesel engine, the thermal input from producer gas was 10.5 kW. (equation (3.2))

$$P_{inpg} = P_{in} x 0.7 \qquad (3.2)$$
$$= 15x10^3 x 0.7$$
$$= 10.5kW$$

Where,

P_{inpg} : Thermal power input from producer gas (kW)

Using the low calorific value for producer gas as 4.6 MJ per $N\text{m}^3$ mentioned by Rezaiyan and Cheremisinoff [2005], then the volume flow rate of the producer gas needed can be calculated as shown in the equation (3.3).

$$P_{inpg} = Q_{pg} x LCV_{pg} \qquad (3.3)$$
$$Q_{pg} = \frac{P_{inpg}}{LCV_{pg}}$$
$$= \frac{10.5x10^3}{4.6x10^6}$$
$$= 2.283x10^{-3} \frac{Nm^3}{s} @136.96 \frac{L}{\text{min}}$$

Where,

Q_{pg} : Volume flow rate of the producer gas ($N\text{m}^3$ per sec)

LCV_{pg} : Low calorific value for producer gas (MJ per Nm^3)

Rezaiyan and Cheremisinoff [2005] also wrote the efficiency of gasifier for the cold producer gas named the cold efficiency is around 60 to 70%. If the cold efficiency for downdraft gasifier assuming as 60% and the low calorific value of furniture wood was 18 MJ per kg, the amount of furniture wood needed in term of mass flow rate can be calculated. As shown in equation (3.4), the mass flow rate of furniture wood needed was 3.5 kg per hour.

$$\eta_{coldgasi} = \frac{Q_{pg} x LCV_{pg}}{\dot{m}_{wood}\, x LCV_{wood}} \qquad (3.4)$$
$$\dot{m}_{wood} = \frac{Q_{pg} x LCV_{pg}}{\eta_{coldgasi} x LCV_{wood}}$$
$$= \frac{2.283x10^{-3} x 4.6x10^6}{18x10^6 x 0.6}$$
$$= 9.72x10^{-4} \frac{kg}{s} @3.5 \frac{kg}{hr}$$

Where,

$\dot{m}_{wood}$: Volume flow rate of the producer gas (Nm^3 per sec)

LCV_{wood} : Low calorific value of furniture wood (MJ per Nm^3)

$\eta_{coldgasi}$: Cold efficiency of gasifier (%)

The amount kg required for the calcium oxide in the reactor can be calculated based on the mass flow rate of the furniture wood. Considered in 1 hour of operation, about 3.5 kg of furniture wood needed as calculated before. Using chemical equation of stoichiometric gasification with oxygen and air for the furniture wood as shown in equation (3.7) respectively, the amount of carbon dioxide, CO_2 produced for 3.5 kg of furniture wood can be calculated.

For stoichiometric gasification with air,

$$CH_{1.44}O_{0.66} + 0.183O_2 + 0.183\left(\frac{79}{21}\right)N_2 \rightarrow 0.026H_2 + 0.333CO + 0.333CO_2 + 0.026H_2O + 0.333CH_4 + 0.183\left(\frac{79}{21}\right)N_2 \qquad (3.7)$$

per kg of furniture wood,

$$12 + 1.44(1) + 0.66(16)kgCH_{1.44}O_{0.66} + 0.183[2(16)]kgO_2 + 0.688[2(14)]kgN_2 \rightarrow 0.026[2(1)]kgH_2 + 0.333[2+16]kgCO + 0.333[12+2(16)]kgCO_2 + 0.026[2(1)+16]kgH_2O + 0.333[12+4(1)]kgCH_4 + 0.688[2(14)]kgN_2$$

$$1kgCH_{1.44}O_{0.66} + 0.244O_2 + 0.803N_2 \rightarrow 0.002H_2 + 0.25CO + 0.61CO_2 + 0.019H_2O + 0.222CH_4 + 0.803N_2 \qquad (3.8)$$

From equation (3.8), 1 kg of furniture wood, $CH_{1.44}O_{0.66}$ will produce $0.61kgCO_2$, for 3.5 kg of furniture wood used, will produced 2.14 kg CO_2 gas. With the amount of CO_2 gas produced, the calcium oxide needed can be determined by solving equation (3.9),

$$CO_2 + CaO \Leftrightarrow CaCO_3 \qquad (3.9)$$

per kg of CO_2,

$$[12+2(16)]kgCO_2 + [40+16]kgCaO \Leftrightarrow [40+12+3(16)]kgCaCO_3$$

$$1kgCO_2 + 1.27kgCaO \Leftrightarrow 2.27kgCaCO_3 \qquad (3.10)$$

From equation (3.10), 1 kg of carbon dioxide, CO_2 produced, required 1.27 kg calcium oxide, CaO. Therefore 3.5 kg of furniture wood used, and 2.14 kg CO_2 gas produced will need about 2.7 kg of calcium oxide, CaO.

Therefore to operate the 4.5 kW small diesel engines with downdraft gasifier and CO_2 absorption reactor for about 1 hour experiment duration times, the design parameters are as shows in Table 3.1.

Table 3.1: Design parameters for 1 hour duration times experiment

Paramaters	Values
Diesel Engine	4.5 kW
Q_{pg}	2.283 x 10^{-3}NM^3 per sec @ 136.96 L per min
$\dot{m}_{wood}$	3.5 kg per hour
m_{CaO}	2.7 kg

The amount of calcium oxide used to run for 1 hour operation was too expensive, so the design has to be scaled down to the laboratory scale. The finalized design of CO_2 absorption reactor is based on the existing ceramic heater band 90 mm inner diameters that have been used.

3.5 DIMENSION OF BUBBLING FLUIDIZED BED CO_2 ABSORPTION REACTOR

The bubbling fluidized bed CO_2 absorption reactor was designed by Universiti Sains Malaysia and fabricated by local manufacturing firm. It was placed at the bio-energy lab. The main construction features of bubbling fluidized bed CO_2 absorption reactor consist of main furnace, stand and nozzle distributor plate. The reactor was developed for the laboratory scale purpose. The overall height of the reactor is 877.5 mm. The inner diameter of the reactor is 74 mm and the outer diameter is 88 mm. The main furnace and nozzle distributor plate are made from stainless steel 304 to detain high temperature operation around 1200°C while the stand made from mild steel. The height of the furnace is 600 mm and has 6 holes for the thermocouples. The nozzle distributor plate has five small nozzles that protrude up from the surface of the plate. Each nozzle has four holes of 1.6 mm diameter to allow gas to flow. Figure 3.2 shows the drawing of bubbling fluidized bed CO_2 absorption reactor in mm and in appendix 1 was a full detail drawing of the CO_2 absorption reactor.

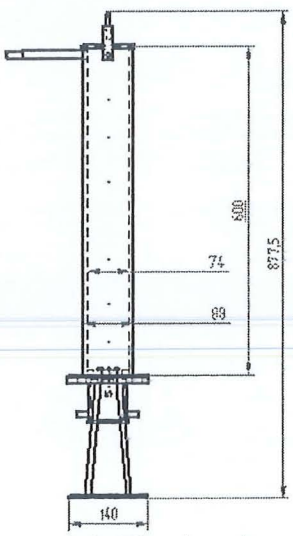

Figure 3.2: The drawing of bubbling fluidized bed CO_2 absorption reactor in mm

3.6 CO_2 ABSORPTION REACTOR OPERATING PARAMETERS

The operation parameters of bubbling fluidized bed CO_2 absorption reactor are important because its help to estimate the values obtained from the design proposed. These values gave the range of the operating condition, whether the design proposed acceptable or not. There are several calculations that have been calculated and shown below.

3.6.1 Aspect Ratio, A_r

Aspect ratio, A_r is the ratio of static bed height, h_s divided by the reactor inner diameter, d_i. It shows the relation between the static bed height and inner diameter of the reactor. In this research study, the static bed height of the calcium oxide, CaO and sand will be determined first. It is desirable to have a high amount of bed material because to increase the residence time of the producer gas to react with calcium oxide. However the static bed height is limited by the pressure drop across the CO_2 absorption reactor. Using equation (3.11), the static bed height can be determined. According to Cao et al. [2006], an aspect ratio of 1 is suitable to be used for the reactor in their experiment. So in this research, the aspect ratio, A_r was operated around 1.

$$A_r = \frac{h_s}{d_i} \tag{3.11}$$

$$d_i = \frac{h_s}{A_r}$$

$$= \frac{0.074}{1}$$

$$= 0.074m$$

3.6.2 Pressure drop, ΔP

According to Geldart [1984], the pressure drop across the fluidized bed is only parameter that can be accurately predicted. Consider the cylinder unrestrained at its upper surface occupied with CaO at certain static bed height, when the upward superficial fluid velocity is gradually increased, the pressure drop gradually increased. Then the pressure drop levels off and no longer increases as the superficial velocity is increased. This is when the upward force exerted by the fluid on the particles is sufficient to balance the net weight of the bed and the particles begin to separate from each other and float in the fluid. As the velocity is increased further, the bed continues to expand in height, but the pressure drop stays constant. It is possible to reach large superficial velocities without having the particles carried out with the fluid at the exit. This is because the settling velocities of the particles are typically much larger than the largest superficial velocities used. Figure 3.3 shows this phenomenon.

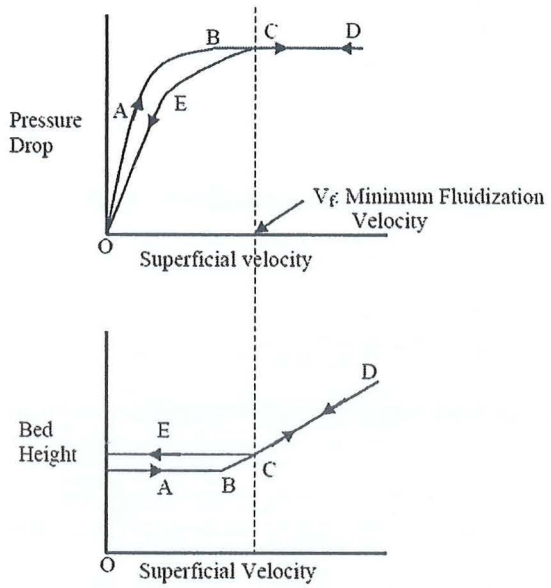

Figure 3.3: Relation between pressure drop, bed height and superficial velocity, Geldart [1984]

The pressure drop across the fluidized bed can be determined using equation (3.12).

$$\Delta P = \frac{m_s(g)}{A} \tag{3.12}$$

$$= \frac{0.526(9.81)}{\frac{\pi(0.074)^2}{4}}$$

$$= 1199.78Pa$$

Where,

m_s : Mass of CaO-Sand particle 100 micron, (kg)

A : Cross sectional area of CO^2 absorption reactor (m^2)

g : Gravitational acceleration (m per s^2)

3.6.3 Minimum Fluidization Velocity, u_{mf}

The minimum fluidization velocity, u_{mf} is important to know because it is used as a basic to determine the fluidized bed gasifier. If the velocity is too small the bed stays fixed and operates as a packed bed. The solid particles in the cylinder will begin to fluidize when minimum fluidization is achieved [Botterill, 1975]. To determine the minimum fluidization velocity, u_{mf} the equation (3.13) as rewritten from the modified Ergun Equation can be used.

$$u_{mf} = \frac{\mu_g}{\rho_g d_s}\left[\left(33.7^2 + 0.0408 Ar_{numb}\right)^{\frac{1}{2}} - 33.7\right] \tag{3.13}$$

Where,

μ_g : Dynamic viscosity of the carrier gas (kg per m.s)

ρ_g : Density of the carrier gas (kg per m^3)

d_s : Solid particles size (m)

Ar_{numb} : Archimedes number

Archimedes number is a dimensionless number in which to determine the motion of fluids due to density differences. It is represented as

$$Ar_{numb} = \frac{\rho_g d_s^{\,3} g(\rho_s - \rho_g)}{\mu_g^{\,2}} \tag{3.14}$$

Where,

g : Gravitational acceleration (m per s^2)

ρ_s : Density of solid particle (kg per m^3)

Table 3.3 shows the design parameters of CO_2 absorption reactor. These parameters have been used to determine the minimum fluidization velocity.

Table 3.3: Design parameters of CO_2 absorption reactor

CO_2 absorption reactor dimensions	
Geometrical shape	Cylindrical
Height, h (m)	0.6
Inner diameter, d_i (m)	0.074
Cross section area, A (m^2)	4.301×10^{-3}
Bed material properties	
Type	Calcium oxide, CaO and Sand
Bulk Density, $\rho_{CaO\text{-}sand}$ (kg per m^3)	5649
Particle size d_s (um)	100
Fluidizing gas properties	
Type	Air
Temperature, T (°C)	35
Density, ρ_g (kg per m^3)	1.145
Dynamic Viscosity, μ (kg per m.s)	1.895×10^{-5}

Refer back to equations (3.14) and (3.13), the archimedes number and the minimum fluidization velocity are,

$$Ar_{numb} = \frac{1.145(0.0001)^3(9.81)(3340-1.145)}{(1.895x10^{-5})^2}$$

$$= 176.44$$

Then $$u_{mf} = \frac{1.895x10^{-5}}{1.145(0.0001)}\left[(33.7^2 + 0.0408(176.44))^{\frac{1}{2}} - 33.7\right]$$

$$= 0.0176\frac{m}{s}$$

3.6.4 Terminal Velocity, u_t

When superficial velocity operated above the terminal velocity of the bed particles, the fast fluidization will occurred and lift a single particle and then carry it out of the reactor. Therefore in bubbling fluidized bed, the superficial velocity must be controlled in between the minimum fluidizing velocity, u_{mf} and terminal velocity, u_t.

Kunni and Levenspiel [1991] have wrote the estimation of the terminal velocity can be calculated by evaluating the dimensionless particle size, d_s^* and dimensionless terminal velocity, u_t^*. These two dimensionless equations were presented in equation (3.15) and (3.16) respectively.

$$d_s^* = d_s\left[\frac{\rho_g(\rho_s - \rho_g)g}{\mu^2}\right] \qquad (3.15)$$

$$= [Ar_{numb}]^{\frac{1}{3}}$$

$$u_t^* = \left[\frac{18}{(d_s^*)^2} + \frac{2.335 - 1.744\phi_s}{(d_s^*)^{\frac{1}{2}}}\right]^{-1}, \quad 0.5 < \phi_s < 1 \qquad (3.16)$$

Where,

μ : Dynamic viscosity of the carrier gas (kg per m.s)

ρ_g : Density of the carrier gas (kg per m^3)

d_s : Solid particles size (m)

Ar_{numb} : Archimedes number

ρ_s : Density of the solid particle (kg per m^3)

g : Gravitational acceleration (m per s^2)

ϕ_s : sphericity of solid particle = 0.78 for CaO particles

Refer back to equations (3.15) and (3.16), the dimensionless particle sizes, d_s^* and dimensionless terminal velocity, u_t^* are,

$$d_s^* = [Ar_{numb}]^{\frac{1}{3}}$$

$$= [104.44]^{\frac{1}{3}}$$

$$= 5.68$$

$$u_t^* = \left[\frac{18}{(5.68)^2} + \frac{2.335 - 1.744(0.78)}{(5.68)^{\frac{1}{2}}}\right]^{-1}$$

$$= 0.43$$

Finally the terminal velocity can be determined using equation (3.17).

$$u_t = u_t^* \left[\frac{\mu(\rho_s - \rho_g)g}{\rho_g^2} \right]^{\frac{1}{3}} \qquad (3.17)$$

$$= 0.43 \left[\frac{1.895x10^{-5}(5649 - 1.145)9.81}{1.145^2} \right]^{\frac{1}{3}}$$

$$= 0.4 \frac{m}{s}$$

3.6.5 Volume Flow Rate, Q

The volume flow rate of minimum fluidizing velocity and terminal velocity were determined. The operation range in between these two volume flow rate are considered as bubbling fluidization regime. The volume flow rate is calculated by solving equation (3.18) and (3.19) for the minimum fluidizing velocity and terminal velocity, respectively.

$$Q_{u_{mf}} = Au_{mf} \qquad (3.18)$$

$$= \frac{\pi(0.074)^2}{4}(0.0104)$$

$$= 4.473x10^{-5} \frac{m^3}{s} \text{ @ 2.68 L per min}$$

$$Q_{u_t} = Au_t \qquad (3.19)$$

$$= \frac{\pi(0.074)^2}{4}(0.62)$$

$$= 2.666x10^{-3} \frac{m^3}{s} \text{ @ 160 L per min}$$

The estimate operation parameters for the CO_2 absorption reactor of the carbonation process with air, simulate gas and producer gas are performed on various temperature ranges. These parameters are listed in the Table 3.5, 3.6 and 3.7 respectively.

In Table 3.4 shown also the estimate operation parameters of the CO_2 absorption reactor but on the process of calcination. Air is only used as the fluidizing gas for the calcination process due to small percentage of CO_2 gas. The estimate operation parameters are performed on various temperature ranges of 700°C, 750°C, 800°C and 850°C.

Table 3.4: Estimate operation parameters of CO_2 absorption reactor for calcination process using air ($CaCO_3 \rightarrow CaO+CO_2$)

Paramaters	Values			
Temperature (°C)	700	750	800	850
Density, ρ_g (kg per m^3)	0.362	0.345	0.328	0.314
Dynamic Viscosity, μ (kg per m.s)	4.111e^{-5}	4.236e^{-5}	4.362e^{-5}	4.481e^{-5}
Archimedes number, Ar_{numb}	5.68	5.10	4.58	4.15
minimum fluidizing velocity, u_{mf} (m per s)	0.0039	0.0038	0.0037	0.0036
terminal velocity, u_t (m per s)	0.32	0.31	0.30	0.29

volume flow rate of minimum fluidizing velocity, $Q_{u_{mf}}$ (m^3 per s) / L per min	$1.677e^{-5}$ / 1.0	$1.634e^{-5}$ / 0.98	$1.591e^{-5}$ / 0.95	$1.548e^{-5}$ / 0.93
volume flow rate of terminal velocity, Q_{u_t} (m^3 per s) / L per min	$1.376e^{-3}$ / 82.56	$1.333e^{-3}$ / 79.98	$1.290e^{-3}$ / 77.40	$1.247e^{-3}$ / 74.82

Table 3.5: Estimate operation parameters of CO_2 absorption reactor for carbonation process using air ($CaO+CO_2 \longrightarrow CaCO_3$)

Paramaters	Values
Temperature (°C)	35
Density, ρ_g (kg per m^3)	1.145
Dynamic Viscosity, μ (kg per m.s)	$1.895e^{-5}$
Archimedes number, Ar_{numb}	104.44
minimum fluidizing velocity, u_{mf} (m per s)	0.0104
terminal velocity, u_t (m per s)	0.62
volume flow rate of minimum fluidizing velocity, $Q_{u_{mf}}$ (m^3 per s) / L per min	$4.473e^{-5}$ / 2.68
volume flow rate of terminal velocity, Q_{u_t} (m^3 per s) / L per min	$2.666e^{-3}$ / 160

Table 3.6: Estimate operation parameters of CO_2 absorption reactor for carbonation process using simulate gas ($CaO+CO_2 \longrightarrow CaCO_3$)

Paramaters	Values			
Temperature (°C)	500	550	600	650
Density, ρ_g (kg per m^3)	0.492	0.473	0.453	0.434
Dynamic Viscosity, μ (kg per m.s)	$3.444e^{-5}$	$3.565e^{-5}$	$3.686e^{-5}$	$3.807e^{-5}$
Archimedes number, Ar_{numb}	13.59	12.19	10.92	9.81
minimum fluidizing velocity, u_{mf} (m per s)	0.0057	0.0055	0.0053	0.0052
terminal velocity, u_t (m per s)	0.44	0.43	0.42	0.41
volume flow rate of minimum fluidizing velocity, $Q_{u_{mf}}$ (m^3 per s) / L per min	$2.451e^{-5}$ / 1.47	$2.365e^{-5}$ / 1.42	$2.280e^{-5}$ / 1.37	$2.236e^{-5}$ / 1.34
volume flow rate of terminal velocity, Q_{u_t} (m^3 per s) / L per min	$1.892e^{-3}$ / 113.00	$1.850e^{-3}$ / 110.96	$1.806e^{-3}$ / 108.40	$1.764e^{-3}$ / 105.80

Table 3.7: Estimate operation parameters of CO_2 absorption reactor for carbonation process using producer gas ($CaO+CO_2 \longrightarrow CaCO_3$)

Paramaters	Values			
Temperature (°C)	500	550	600	650
Density, ρ_g (kg per m^3)	0.435	0.418	0.401	0.384
Dynamic Viscosity, μ (kg per m.s)	$3.187e^{-5}$	$3.302e^{-5}$	$3.418e^{-5}$	$3.533e^{-5}$
Archimedes number, Ar_{numb}	14.03	12.56	11.25	10.08
minimum fluidizing velocity, u_{mf} (m per s)	0.0062	0.0060	0.0058	0.0056
terminal velocity, u_t (m per s)	0.47	0.46	0.45	0.44

volume flow rate of minimum fluidizing velocity, $Q_{u_{mf}}$ (m^3 per s) / L per min	$2.666e^{-5}$ / 1.60	$2.580e^{-5}$ / 1.55	$2.490e^{-5}$ / 1.49	$2.410e^{-5}$ / 1.44
volume flow rate of terminal velocity, Q_{u_t} (m^3 per s) / L per min	$2.040e^{-3}$ / 122.50	$1.990e^{-3}$ / 119.30	$1.938e^{-3}$ / 116.30	$1.892e^{-3}$ / 113.50

CHAPTER 4: METHODOLOGY

4.0 INTRODUCTION

In this chapter, the experimental setup and procedure of the experimental works were shown. The block of furniture woods from the factory nearby were selected as a primary feedstock for producing the producer gas in downdraft gasifier. To enhance the quality of the producer gas, the calcium oxide powders (range 100 -1000 micron) was selected as a sorbent to absorb the carbon dioxide gas in the producer gas.

The CO_2 absorption reactor experimental study is carried out at the biomass energy lab, Universiti Sains Malaysia, Transkrian Pulau Pinang. The experiments are designed to examine the absorption process of CO_2 in the reactor and the performance of diesel engine. Three main experiments have been identified to achieve the objectives of the research. Figure 4.1 shows the types of the experimental work.

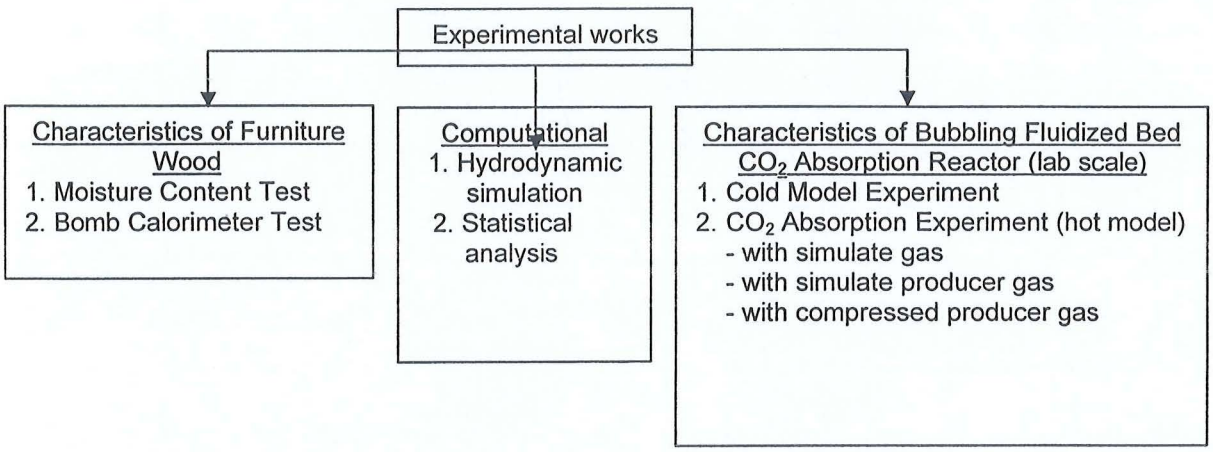

Figure 4.1: Types of the experimental work.

4.1 CHARACTERISTICS OF FURNITURE WOOD

The characteristics of furniture wood have a significant effect to the performance of gasifier system. The calorific value of the producer gas produced from downdraft gasifier is depended from the furniture wood characteristics. At present study, two tests are selected for characterize the furniture wood such as moisture content test and bomb calorimeter test. Figure 4.2 shows the flow process to characterize the furniture wood.

4.1.1 Moisture Content Test

The Infrared Moisture Balance Machine as shown in Plat 4.1 is used to determine the percentage of moisture content in furniture wood. The test was operated at Heat Transfer Laboratory, School of Mechanical Engineering. The moisture content is a weight of moisture contained in a piece of wood as a percentage of its oven dry weight.

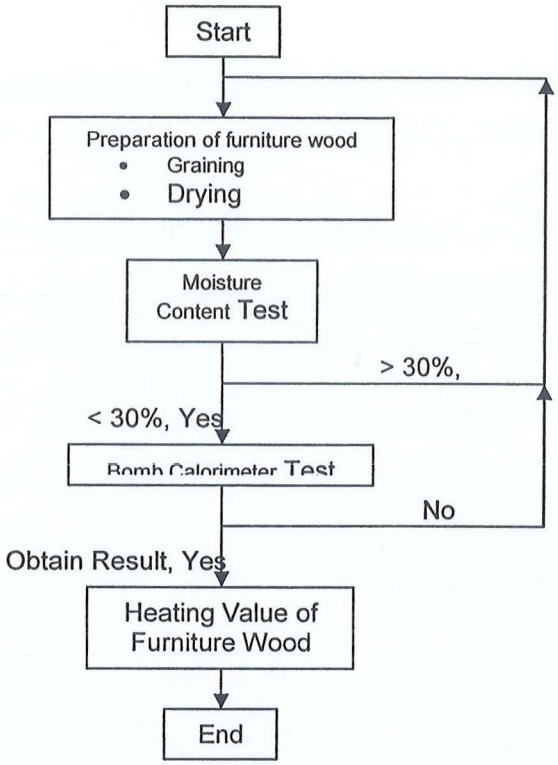

Figure 4.2: The flow process to characterize the furniture wood

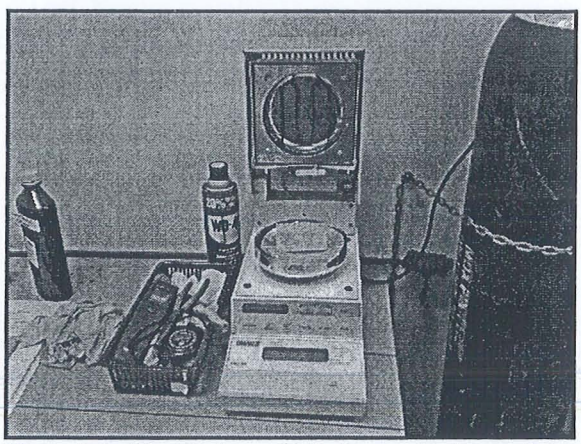

Plate 4.1: The Infrared Moisture Balance Machine

A small block of wood 7.6 (L) x 3.3 (H) x 3.2 (W) cm dimension size has been cut, weighted and recorded. The wood then has been placed on the plate of the Infrared Moisture Balance Machine. The temperature was set started from 120°C for 180 minutes.

The button has been pushed after the cover of Infrared Moisture Balance Machine closed. Three parameters such as percentage of moisture content, percentage of solid weight and current weight in gram have been recorded for every 5 minutes until reached the constant wood weight.

4.1.2 Bomb Calorimeter Test

Bomb Calorimeter as show in the Plate 4.2 was used to determine the heating value of the furniture wood. The test was done at Heat Transfer Laboratory, School of Mechanical Engineering. The block of furniture wood was crushed to be woodchips. A sample of 1 gram of woodchips was wrapped and tied by nickel wired before placing it in the crucible. The crucible was placed in the bomb filled with the oxygen and immersed in water. The Beckman's thermometer was placed into inner cylinder and outer tank. Then, the water temperature of the outer tank was controlled to obtain approximate water temperature of inner cylinder within the range of 0.1°C. The initial temperature was recorded every minute until ignition was started after 5 minutes. The calorimeter water in the inner cylinder was changed because of the ignition. Then the changes were recorded every thirty second until its reached maximum temperature. The test was done almost 15 minutes.

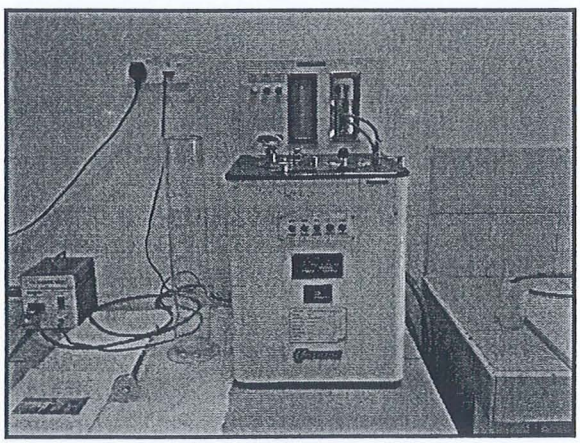

Plate 4.2: Bomb Calorimeter

4.2 CFD SIMULATION

The present study is to know the hydrodynamic characteristics of the Calcium oxide-sand mixture using software called Fluent version 6.2.16. The 2-D model of the bubbling fluidized bed CO_2 absorption reactor (BFBR) was generated in Gambit version 2.3.16 pre-processor. A multiphase flow consist of a gas-solid phases flow is used inside the bubbling fluidized bed CO_2 absorption reactor model. A structured face mesh of quadrilateral is used to generate grid due to less complexity and time required to grid over such geometry when imported to Fluent. The gas enters into the BFRB from bottom side. Figure 4.3 shows the 2-D model.

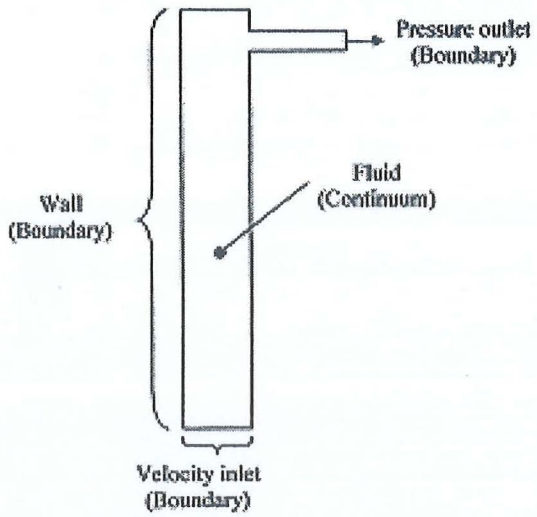

Figure 4.3: 2-D model of the bubbling fluidized bed CO_2 absorption reactor

The 2-D model was export to Fluent in ".msh" file type after meshing and zone specifying completed. The Eulerian multiphase model was used to model multiphase flow. This model allows the multiple separate and interacting phases. The material properties for the bed material (calcium oxide and sand) were set to a density of 3340 kg/m^3 and to a particle size of 100 micron. It was set as a phase 2 or secondary phase. Phase 1 or primary phase is air, having the density of 1.16 kg/m^3, a specific heat of 0.994 kJ/kg.K and a viscosity of 1.7894×10^{-5} kg/ms. The air distribution plate was modeled as a uniform surface velocity inlet. The inter-particle forces were able to be modeled by enabling the interaction forces. Then the boundary conditions are set up closed to the experiment condition needed.

The contours of the volume fraction of the bed material were monitored with respect to the flow time. The change in the volume fraction with flow time was checked to know the bed material motion. To reconfirm the air and calcium oxide–sand mixture motion, the velocity vectors were also plotted. Instead of volume fraction, the bed expansion height was also monitored. Three different of particle sizes, 100, 500 and 1000 micron were tested at various volume flow rate. Figure 4.4 shows the flow process of the simulation.

4.2 STATISTICAL ANALYSIS

Statistical analysis using a cold model experiments were conducted to analyze the data. Calcium oxide 100 microns in size was used and it was performed 8 times in a row to determine the error analysis. The commercial software "SPSS Statistics version 17 for windows" was used to perform the analysis. The statistical tools used in this study was descriptive analysis.

The descriptive analysis is used to explore the data and then described the observations. In case of observations, the frequency distribution can be performed in tabular form or graphical form. According to Sheridan and Lyndall (2003), the bar charts are appropriate for the categorical variables. In this study the frequency distribution was the display of the occurrence of the items. The demographic data of the fluidization bed height was

collected and analyzed using description analysis. Then the frequencies and the data of the information were gathered.

4.3 INSTRUMENT AND MEASUREMENT

In this section, the description of the instruments and measurements used were introduced. The instruments used in the experiment are described below:

4.3.1 Ceramic band heater and controller

The ceramic band heater and controller are used to control and transmit heat energy through both conduction and radiation mechanisms to the bubbling fluidized bed CO_2 absorption reactor. The maximum working temperature of the ceramic band heater is 1200 deg Celsius. It is constructed with a stainless steel shroud enclosing high quality ceramic knuckles through which run coiled high temperature nickel-chromium element wire. Plate 4.3 shows the the ceramic band heater and it controller.

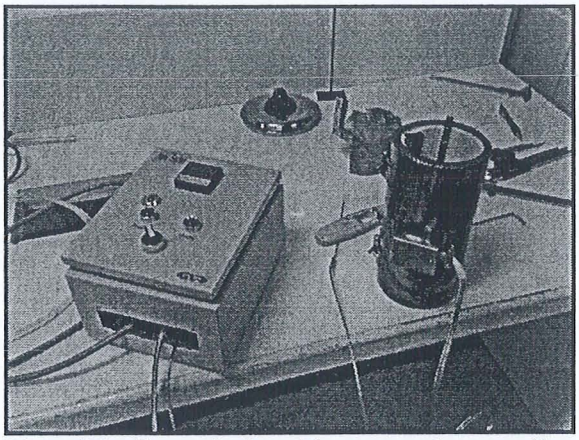

Plate 4.3: Ceramic band heater and controller

The electrical cable from controller is connected to the screw terminal of ceramic band heater. The ceramic heater was clamped tight to the CO_2 absorption reactor to transmit heat energy. Plate 4.4 shows the heat energy produced inside the ceramic band heater.

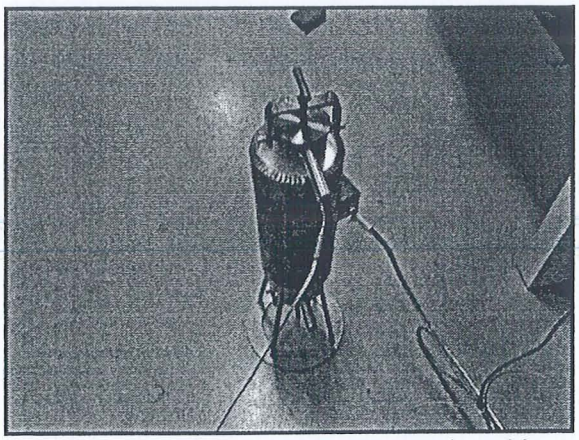

Plate 4.3: Ceramic band heater produced heat energy

4.3.2 Data acquisition

The data acquisition is capable of logging the temperature for every 4 second during the tests using thermocouple type-K. The data acquisition used was DIGI-SENSE scanning Thermometer with 12 channel thermocouple scanner Model 69202-30. Plat 4.4 shows the data acquisition.

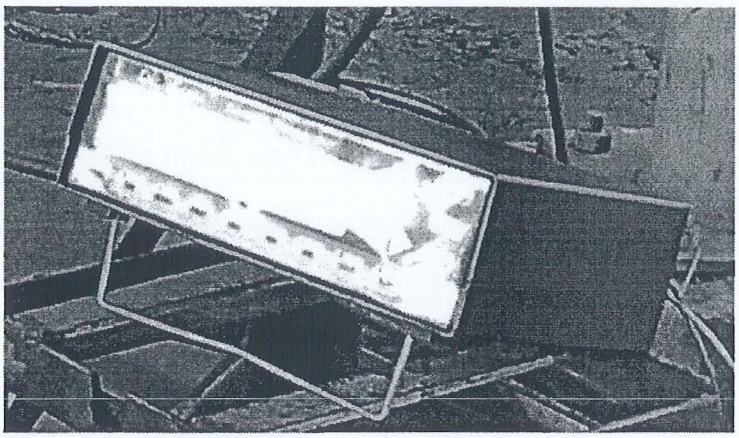

Plate 4.4: DIGI-SENSE scanning Thermometer

4.3.3 Gas Chromatograph

The producer gas composition was analyzed using a Gas Chromatograph Hewlett Packard Module 4890. It consists an injector port, a separation part contain of column, detector and recorder. Plate 4.5 shows the gas chromatograph.

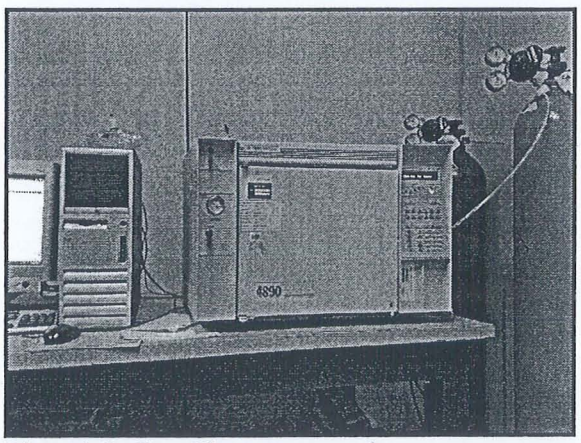

Plate 4.5: Gas Chromatograph

In the analysis, helium gas was used as a carrier gas. Propack-Q and molecular sieve, where the 2 columns were used to identify the gases. The Propack-Q column is used to detect CO_2 and the molecular sieve column is used to detect H_2, CO, CH_4, O_2 and N_2 using thermal conductivity detector (TCD).

4.3.4 Gas Analyzer

The gas analyzer was used to determine the emission of diesel engine fuelled with the producer gas. It measured CO (%), CO_2 (%), NO_x (ppm) and O_2 (%). Plate 4.6 shows the gas analyzer drager MSI compact.

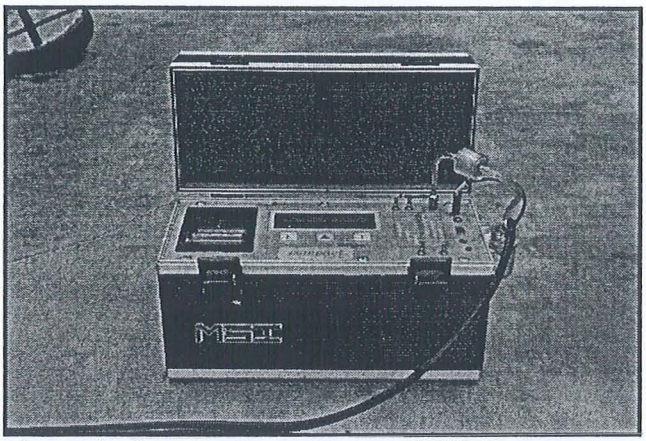

Plate 4.5: Gas Analyzer (Drager MSI Compact)

4.4 CHARACTERISTICS OF BUBBLING FLUIDIZED BED CO_2 ABSORPTION REACTOR

4.4.1 Cold Model Experiment

A cold model experiment is conducted to gain the hydrodynamic study of a bubbling fluidized bed CO2 absorption reactor (BFBR) with pressurized air at ambient temperature. Plate 4.6 shows photograph of cold model experiment apparatus. The BFBR is made of transparent perspex with an inner diameter of 74 and 600 mm height. The distributor plate has five nozzles each having four holes of 1.6 mm diameter. Detail of the schematic diagram of bubbling fluidized bed CO_2 absorption reactor (BFBR) is shows in Figure 4.5.

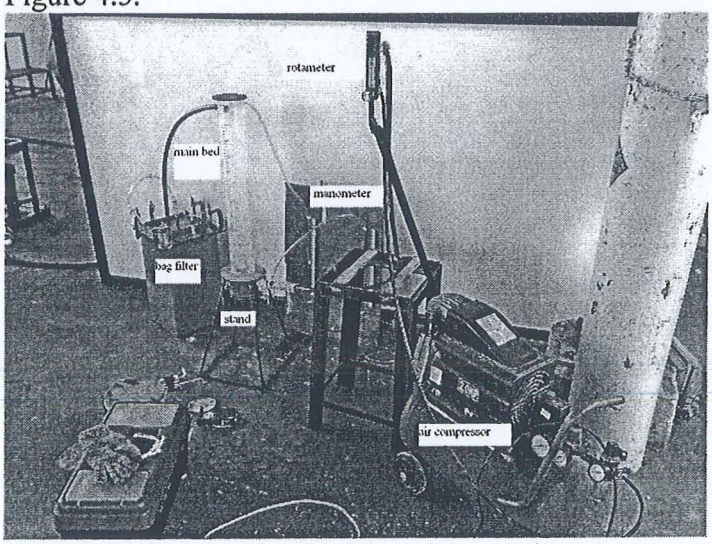

Plate 4.6: Photograph of cold model experiment apparatus

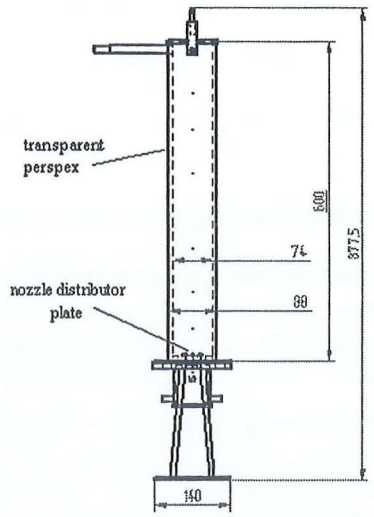

Figure 4.5: Detail of the schematic diagram of BFBR

The BFBR is connected to a 1.9 kW air compressor model HD47C to provide compressed air at various pressures and a filter bag to capture any of the bed material entrained from the bubbling fluidized bed CO2 absorption reactor. A simple U-tube manometer is connected across the bubbling fluidized bed CO2 absorption reactor to monitor the pressure drop. Figure 4.6 shows the schematic diagram of cold model experimental set-up.

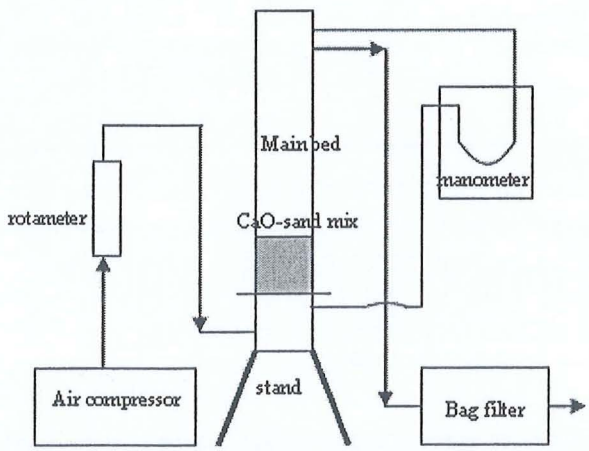

Figure 4.6: Schematic diagram of cold model experiment set-up.

The CaO mixed with sand was used as the bed material in the BFBR. Variables affecting the fluidization height were studied such as CaO-sand mixture percentages (70, 60, 50, 40% CaO), air volume flow rates (5, 15, 25, 35, 45, 55 $Lmin^{-1}$), air intake pressures (2, 3, 4, 5, 6 bar) and different CaO particles sizes (100, 500 and 1000 micron). For each run, 4 cm arbitrary chosen constant height of the CaO was measured (Table 4.1) and mixed with 1.7, 2.7, 4 and 6 cm of sand where the particle size used were 100, 500 and 350 micron.

Table 4.1: CaO weight for 4 cm height

CaO particle size (micron)	CaO weight (g)
100	172.30
500	198.65
1000	240.00

The air flow from the air compressor was set to the desired pressure and volume flow rate by using manometer. During the experiment, the hydrodynamic behaviors such as the bed expansion height and the pressure drop across the bubbling fluidized bed CO_2 absorption reactor were recorded. Fine particles found in the filter bag was weighed and recorded at the end of each experiment run. All the data recorded and analyzed are shows in Chapter 5.

4.4.2 Carbonation Hot Model Experiment

As mention in the chapter 2, the carbonation or sequestration process is a reaction process of calcium oxide, CaO with carbon dioxide, CO_2 to produce final product called calcium carbonate, $CaCO_3$ at certain temperature. To determine the exactly temperature perform the carbonation process of CaO, the carbonation hot model experiment has been conducted. The bubbling fluidized bed CO_2 absorption reactor (BFBR) made from stainless steel 304 has been coupled to a 3 kW electrical ceramic heater band to heat the CaO-sand mixture. One connection been connected to the simulated gas tank consisting of 30% CO_2 and 70% N_2 and other side of BFBR is connected to the filter bag. Five set of temperature range have been selected as variables (500-549, 550-599, 600-649, 650-699, 700-749 deg C). A 40% CaO-sand mixture ratio (density ???) is poured inside the BFBR, at the same time the heater band is switch on and set to the 500-549 deg C. When the temperature has reached to the selected range, the simulated gas regulator valve is opened and set to 3 bar. Using the rotameter, the gas volume flow rate is set to 15 $Lmin^{-1}$.

4.4.3 CO_2 Absorption Experiment (Hot model)

To know the ability of CO_2 absorption of CaO-sand mixture in the bubbling fluidized bed CO_2 absorption reactor, the CO_2 absorption experiment or hot model experiment has been conducted. A number of the experiments using three types of gas with different composition have been done by flow in to the bubbling fluidized bed CO_2 absorption reactor. The operational procedures using these gases have been described below:

4.4.3.1 Simulated gas

The hot model experiment with simulated gas consisting of 20% CO_2 and 80% N_2 has been applied to the bubbling fluidized bed CO_2 absorption reactor (BFBR) at selected temperatures. In this hot model experiment, the BFBR is made from stainless steel 304. The same distributor plate was used to allow the simulated gas to flow. Plate 4.7 shows a photograph of the hot model apparatus and Figure 4.7 described the schematic diagram of the hot model experimental setup respectively.

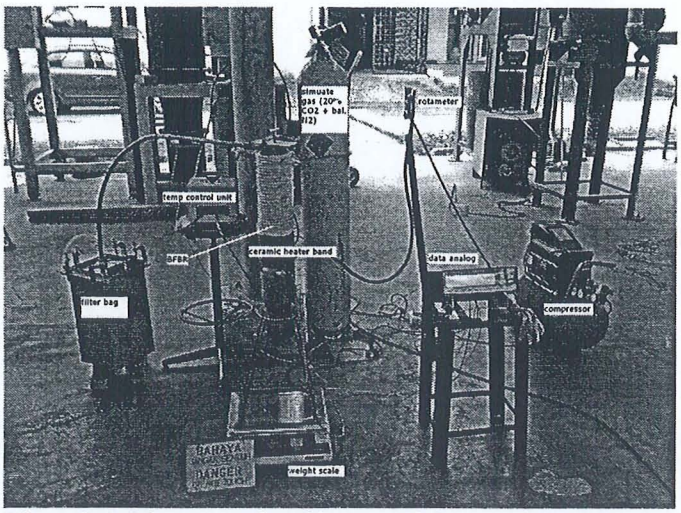

Plate 4.7: Photograph of hot model experiment apparatus with simulated gas

A 3 kW electrical ceramic heater band was coupled to the bubbling fluidized bed CO_2 absorption reactor for heating the bed material (CaO-sand mixture) at various temperatures. The selected variables were obtained from the cold model experiment after analyzed (refer to chapter 5) such as CaO-sand mixture percentages (50 and 40% CaO), volume flow rates (15, 25 and 45 $Lmin^{-1}$), intake pressures (2, 3 and 4 bar) and the CaO particle size of 1000 micron. For each run, 4 cm constant height of the 1000 micron CaO was used and mixed with 4 and 6 cm of the 350 micron sand. These particles sizes were sieved using an Endecott's multi-layer test sieve shaker.

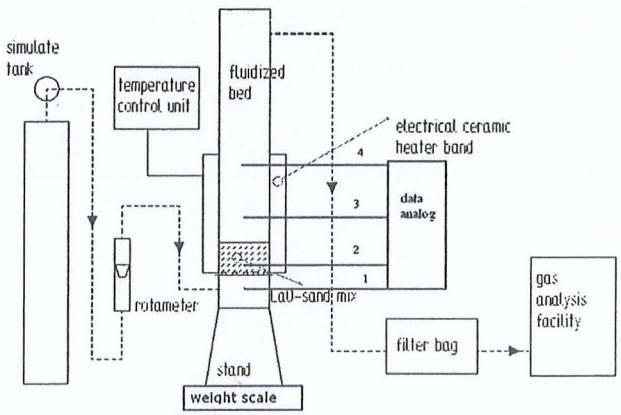

Figure 4.7: Schematic diagram of hot model experiment set-up.
1-4 refer to thermocouples used

The controller of the ceramic heater band was set to 900°C. When the temperature inside the fluidized bed reached 650-750°C, the simulated gas was set to 2 bar using a pressure regulator with a gas flow rate of 15 $Lmin^{-1}$ controlled by a rotameter. The simulated gas at the exit of the fluidized bed was collected by gas sampling bags at an interval of 5 minutes for 60 minute experiment. The gas samples were analyzed in a gas chromatograph (Hewlett Packard Module 4890) as soon as possible to avoid any diffusion of gases into or out the sampling bags. This process was repeated for the other

variables. Some of the fine particles found in the filter bag was weighed and recorded at the end of each experiment. At the end of the CO_2 absorption experiment, the CO_2 is released from the $CaCO_3$ via calcination process at temperature above 850°C for about 90 min.

4.4.3.2 Simulated producer gas

The simulated producer gas was obtained from the MOX manufacture nearby. It was consisting of 16% CO_2, 24% CO, 12% H_2 and 48% N_2 gas composition. Using the best variables obtained from hot model experiment with simulated gas, the experiment was started again. A 3 kW electrical ceramic heater band was heated to heat the CaO-sand mixture in the bubbling fluidized bed CO_2 absorption reactor (BFBR). When the temperature inside the BFBR reached 650-750°C, the simulated producer gas was set to craving bar and gas flow rate using a pressure regulator and a rotameter. The simulated producer gas passed through the BFBR and the exit of new simulated producer gas was collected in the sampling bag. The gas was collected at an interval of 10 minutes for 60 minute experiment. Then using the gas chromatograph, the collected simulated producer gas was recorded and analyzed. All the data results and analysis were presented in the Chapter 5.

4.4.3.3 Compressed producer gas

In this section, the compressed producer gas was used by flow in to the bubbling fluidized bed CO_2 absorption reactor (BFBR) of the hot model experiment. To gain the compressor producer gas, the preparation must be done. A 50 kg of block wood (size: 0.076 (L) x 0.033 (H) x 0.032 (W) m) was prepared and feed to the downdraft gasifier. The thermocouples were placed at certain places and connected on the data logger. The block wood in the download gasifier was burn using the LPG gas burner until it can combust it self. While waiting the block wood to combust and resulted with producer gas, the CaO-sand mixture was prepared. An optimum values of parameters obtained from the hot model experiment with simulate producer gas were used. Using 3 kW electric ceramic heater band, the bubbling fluidized bed CO_2 absorption reactor (BFBR) was heated until the temperature inside the BFBR reached 650-750°C. When the blue flare at point 3 was obtained (Figure 4.8), the gas collecting process was conducted using sampling bags at point SP 2. The compressed producer gas was analyzed using Gas Chromatograph and recorded.

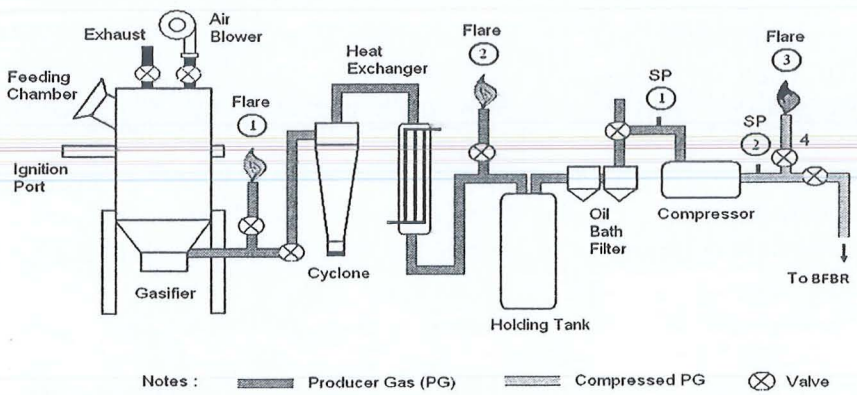

Figure 4.8: Compressed producer gas experiment set-up

After collected gas sample at SP 2, then the compressed producer gas is passed to the BFBR controlled by the rotameter. The rotameter was set to 45 $Lmin^{-1}$ (0.00075 m^3s^{-1}). The outlet compress producer gas was passed to the filter bags and cooling system before been collected by sampling bags. The gas collecting process was conducted for an interval of 15 minutes in 60 minutes experiment. Then compressed producer gas before and after passed through the BFBR was analyzed and recorded. The fine particles found in the filter bag was weighed and recorded. These data results and analysis were presented in the Chapter 5. Figure 4.9 shows the schematic diagram BFBR set-up using compressed producer gas.

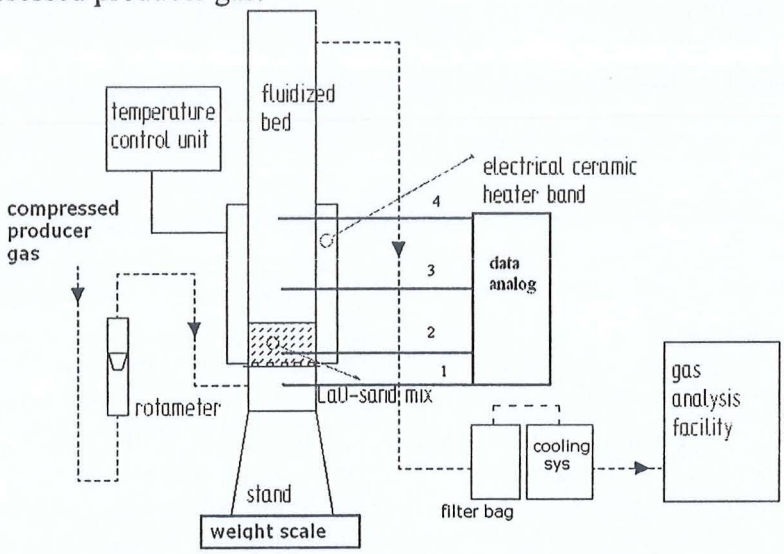

Figure 4.9: BFBR set-up using compressed producer gas

CHAPTER 5: RESULTS AND DISCUSSIONS

5.0 INTRODUCTION

The results obtained from the experimental have been analyzed and shown in this chapter. All experimental and simulation done is presented as follow:

Moisture Content Test
Bomb Calorimeter Test
Fluent Simulation
Statistical Analysis
Cold Model Experiment
CO_2 Absorption Experiment with Simulate Gas
CO_2 Absorption Experiment with Simulate Producer Gas
CO_2 Absorption Experiment with Compressed Producer Gas

5.1 CHARACTERISTICS OF FURNITURE WOOD

5.1.1 Moisture Content Test

A small block of wood 0.076 (L) x 0.033 (H) x 0.032 (W) m dimension size has been cut.

As seen in Figure 5.1 after 135 min, the mass of wood became constant. The percentage of moisture content obtained was 11.1%. This value is below than 30% wood moisture content and it suitable to be used for the next stage. The moisture content will affect the performance of the gasifier because of the ignition difficult and reduced the calorific value of the producer gas. This has been mentioned in section 2.2.2. Some researchers implement a pre-treatment process to reduce the moisture of the wood and give the maximum operating condition. The acceptable maximum amount of moisture content of wood for gasification process is in the range of 30% to 60% and it depends on types of the gasifier design.

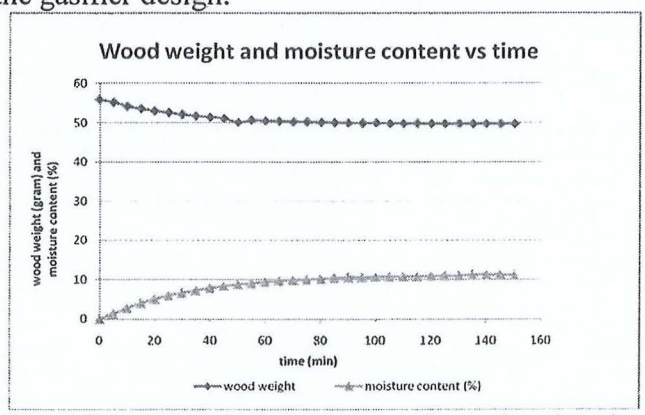

Figure 5.1: A graph shows mass of wood and moisture content versus time

5.1.2 Bomb Calorimeter Test

Using the HHV wood on dry basis given by Zainal, 1996 (Equation 5.2), the low heating value (LHV) of wood can be determined as:

$$HHV_{wood(dry\ basis)} = LHV + W\lambda \qquad (5.2)$$

$$LHV_{wood} = HHV_{wood(dry\ basis)} - W\lambda$$

$= 17.35 - 0.111\ (2.260)$
$= 17.1$ MJ/kg

where the latent heat of vaporization, λ is 2.260 MJ/kg. The result obtained was in the range of various types of wood between 15.3 MJ/kg to 21.2 MJ/kg stated by Negi and Todaria, 1993. The low heating value is used rather than the high heating value (producer gas is in the gaseous form) in the calculation for gasification.

5.2 FLUENT SIMULATION

The Fluent simulation is done to know the hydrodynamic expansion of the static bed material. In addition, comparable between the simulations and experiments are also performed. The fluidization dynamics modeled in isothermal conditions from Fluent are presented. The simulation is conducted for particle sizes 100, 500 and 1000 Calcium Oxide. The bulk densities of the 50% CaO-sand mixture are 5649, 7056 and 6695 kgm^{-3} for 100, 500 and 1000 CaO respectively. Using the variables that have been determined, the bubble, bed material volume fraction and the expansion height were able to be determined.

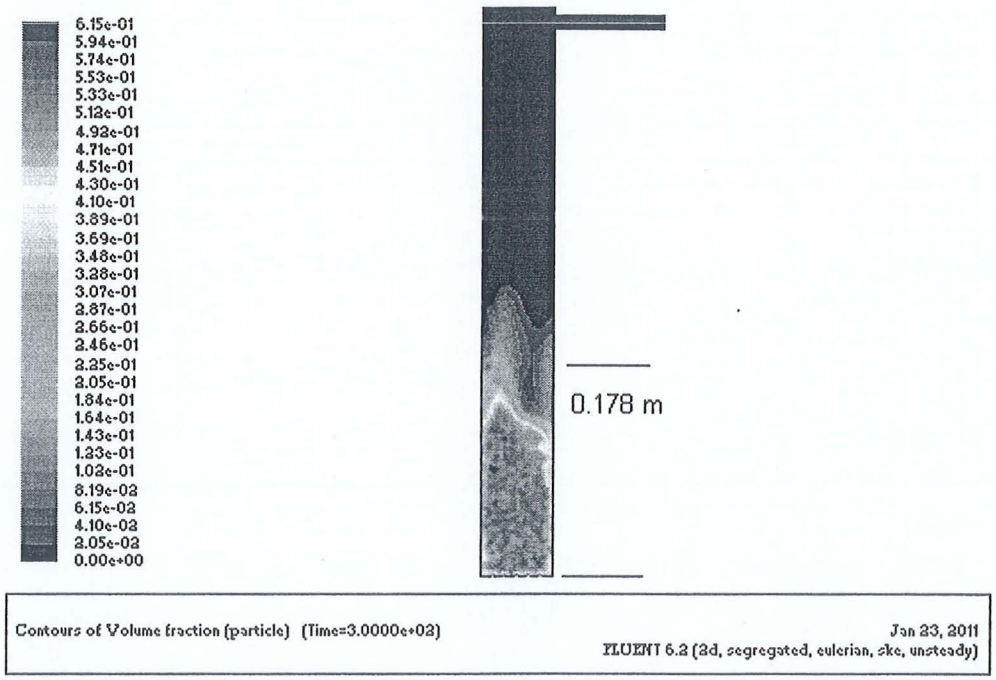

Figures 5.17: Contour of volume fraction of CaO-sand mixture in BFBR (1000 micron, 0.00092 m^3s^{-1})

From the observation, the used of large particle density and size of the solid material will caused the inter–particle forces or the cohesive forces to be lower and this will allowed more bubble to be formed. On the other side, the used of the fine and small particles will have high inter-particle forces and it is resulted in difficult fluidization.

The comparison of bed expansion height of the fluidization achieved by fluent simulation versus the actual experiment data were listed in Table 5.3. The total relative errors in percentages for all particle sizes are below than 24%. Simulation model gave the acceptable resulted match to the experimental cases, although some point has a large

relative error. Therefore the Fluent is a powerful tool to investigate the behavior of fluidization. This has been mentioned by Vuthalurua et al. (2009) in Chapter 2.

Table 5.3: Comparison between simulation and experiment of bed expansion height (100, 500, 1000 CaO particle size, 50% CaO)

100 micron CaO		
expansion bed height x 10^{-2}(m)		
at selected volume flow rate		
experimental	simulation	relative error (%)
4.5	1.7	62.22
8.5	7.6	10.59
10.8	12.5	15.74
12.5	14.8	18.40
13.0	19.5	50.00
		23.15
500 micron CaO		
expansion bed height x 10^{-2}(m)		
at selected volume flow rate		
experimental	simulation	relative error (%)
7.3	6.11	16.30
9.9	7.53	23.94
11.8	12.00	0.14
14.0	14.23	1.64
15.0	18.90	26.00
		13.60
1000 micron CaO		
expansion bed height x 10^{-2}(m)		
at selected volume flow rate		
experimental	simulation	relative error (%)
2.0	2.70	35.00
5.0	5.94	18.8
7.0	7.60	8.6
8.0	9.40	17.5
9.0	10.30	14.4
		18.86

COLD MODEL EXPERIMENT

The cold model experiment raw data have been recorded and show in Appendix 5. The experiment has been run for 10 times according to the difference variables selected. Based on the raw data recorded, the bed expansion height of the material inside the bubbling fluidized bed CO_2 absorption reactor is determined and analyzed. The graphs of the bed expansion height focus on the effect of the CaO-sand mixture ratio, the CaO particle size, the air volume flow rate and air pressure are presented. Instead of that, the CaO mass flow rate is also determined and analyzed. Table 5.6 shows the CaO-sand mixture data recorded.

Table 5.6: CaO-sand mixture data

CaO-sand mixture (%)	Mass of CaO-sand mixture (kg)	Static bed height (m)	Bulk density of CaO-sand mixture (kgm^{-3})
70	0.3300	0.055	4377
60	0.4560	0.065	5114
50	0.5810	0.075	5649
40	0.7520	0.090	6094

100 CaO

CaO-sand mixture (%)	Mass of CaO-sand mixture (kg)	Static bed height (m)	Bulk density of CaO-sand mixture (kgm^{-3})
70	0.4115	0.055	5465
60	0.5662	0.065	6893
50	0.6762	0.070	7056
40	0.8719	0.085	7492

500 CaO

CaO-sand mixture (%)	Mass of CaO-sand mixture (kg)	Static bed height (m)	Bulk density of CaO-sand mixture (kgm^{-3})
70	0.4534	0.050	6625
60	0.5369	0.060	6537
50	0.6695	0.070	6987
40	0.8601	0.090	7411

1000 CaO

5.4.1 Effect of CaO-Sand Mixture Ratio

The graph of the bed expansion height versus constant superficial velocity at different CaO-sand mixture ratio is shown in Figures 5.19, 5.20 and 5.21. In the experiment, the constant variables 100, 500 and 1000 micron particle size and 3 bar air pressure were used. The selected constant variables have to be done because to determine and analyze the bed expansion height cause of the effect of the CaO-sand mixture ratio.

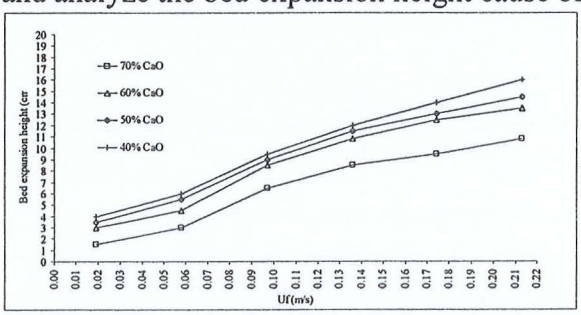

Figure 5.19: Effect of CaO-sand mixture ratio to the bed expansion height (100 micron)

As shown in Figure 5.19, the bed expansion height increased when used different ratio of CaO-sand mixture. The maximum bed expansion height was achieved for 40% CaO-sand mixture followed by 60, 50 and 70% CaO. The similar result is also can be observed for 500 and 1000 micron particle size as shown in Figures 5.20 and 5.21, respectively.

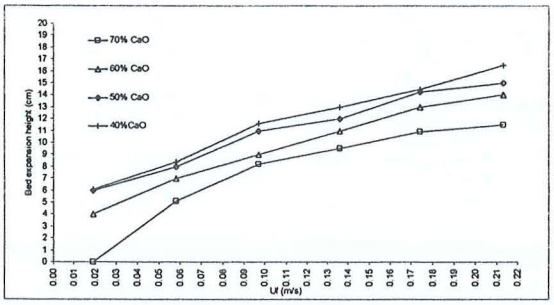

Figure 5.20: Effect of CaO-sand mixture ratio to the bed expansion height (500 micron)

The amount of CaO percentages in the mixture has an effect on the bed expansion height. With the decrease in CaO percentages from 70, 60, 50 to 40%, it was found that the bed expansion height increased between 0 to 17 cm for all constant superficial velocity. This is evidence of adhesive force between CaO particles such as the Van der Waals force, the electronic force and the liquid bridge that exists in the powder as defined by Hiroaki, 2006. The adhesive force between CaO particles was reduced with the increase of sand % in the mixture.

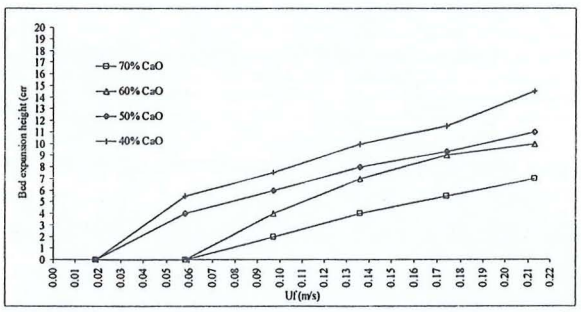

Figure 5.21: Effect of CaO-sand mixture ratio to the bed expansion height (1000 micron)

Although the fluidization of the bed expansion height was observed however at the early stages of the constant superficial velocity there was no fluidization happened at low superficial velocity of 0.02 ms^{-1} for all percentages of CaO mixture with 1000 micron particle size (Figure 5.21). The superficial velocity has not reach the minimum superficial velocity where the upward force exerted by the fluid on the particles is not sufficient to force the weight of CaO-sand mixture of the bed. Once increasing the sand % to 50% and 40% CaO-sand mixture, the fluidization occurred at 0.06 ms^{-1}. The amount of sand at first was insufficient to overcome the adhesive forces of the CaO particles which prevented fluidization at early stages of the constant superficial velocity. The similar trends can be seen used 70% CaO-sand mixture ratio for 500 micron as shown in Figure 5.20.

5.4.2 Effect of CaO Particle Size

To investigate the effect of particle size on the bed expansion height, three particle sizes of 100, 500 and 1000 micron CaO were tested. Previous studies stated in Chapter 3, showed that the particle size in the range of 100-600 micron (Geldart Group B) with density of 1500-4000 kgm^{-3} has a better fluidization compared to the 30-100 micron (Geldart Group A) and above 600 micron (Geldart Group D). Relatively in this experiment, as seen in Figure 5.22 is a bar graph of the bed expansion height versus CaO

particle size between air pressure 2-6 bar. Its can be observed that the fluidization happened in every CaO particle size used. The bed expansion height increased between 11-14 cm used 100 and 500 CaO particles size, and only 8 -11 cm using 1000 micron.

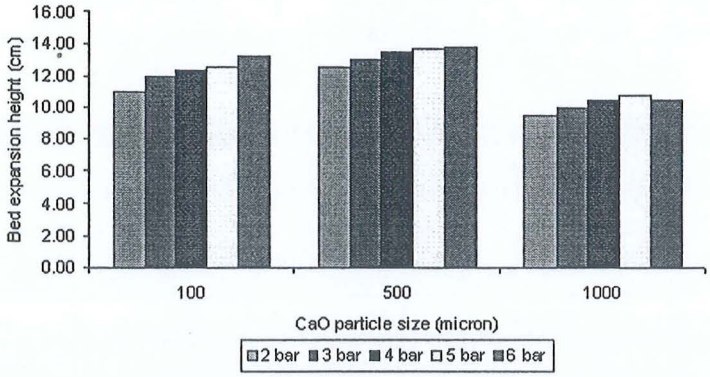

Figure 5.22: Effect of CaO particle size to the bed expansion height

The CaO particle size of 500 micron has better bed expansion height than 100 and 1000 micron. The 500 micron particle size has negligible inter-particle forces compared to 100 micron, which can fluidize well with vigorous bubbling actions. The 1000 micron particle size is large and dense, hence the inter-particle forces between particles are negligible, but the high density of the particle makes it difficult to fluidize and enormous amount of air is needed to overcome the size and weight.

5.4.3 Effect of Air Volume Flow Rate and Pressure

Air volume flow rate and pressure are important operating parameters in fluidized bed. The bed expansion height of CaO–sand mixture was tested at 5, 15, 25, 35, 45 and 55 $Lmin^{-1}$ flow rates with different air pressures to determine the hydrodynamic behavior. As seen in Figure 5.23, the graph bed expansion height versus volume flow rate of air at different air pressure has been plotted.

Once the air volume flow rate increases, the bed expansion height also increased at all air pressures except at the volume flow rate less than 15 $Lmin^{-1}$ at 2 bar and 5 $Lmin^{-1}$ at 3 bar (500 micron and 70% CaO mixture), where no fluidization was found. The similar trends also occurred for 1000 micron and 70% CaO mixture ratio as shown in Figure 5.24. When the volume flow rate is 5 $Lmin^{-1}$ there is no fluidization at all air pressure. The bed expansion height only observed when the volume flow rate reached 15 $Lmin^{-1}$ for 6 bar air pressure. This is due to strong interacting force between the molecules of the 70% CaO particles, even though the minimum fluidization velocity has been reached.

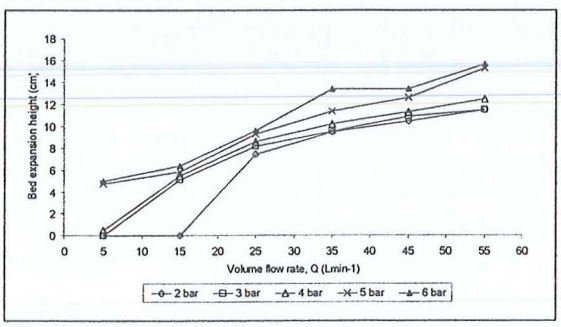

Figure 5.23: Effect of air volume flow rate and pressure to bed expansion height (500 micron and 70% CaO mixture)

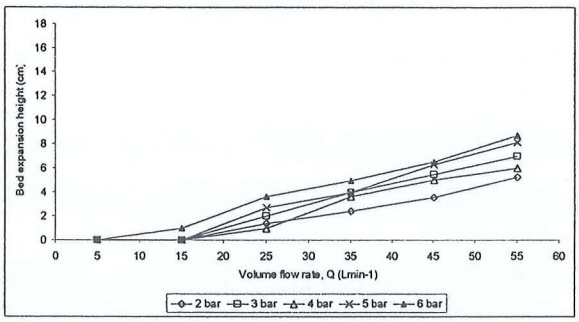

Figure 5.24: Effect of air volume flow rate and pressure to bed expansion height (1000 micron and 70% CaO mixture)

Plat 5.1 shows the picture where the "rat hole" was observed in the CaO-sand mixture when fluidization not occurred.

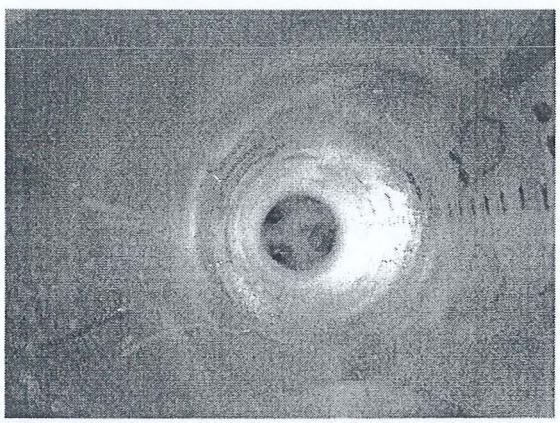

Plat 5.1: Rat holes formed during operation (15 $Lmin^{-1}$, 500 micron, 70% CaO mixture, 2 bars)

5.4.4 Mass Flow Rate of CaO Entrained

The experiment results of mass flow rate of CaO entrained from the bubbling fluidized bed CO_2 absorption reactor (BFBR) are shown in Figures 5.25 -5.29. The graphs of CaO mass flow rate versus volume flow rate were plotted. Its can be observed that with the increases of the air volume flow rate, the mass flow rate of the CaO entrained increased. The minimum and maximum mass flow rates obtained are 0.2 and 1.42 g/min, respectively. The constant values of mass flow rate CaO entrained obtained around 0-0.6 g/min for 1000 micron particle size at all CaO-sand mixture percentages and pressures, although the air volume flow rate has been increased.

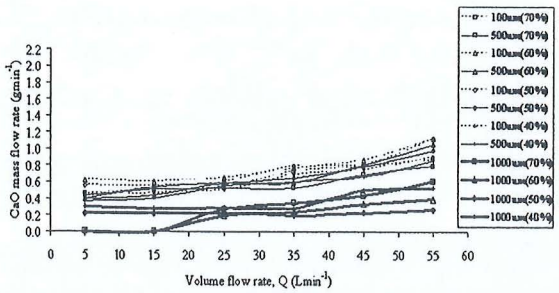

Figure 5.25: Amount of CaO entrained from BFBR (2 bar)

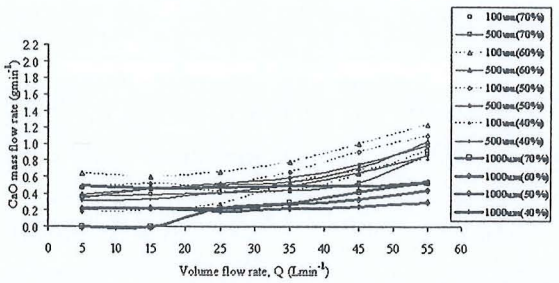

Figure 5.26: Amount of CaO entrained from BFBR (3 bar)

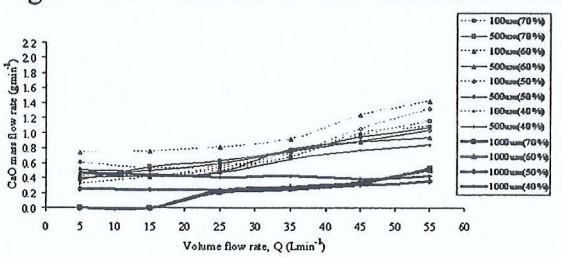

Figure 5.27: Amount of CaO entrained from BFBR (4 bar)

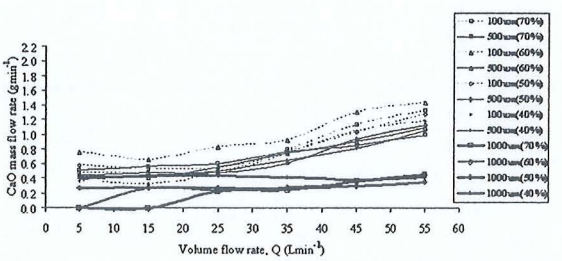

Figure 5.28: Amount of CaO entrained from BFBR (5 bar)

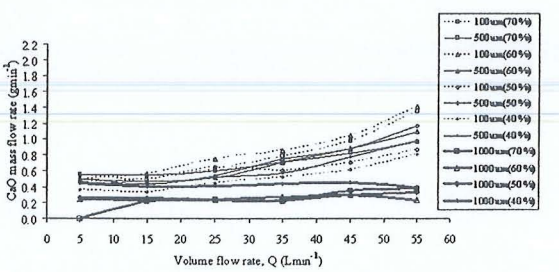

Figure 5.29: Amount of CaO entrained from BFBR (6 bar)

It also can be observed that after 35 $Lmin^{-1}$ volume flow rate, the CaO mass flow rate is increased for 100 and 500 micron compare to 1000 micron particle size. The high density of the 1000 micron particle is the factor why the mass flow rate of CaO entrained is less compared to 100 and 500 micron. In addition, the attrition phenomena occurred for 100 and 500 micron is greater than 1000 micron because of the sand existing.

After investigated and analyzed the cold model experiments, some important thing can be listed:

The CaO percentages ratio of 60, 50 and 40 for 100 and 500 micron sizes were found to have good fluidization for all air pressures (2, 3, 4, 5 and 6 bars).

The volume flow rates of air between 15 – 55 $Lmin^{-1}$ were found to have a good fluidization for all variables except for 70% CaO – sand mixture at 100 and 500 micron sizes.

The 500 micron CaO particle size shows better fluidization characteristics behavior compared to 100 and 1000 micron particles size. However the 1000 micron CaO size is utilized because it gave good fluidization with less CaO entrained compare to 100 and 500 micron sizes.

The 50 and 40% CaO mixture for 1000 micron were found to have a good fluidization in the range 15-55 $Lmin^{-1}$ for all air pressures (2, 3, 4, 5 and 6 bars). Only at 5 $Lmin^{-1}$, no fluidization was found.

CO_2 ABSORPTION EXPERIMENT WITH SIMULATE GAS

The CO_2 detected by gas chromatograph versus time at constant pressure 2, 3 and 4 bars for 50% and 40% CaO-sand mixtures of 1000 micron are shown in Figures 5.30 and 5.31. The low CO_2 concentration was obviously seen for 50% CaO-sand mixture compared to 40% CaO-sand mixture for all elevated pressure at 15 $Lmin^{-1}$ and 45 $Lmin^{-1}$ detected by gas chromatograph. Appendix 6 shows sample of output from gas chromatograph.

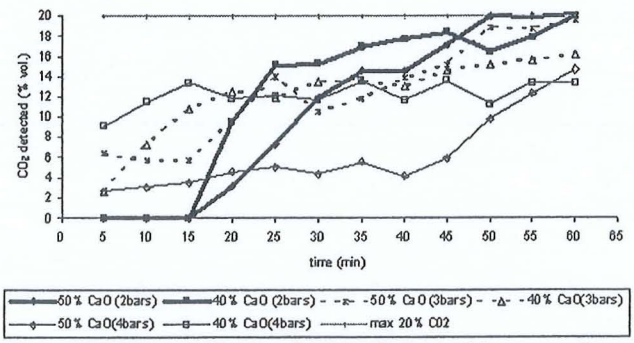

Figure 5.30: Amount of CO_2 detected by gas chromatograph
(15 $Lmin^{-1}$, 650-750^{O}C, 1000 micron)

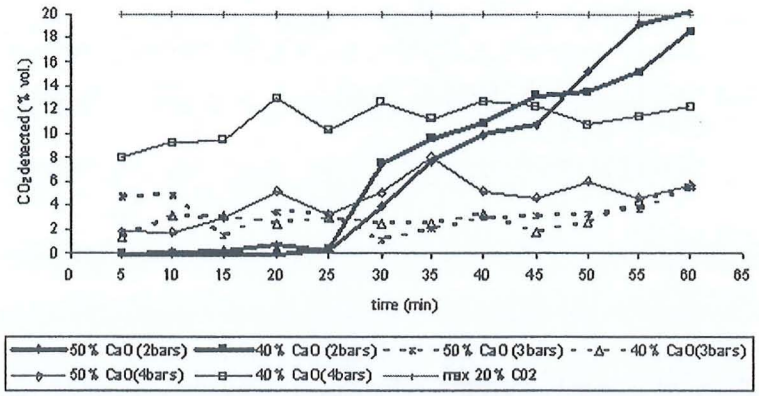

Figure 5.31: Amount of CO_2 detected by gas chromatograph (45 $Lmin^{-1}$, 650-750^{O}C, 1000 micron)

The 20% CO_2 absorption only occurred for 15 min at 2 bars then increased to the max 20% vol. CO_2 in 60 min (Figure 5.30). This similar trend was also been found at the pressures of 3 and 4 bars. In 40% CaO-sand mixture, the collision between the CaO and sand particles is higher compared to 50% CaO-sand mixture. This is because large amount of sand is used in the 40% CaO-sand mixture. The decrease in particle diameter due to impact attritions increased the particle velocity. Some of the 1000 micron CaO particle size became smaller and then entrained from the reactor. This is why the ability of the 40% CaO-sand mixture to absorb 20% CO_2 becomes less.

CO_2 ABSORPTION EXPERIMENT WITH SIMULATE PRODUCER GAS

From the analysis of CO_2 absorption experiment with simulate gas, 3 bar air pressure with 45 $Lmin^{-1}$ of volume flow rate and 50% CaO-sand mixture ratio (1000 micron) will be used to test the ability of CO_2 absorption using the simulate producer gas. Figure 5.32 shows the graph of the CO_2 detected by gas chromatograph versus time. It can be observed that the 16 % vol. concentration of CO_2 in the simulated producer gas before flow through the bubbling fluidized bed reactor (BFBR) has been absorbed after exit from the BFBR. Within the first 10 min experiment, the CO_2 concentration of simulate producer gas decreased from 16% to 6.8% by vol when it is analyzed by gas chromatograph. The carbonation process occurred during 60 min run with slower rate at end of the experiment. As seen in Figure 5.32, only 11.7% by vol. the CO_2 detected by gas chromatograph. Although, the maximum CO_2 % is 11.7% but it still less than 16% CO_2 gas supplied from the simulated producer gas tank.

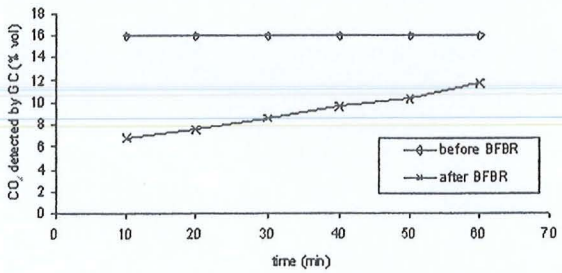

Figure 5.32: CO_2 gas detected by gas chromatograph (Simulated producer gas) (45 $Lmin^{-1}$, 650-750^{O}C, 1000 micron)

In 50% CaO-sand mixture, the collision between the CaO and sand particles is occurred because of the fluidization phenomena in the bed. During 60 min of experiment run, the 1000 micron particle size became smaller and then

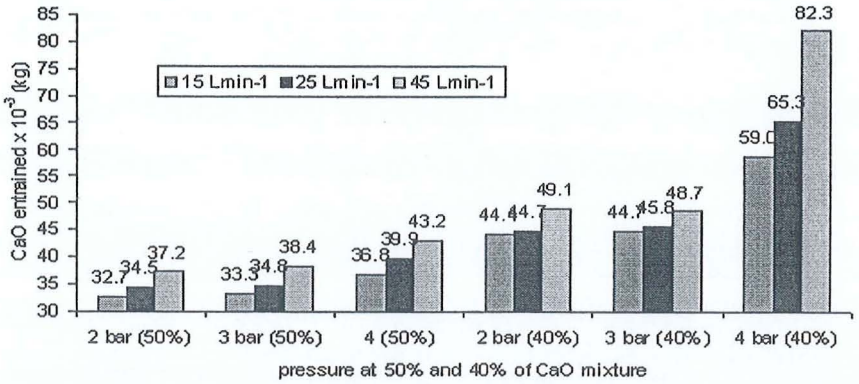

Figure 5.33: Amount of CaO-sand mixture entrained

entrained from the reactor. The ability of the 50% CaO-sand mixture to absorb 16% CO_2 composition of the simulated producer gas becomes less at the end of the experiment. Figure 5.33 shows the amount of CaO mass entrained from BFBR.

The simulated producer gas compositions before and after reach carbonation process have been recorded and listed in Table 5.7. It can been seen that the simulated producer gas content of Hydrogen 12% vol., Carbon Oxide 24% vol. and Nitrogen 48% vol., were improved during 60 min experiment after carbonation process with CaO-sand mixture. Figure 5.34 shows the graph amount of gasses detected by gas chromatograph by vol. versus time for the simulated producer gas experiment.

Table 5.7: Simulated producer gas composition before and after BFBR

	Simulated Producer Gas Composition (vol.) detected by GC							
time (min)	H_2 aft.	H_2 bef.	N_2 aft.	N_2 bef.	CO aft.	CO bef.	CO_2 aft.	CO_2 bef.
10.00	15.07	12.00	51.07	48.00	27.07	24.00	6.80	16.00
20.00	14.83	12.00	50.83	48.00	26.83	24.00	7.50	16.00
30.00	14.47	12.00	50.47	48.00	26.47	24.00	8.60	16.00
40.00	14.13	12.00	50.13	48.00	26.13	24.00	9.60	16.00
50.00	13.90	12.00	49.90	48.00	25.90	24.00	10.30	16.00
60.00	13.43	12.00	49.43	48.00	25.43	24.00	11.70	16.00

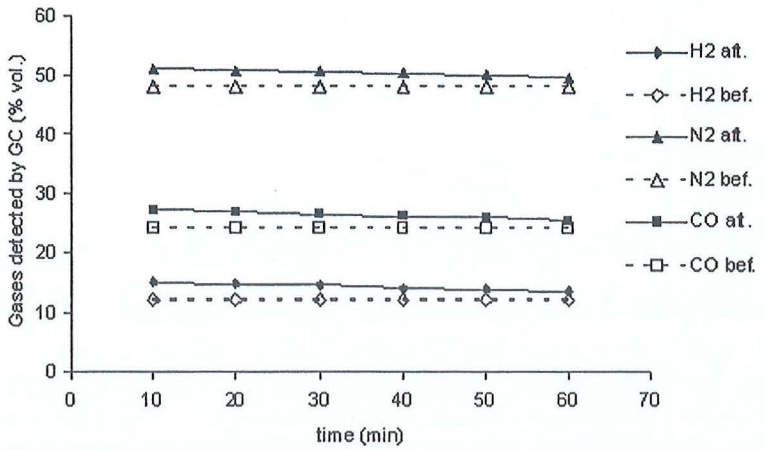

Figure 5.34: Gases detected by gas chromatograph (simulated producer gas)

All the gases compositions content in the simulated producer gas were improved after flow out from the CaO-sand mixture in BFBR. The amount of CO_2 been absorbed during the experiment, resulted in the improvement of the simulated producer gas. The absorption of CO_2 used CaO as a sorbent also has been done by Mahishi and Goswami (2007) in their research. Although, the gases percentage vol. in the producer gas have been improved, but the improvement rate at the end of the experiment is decreased about 10% by vol. for all gases compared to the first 10 min. The saturated absorption of carbonation process occurred for the 50% CaO-sand mixture and the attrition as mentioned previously was the factor why the improvement rate is less at the end of the experiment. This phenomenon also has been stated and studied by Chen et al. (2008).
The heating value of the simulated producer gas before and after through the carbonation process in the bubbling fluidized bed CO_2 absorption reactor (BFBR) is one important element has to know. It is depends on the relative amount of different combustible gas components such as Hydrogen and Carbon Oxide used. The low heating value can be calculated using

$$LHV_{simulatedproducergas} = (LHV_{H_2})(V_{H_2}) + (LHV_{CO})(V_{CO}) \qquad (5.3)$$

Where:
V_{H_2}, V_{CO} are the volumetric concentration of the combustible gas composition.

Table 5.8 shows the low heating value of simulated producer gas before and after through the carbonation process in the BFBR. It is seemed that the LHV of simulated producer gas after through the carbonation process been improved during the 60 min experiment. The absorbed of CO_2 gas by 50% CaO-sand mixture during carbonation process and the improvement of percentage volumetric for every combustible gas in simulated producer gas, resulted higher simulated producer gas.

Table 5.8: LHV of simulated producer gas before and after BFBR

time	before MJ/N m3	after MJ/N m3
10.00	4.32	5.04
20.00	4.32	4.99
30.00	4.32	4.90
40.00	4.32	4.82
50.00	4.32	4.77
60.00	4.32	4.66

CO_2 ABSORPTION EXPERIMENT WITH COMPRESSED PRODUCER GAS

In this stage the compressed producer gas is used to validate the ability of CO_2 absorption. The same conditions: 300 kNm^{-2} air pressure with 0.00075 m^3s^{-1} volume flow rate and 50% CaO-sand mixture ratio (1000 micron) were used. Table 5.9 shows the results analysis of the compressed producer gas compositions before flow through the carbonation process of CaO-sand mixture and the low heating value calculated based on the equation 5.3.

Table 5.9: Compressed producer gas composition and LHV before BFBR

	Compressed producer gas (% vol.) detected by GC					LHV
time (min)	H_2	N_2	CO	CO_2	CH_4	(MJ/N m^3)
15.00	12.16	54.68	20.12	11.58	1.46	4.37
30.00	13.11	52.98	20.36	12.08	1.47	4.51
45.00	12.34	54.94	20.75	10.60	1.38	4.44
60.00	12.57	51.73	21.89	12.52	1.30	4.58

It can be observed that, the heating value of the compressed producer gas before passed through to the 50% CaO-sand mixture for carbonation process were approximately constant during 60 minutes experiment.

In Figure 5.35, the graph of the CO_2 detected by gas chromatograph versus time after passed through the 50% CaO-sand mixture is shown. It can be seen that every 15 minutes the CO_2 concentration of the compressed producer gas supplied was absorbed. In the first 15 minutes, the CO_2 concentration content in the compressed producer gas is decreased from 11.58 to 2.62% vol. when it is analyzed by gas chromatograph. The carbonation process still occurred during 60 minutes experiment with slower rate at end of the experiment. Although, the CO_2 detected by GC is 7.80% vol. but it still showed the ability to absorb CO_2 gas.

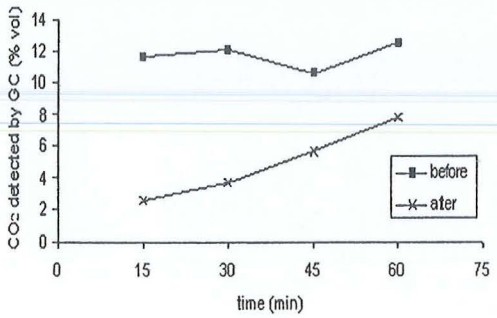

Figure 5.35: CO_2 gas detected by gas chromatograph (compressed producer gas) (45 $Lmin^{-1}$, 650-750^{O}C, 1000 micron)

Figure 5.36 shows the graph of the composition of combustible gases in the compressed producer gas against time after passed through the 50% CaO-sand mixture. It can be observed, for the three combustible gases H_2, CO and CH_4 there is an improvement on the percentage concentration gases by vol. after passed through the carbonation process in the BFBR. The effective of CO_2 absorption from the compressed producer gas during the experiments conducted results in an increase of the gas percentage vol.

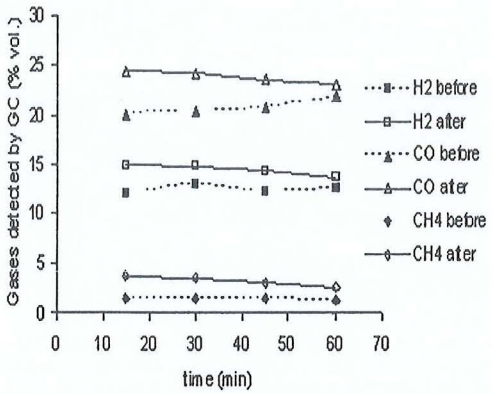

Figure 5.36: Amount of combustible gases detected by gas chromatograph (compressed producer gas)

Table 5.10 shows the low heating value (LHV) of compressed producer gas after through the carbonation process in the BFBR. The calculation of the LHV is based on the equation 5.3. It is seen that the LHV of compressed producer gas after through the carbonation process has been improved during the 60 minutes experiment. In the early of 15 minute experiment about 38% LHV has increased and then followed with 16% in 60 minutes experiment run. The turn down of the percentage was due to the saturation state of the CaO to absorb CO_2 and due to loss of small particle of CaO from the bubbling fluidized bed reactor. This has been discussed in the earlier discussion.

Table 5.10: Compressed producer gas composition and LHV after BFBR

	Compressed producer gas (% vol.) detected by GC					LHV
time (min)	H_2	N_2	CO	CO_2	CH_4	(MJ/Nm^3)
15.00	14.99	54.20	24.48	2.62	3.71	6.04
30.00	14.85	53.75	24.23	3.70	3.47	5.90
45.00	14.29	53.45	23.59	5.66	3.01	5.60
60.00	13.77	52.82	23.13	7.80	2.48	5.29

CHAPTER 6: CONCLUSION

The development of a bubbling fluidized bed reactor to absorb CO_2 in the producer gas using Calcium Oxide (CaO) mixed with sand as absorbent reagent for improving the quality of the producer gas has been successfully built and operated. The conclusion can be broken down into three parts: the hydrodynamic simulation, design and development of bubbling fluidized bed CO_2 absorption reactor (BFBR) and the experiments: cold model and hot model to determine the absorption of CO_2 on the simulation of gas, compressed producer gas generated.

6.1 HYDRODYNAMIC SIMULATION

The computerized simulation software named Fluent has been successfully carried out to determine the ability of the fluidized calcium oxide (CaO) contained in the bubbling fluidized bed CO_2 absorption reactor (BFBR). The comparison between fluent computer simulation of the cold model experiments show that particular bed height expansion produced by computer simulation is almost identical to that carried out by experiments using several parameters setting. The relative error is found to be less than 24 percent. In addition, the formation of bubbles is occured in the calcium oxide material inside the BFBR and it has been successfully demonstrated in the simulation.

6.2 DESIGN OF BUBBLING FLUIDIZED BED CO_2 ABSORPTION REACTOR

The laboratory scale design of the bubbling fluidized bed CO_2 absorption reactor (BFBR) has successfully done and developed according to the size of the ceramic heater band available. The design has been shown detail in the engineering drawings and fabricated one by one. The calculation for the estimated parameters showed BFBR operations should be designed to have a diameter of 0.074 m. Moreover, the pressure drop produced when using 100 micron particle size in BFBR is 1199 Pa only. The estimation operating parameters of the CO_2 absorption reactor for the carbonation process using water, simulate gas, producer gas have been calculated successfully. These value obtained are show in chapter 3 of this thesis.

6.3 EXPERIMENTS

In the moisture content test, the percentage obtained was 11.1%. The value is below than 30% wood moisture content, so it is found to be suitable for combustion in the gasification process to produce the optimum heating value for the producer gas. Based on the moisture content of the wood, the wood furniture used in the experiment has a low heating value of 17.1 MJ/kg.

An experiment to characterize the ability of the fluidization of the calcium oxide (CaO) - sand mixture in the BFBR called cold model experiment was successfully carried out. The results obtained showed that variables such as the different size of the CaO particles, percentage ratio of CaO - sand, air volume flow rate and air pressure, mass flow rate of the CaO out from BFBR are affects the ability of fluidization material. The CaO particle

size of 1000 micron with air pressure of 2, 3 and 4 bars, and 50% to 40% CaO - sand have show successful fluidization ability.

In the hot model experiments using ceramic heater band provided heat energy to the CaO-sand mixture, the carbonation process has been successfully done. The process is to absorb the CO_2 concentration in the simulated gas containing 20% CO_2 and 80% N_2. The results showed the low CO_2 concentration was obviously seen at 50% CaO-sand mixture compared to 40% CaO-sand mixture for all elevated pressure at 15 Lmin-1 and 45 Lmin-1.

To confirm that the 50% CaO-sand mixture is better in terms of acceptance of CO_2 absorption, further testing is done using the simulated producer gas. The gas contains of 16% CO_2, 24% CO, 12% H_2 and 48% N_2 gas composition. The 16% vol. concentration of CO_2 in the simulated producer gas has been absorbed after exit from the BFBR. The carbonation process occurred during 60 min run with slower rate at end of the experiment. Only 11.7% CO_2 of gas found in the simulated producer gas at the end of 60 min. The value of the low heating value of producer gas is found to be 5.04 MJ/Nm^3 after flow out from the BFBR compared before pass through the BFBR is 4.32 MJ/Nm^3. This shows that the quality of the simulated producer gas has been improved after pass through the CaO-sand mixture in the BFBR.

Finally, the experiment was carried out to absorb CO_2 content in the actual compressed producer gas. It contains 11.58% CO_2, 20.12% CO, 12.16% H_2, 1.46% CH_4 and 54.68% N_2 gas composition. The concentration of CO_2 content in the compressed producer gas is decrease from 11.58 to 2.62% vol. after passed through the BFBR. The carbonation process is still occurred within 60 minutes with slower rate at end of the experiment. Although the CO_2 detected by Gas Chromatograph is 7.80% vol. but it still showed the ability to absorb CO_2 gas. Once calculated, the low heating value of compressed producer gas has changed from 4.37 MJ/Nm^3 to 6:04 MJ/Nm^3. It shows the quality of the compressed gas producer has been improved by using selected operation parameters.

Thus in general, this research work is considered successful because its objectives have been achieved. Nevertheless, some suggestions can be forwarded to the next research such as the experiments can be done using the actual size to obtain the real industrial data and using on-line gas chromatograph mechanisms to gain accurate gas concentration data.

Journals:
Abad, A.; Garcı´a-Labiano, F.; de Diego, L.F. ; Gaya´n, P. and Ada´nez, J. (2002). Calcination of calcium-based sorbents at pressure in a broad range of CO2 concentrations. *Chemical Engineering Science*. 57, pp. 2381– 2393.

Abanades, J.C. (2002). The maximum capture efficiency of CO2 using a carbonation/calcination cycle of CaO/CaCO3, *Chemical Engineering Journal*. 90, pp. 303– 306.

Abanades, J.C. and Alvarez, D. (2003). Conversion limits in the reaction of CO_2 with lime. *Energy Fuels*. 17, pp. 308– 315.

Adnan Midilli, Murat Dogru, Galip Akay and Colin R. Howarth (2002). Hydrogen production from sewage sludge via a fixed bed gasifier product gas. *International Journal of Hydrogen Energy*, 27, pp 1035-1041.

Adnan Midilli, Murat Dogru, Teoman Ayhan and Colin R. Howarth (2001). Hydrogen production from hazelnut shell by applying air-blown downdraft gasification technique. *International Journal of Hydrogen Energy*, 26, pp 29-37.

Anderson, W.K.; Bonhous, D.L.; McGhee, R.J. and Walker, B.S. (1995). Navier-Stroke computation and experimental comparisons for multi-element airfoil configurations. *Journal of Aircraft*, 32, pp. 1246-1253.

Anthony, E.J. and Granatstein, D.L. (2001). Sulphation phenomena in fluidized bed combustion systems, *Progress in Energy and Combustion Science*. 27, pp. 215–236.

Aznar, M.P.; Caballero, M.A.; Gil, J.; Martin, J.A and Corella, J. (1998). Commercial steam reforming catalysts to improve biomass gasification with steam-oxygen mixtures. 2. Catalytic tar removal. ***Industrial & Engineering Chemistry Research***. 37, pp 2668-2680.

Banapurmath, N.R.; Tewari, P.G. and Hosmath, R.S. (2008). *Renewable Energy*. 33 , pp. 2007–2018.

Barea, A.G. and Leckner, B. (2010). Modeling of biomass gasification in fluidized bed. *Progress in Energy and Combustion Science*, 36, pp. 444–509.

Barker, R. (1973). The reversibility of the reaction $CaCO_3 \leftrightarrow CaO+CO_2$. *Journal of Applied Chemistry & Biotechnology*. 23, pp. 733–742.

Behjat, Y.; Shahhosseini, S. and Hashemabadi, S.H. (2009). CFD modeling of hydrodynamic and heat transfer in fluidized bed reactors. *International Communications in Heat and Mass Transfer*, 35, pp. 357-368.

Bhatia, S.K. and Perlmutter, D.D. (1983). The effect of product layer on the kinetics of the CO_2-lime reaction, *American Institute of Chemical Engineers Journal*. 29, pp. 79.

Bridgwater, A.V.; Brammer, J.G. and Toft, A.J. (2002). A Techno-economic Comparison of Power Production by Biomass Fast Pyrolysis With Gasification and Combustion. *Renewable and Sustainable Energy Reviews*, 6, pp. 181-248.

Cao, Y.; Wang, Y.; John, T.R. and Pan, W.P. (2006). A novel biomass air gasification process for producing tar-free higher heating value fuel gas. *Fuel Processing Technology*. 87, pp. 343-353.

Chang, J.; Lv, P.M.; Xiong, Z.H.; Wu, C.Z.; Chen, Y. and Zhu, J.X. (2004). An experimental study on biomass air-steam gasification in a fluidized bed. *Bioresource Technology*, 95, pp 95-101.

Chen, Z.; Grace, John R. and Lim, C. Jim (2007). Study of limestone particle impact attrition. *Chemical engineering science*, Vol. 62, pp. 867-877.

Chen, Z.; Grace, John R. and Lim, C. Jim (2008). Limestone particle attrition and size distribution in a small circulating fluidized bed. *Fuel*, Vol. **87** (7), pp 1360-1371.

Cooper, S. and Coronella, C.J. (2005). CFD simulations of particle mixing in a binary fluidized bed. *Powder Technology*, 151, pp. 27– 36.

Courson, C.; Makaga, E.; Petit, C. and Kiennemann, A. (2000). Development of Ni catalysts for gas production from biomass gasification. Reactivity in steam and dry reforming. *Catalysis Today*, 63, pp 427-437.

Curran, G.P.; Fink, C.E. and Gorin, E. (1967). Carbon dioxide-acceptor gasification process: studies of acceptor properties. *Advances in Chemistry Series*, 69, pp. 141-165.

Delgado, J.; Aznar, M.P. and Corella, J.(1996). Calcined dolomite, magnesite and calcite for cleaning hot gas from a fluidized bed biomass gasifier with steam: life and usefulness. *Industrial & Engineering Chemistry Research.*, 35, pp 3637-3643.

Deshmukh, S.J.; Bhuyar, L.B. and Thakre, S.B. (2008). Investigation on performance and emission characteristics of CI engine fuelled with producer gas and esters of hingan (balanites) oil in dual fuel mode. *International Journal of Aerospace and Mechanical Engineering*, 2: 3, pp. 148-153.

Dogru, M.; Howarth, C.R.; Akay, G.; Keskinler, B. and Malik, A.A. (2002). Gasification of hazelnut shells in a downdraft gasifier. *Energy*, 27, pp 415-427.

Flamant, G., N. Fatah, D. Steinmetz, B. Murachman, and C. Laquerie (1991). High-temperature velocity and porosity at minimum fluidization. Critical analysis of experimental results. *International Chemical Engineering*, 31: 673-684. ISSN: 00206318.

Geldart, D. (1973). Types of gas fluidization. *Powder Technology*, 7, pp. 285-292.

Gemma, S.G. and Abanades, J.C. (2006). CO_2 capture capacity of CaO in long series of carbonation/calcination cycles. *Industrial & Engineering Chemistry Research*. 45, pp. 8846-8851.

Gil J.; Corella, J.; Aznar, M.P. and Caballero, M.A. (1999). Biomass gasification in atmospheric and bubbling fluidized bed: effect of the type of gasifying agent on the product distribution. *Biomass and Bioenergy*, 17, pp 389-403.

Guo, Q., G. Yue, T. Suda and J. Sato (2003). Flow characteristics in a bubbling fluidized bed at elevated temperature. *Chemical Engineering and Processing*, **42**: 439-447. DOI:10.1016/S0255-2701(02)00071-5

Hanaoka, T.; Yoshida, T.; Fujimoto, S.; Kamei, K.; Harada, M.; Suzuki, Y.; Hatano, H.; Yokoyama, S. and Minowa, T. (2005). Hydrogen production from woody biomass by steam gasification using a CO_2 sorbent. *Biomass and Bioenergy*, 28, pp 63-68.

Hu, N. and Scaroni, A.W. (1996). Calcination of pulverised limestone particles under furnace injection conditions. *Fuel*. 75, pp.177– 186.

Hollingdale, A.C., G.R. Breag and D. Pearce, 1988. Producer Gas Fuelling of a 20 KW Output Engine by Gasification of Solid Biomass. *Energy and power & Propulsion and fuels*, pp. 10-21. ISBN 0-85954-243-2.

Jorapur, R.M. and Rajvanshi, A.K. (1995). Development of Sugarcane Leaf Gasifier for Electricity Generation. *Biomass and Bioenergy*. Volume 8, No. 2, pp 91-98.

Kramlich, J.C.; Silcox, G.D. and Pershing, D.W. (1989). A mathematical model for the flash calcination of dispersed $CaCO_3$ and $Ca(OH)_2$ particles, *Industrial & Engineering Chemistry Research*. 28, pp. 155–160.

Lin, S.Y.; Suzuki, Y.; Hatano, H. and Harada, M. (2002). Developing an innovative method, HyPr-RING, to produce hydrogen from hydrocarbons. *Energy Conversion and Management*, 43, pp 1283-1290.

Magnus Ryden; Anders Lyngfelt (2006). Using steam reforming to produce hydrogen with carbon dioxide capture by chemical-looping combustion. *International Journal of Hydrogen Energy*, Vol. 31, pp. 1271-1283.

Mahishi M.R. and Goswami D.Y., (2007). An experiment study of hydrogen production by gasification in presence of CO2 sorbents. *International Journal of Hydrogen Energy*, 32: pp. 2803-2808.

Manovic, V.; Charland, J.P.; Blamey, J.; Fennell, P.S.; Lu, D.Y. and Anthony, E.J. (2009). Influence of calcination conditions on carrying capacity of CaO-based sorbent in CO_2 looping cycles. *Fuel*, 88, pp. 1893-1900.

Mathieu, P. and Dubuisson, R.(2002). Performance analysis of a biomass gasifier. *Energy Conversion and Management*, 43, pp 1291-1299.

McKendry, P. (2001). Energy production from biomass (part 1): overview of biomass. *Bioresource Technology*, 83 (1), pp. 37–46.

McKendry, P. (2002b). Energy production from biomass (part 2): conversion technologies. *Bioresource Technology*, Vol. 83, pp. 47-54.

McKendry, P. (2002c). Energy production from biomass (part 3): gasification technologies. *Bioresource Technology*, Vol. 83, pp. 55-63.

Mess, D.; Sarofim, A.F. and Longwell, J.P. (1999) Product layer diffusion during the reaction of calcium oxide with carbon dioxide, *Energy Fuels*, 13, pp. 999–1005.

Mohammadi Ali, Shioji Masahiro, Ishiyama Takuji and Kitazaki Masato (2006). Utilization of low-calorific gaseous fuel in a direct-injection diesel engine. *Gas Turbines Power*, 128, pp. 915–920.

Munoz, M.; Moreno, F.; Morea-Roy, J.; Ruiz, J. and Arauzo, J. (2000). Low heating value gas on spark ignition engines. *Biomass and Bioenergy*, 18, pp 431-439.

Nikulshina, V.; Gebald, C. and Steinfeld, A. (2009). CO_2 capture from atmospheric air via consecutive CaO-carbonation and $CaCO_3$-calcination cycles in a fluidized-bed solar reactor. *Chemical Engineering Journal*. **146**, pp. 244-248.

Ramadhas A.S., Jayaraj S. and Muraleedharan (2006). Power generation using coir-pith and wood derived producer gas in diesel engines. *Fuel Process Technology*, 87, pp. 849–853.

Rapagna, S.; Jand, N.; Kiennemann, A. and Foscolo, P.U. (2000). Steam gasification of biomass in a fluidized bed of olivine particles. *Biomass and Bioenergy*, 19, pp 187-197.

Salvador, C.; Lu, D. ; Anthony, E.J. and Abanades, J.C. (2003). Enhancement of CaO for CO_2 capture in an FBC environment. *Chemical Engineering Journal*. 96, pp. 187– 195.

Schuster, G.; Loffler, G., Weigl, K and Hofbauer, H. (2001). Biomass steam gasification an extensive parametric modeling study. *Bioresource Technology*, 77, pp 71-79.

Singh, R.N.; Singh, S.P. and Pathak, B.S. (2007). Investigations on operation of CI engine using producer gas and rice bran oil in mixed fuel mode. *Renewable Energy*, 32, pp. 1565–1580.

Squires, A.M., (1967). Cyclic use of calcined dolomite to desulfurize fuels undergoing gasification. *Advances in Chemistry Series*, 69, pp. 205-229.

Sridhar, G.; Paul, P.J.; and Mukunda, H.S. (2001). Biomass derived producer gas as a reciprocating engine fuel-an experimental analysis. *Biomass and Bioenergy*, 21, pp 61-72.

Klass, D.L. (1998). *Biomass for Renewable Energy, Fuels, and Chemicals*. Academic Press, San Diego.

Kunii, D. and Levenspiel, O. (1991). *Fluidization Engineering*, 2nd Edition. Butterworth-Heinemann, USA.

Lee S. (1996). *Alternative Fuels*. Washington DC: Taylor & Francis, pp. 427.

Levin, R.I. and Rubin, D.S. (2009). *Statisticals for Management*, seventh edition . Pearson Prentice Hall.

McCabe, W.E., J.C. Smith, and P. Harriott (2004*). Unit Operations of Chemical Engineering*. 7th edition. McGraw Hill, New York. ISBN 0-07-284823-5.
Mukherjee, D. and Chakrabarti, S. (2004). *Fundamentals of renewable energy systems*. New Age International (P) Ltd, New Delhi.

Reed, T. and Das, A. (1988). Handbook of biomass downdraft gasifier engine systems. Solar Technical Information Program, Solar Energy Research Institute in Golden, Colo.

Rezaiyan, J. and Cheremisinoff, N.P. (2005). *Gasification Technologies: A Primer for Engineers and Scientists*. CRC Press, Taylor and Francis Group. United Stated of America.

Sheridan, J.C. and Lyndall, G.S. (2003). *SPSS Analysis without anguish Version 11.0 for windows*. John Wiley & Sons Australia Ltd.
U.S. Departments of Agriculture (2007). *The Encyclopedia of Wood*. Skyhorse Publishing.

Walawender, W.P.; Chern, S.M. and Fan, L.T. (1985). *Wood chips gasification in a commercial downdraft gasifier*. In: Overend RP, editor. Fundamentals of thermo chemical biomass conversion, Amsterdam: Elsevier Applied Science, pp 911.

Wen, C.Y. (2003). Handbook of fluidization and fluid-particle systems. Crc Press. ISBN-13: 9780824702595.

Yates, J.G. (1983). *Fundamentals of fluidized-bed chemical processes. Butterworth-Heinemann*. ISBN-13: 978-0408709095.

Zainal, Z.A. (1996). Performance and Characteristics of A Biomass Gasifier System. Ph.D Dissertation, Division of Mechanical Engineering and Energy Studies, School of Engineering, University of Wales, College of Cardiff, United Kingdom.

Proceedings:
Alvarez, D. ; Abanades, J.C.; Anthony, E.J. and Lu, D. (2003). In-situ capture of CO_2 in a fluidized bed combustor, *Proceeding 17th International Fluidized Bed Combustion Conference*, Jacksonville Florida, May.

Graham, R.G. and Huffman, D.R. (1981). Gasification of Wood in A Commercial Scale Downdraft Gasifier. In: *Energy from Biomass 5*, Lake Buena Vista, FL. Jan., pp 633-650.

Gunderson, J.R. and Darren D. Schmidt (2000). Opportunities for hydrogen: An analysis of the application of biomass gasification to farming operations using microturbines and fuel cells. In *Proceedings of the 2000 hydrogen program review* NREL/CP-570-28890.

Hofbauer, H.; Rauch, R.; Foscolo, P. and Matera, M. (2000). Hydrogen rich gas from biomass steam gasification. *1st World Conference & Exhibition on Biomass for Energy & Industry*, Sevilla. June.

Markus, B.N. and Hofbauer, H. (2004). Gasification demonstration plants in Austria. *IV International Slovak Biomass Forum*, Bratislava. February 9th -10th.

Pfeifer, C.; Rauch, R. and Hofbauer, H. (2004). Hydrogen rich gas production with a catalytic dual fluidized bed biomass gasifier. *2nd World Conference & Technology Exhibition on Biomass for Energy, Industry & Climate Protection*, Rome. May 10-14th.

Rauch, R.; Pfeifer, C.; Hofbauer, H.; Swierczynski, D.; Courson, C. and Kiennemann, A. (2004). Hydrogen-rich gas production with a Ni-catalytic in a dual fluidized bed biomass gasifier. *Science in Thermal & Chemical Biomass Conversion,* Victoria Canada. August 30th – September 2nd.

Singh R.N., Singh S.P. and Pathak B.S. (2007). Investigations on operation of CI engine using producer gas and rice bran oil in mixed fuel mode fuel. *Renewable Energy*, Vol. 32 (9), pp. 1565 -1580.

Skov, N.A. and Papworth, M.L. (1974). The Pegasus Unit: The Lost Art of Driving Without Gasoline, Pegasus. Now available from LaFontaine, H. Biomass Energy Foundation, Inc. Keystone Blvd., Miami.

Xu, G.Q and Wang, Y. (1988). Gasification of Agricultural and Forestry Residues. *23rd Proceeding Intersociety Energy Conversion Engineering Conference*. Denver, U.S.A.

Website:
Energy Information Administration Report (2006).Annual Energy Outlook 2006 with Projections to 2030.http://www.eia.doe.gov/oiaf/archive/ieo06/index.html. [Accessed 5 July 2008].

Energy Information Administration Report (2008). Country Analysis Briefs: Malaysia. Washington DC: EIA.http://tonto.eia.doe.gov/country/country_energy_data.cfm?fips=MY. [Accessed 5 July 2008].

Energy Information Administration Report (2010). Country Analysis Briefs: Malaysia. Washington DC: EIA.http://tonto.eia.doe.gov/country/country_energy_data.cfm?fips=MY. [Accessed 24 January 2011].

Energy Information Bureau, Malaysia (2006). Biomass: http://eib.org.my/index.php?page=article&item=100,136,142. [Accessed 5 July 2010].

Malaysia Energy Centre (2008). Energy Information Bureau (EIB) Malaysia: Biomass. http://eib.ptm.org.my/index.php?page=article&item=100,136,142 [Accessed 5 Januari 2009].

World Energy Outlook (2004). International Energy Agency. http://www.iea.org/textbase/nppdf/free/2004/weo2004.pdf. [Accessed 5 september 2009].

LAMPIRAN B

KERTAS PENERBITAN

An Article Submitted to

INTERNATIONAL JOURNAL OF CHEMICAL REACTOR ENGINEERING

Experimental Study of Hydrodynamic Characteristics and CO2 Absorption in Producer Gas using CaO-sand Mixture in a Bubbling Fluidized Bed Reactor

Mohd Mahadzir Mohammud* Zainal Zainal†

*Universiti Teknologi MARA (UiTM), Penang Branch Campus,, mohdmahadzir@hotmail.com

†universiti sains malaysia kampus kejuruteraan, mezainal@yahoo.com

ISSN 1542-6580

Experimental Study of Hydrodynamic Characteristics and CO2 Absorption in Producer Gas using CaO-sand Mixture in a Bubbling Fluidized Bed Reactor

Mohd Mahadzir Mohammud Mr and Zainal Zainal

Abstract

Producer gas, from biomass gasification process can be used to generate power as an alternative to fossil fuel. Carbon dioxide (CO2) content in the producer gas reduces its heating value as CO2 acts as a diluent. The used of limestone consisting mainly of the mineral calcite (calcium oxide, CaO) as calcium based sorbent to absorb CO2 in the producer gas can make biomass technology more viable. In this paper, the behavior of CaO-sand mixtures in a cold model experiment was studied. The effect of the CaO-sand mixtures, the CaO particle sizes, the volume flow rate and the pressure of air intake were investigated experimentally. The hot model experimental was also conducted to investigate CO2 absorption at the optimum condition obtained from the cold model experiment. The CaO percentages of 50 and 40 in sand were found to have a good fluidization at all air pressures (2 - 6 bar). In addition to that, the 1000 micron particle size of the CaO–sand mixture and the volume flow rate of air between 15 – 55 Lmin-1 were also found to give good fluidization. In the hot model experiment, the best CO2 absorption occurred at 50% CaO mixture with simulated gas pressure of 3 bar and the volume flow rate of 45 Lmin-1 at 650-750oC in a bubbling fluidized bed reactor (BFBR).

KEYWORDS: Biomass, Producer Gas, Fluidization, CaO, CO2 absorption

Experimental Study of Hydrodynamic Characteristics and CO_2 Absorption in Producer Gas using CaO-sand Mixture in a Bubbling Fluidized Bed Reactor

Mahadzir M. M.[a,b*] and Zainal Z. A.[b]

[a]*Faculty of Mechanical Engineering, Universiti Teknologi MARA (UiTM), Penang Branch Campus, Pulau Pinang.*

[b]*School of Mechanical Engineering, Universiti Sains Malaysia, Eng. Campus, Pulau Pinang.*

Email: mohdmahadzir@hotmail.com, mezainal@yahoo.com*

Abstract

Producer gas, from biomass gasification process can be used to generate power as an alternative to fossil fuel. Carbon dioxide (CO_2) content in the producer gas reduces its heating value as CO_2 acts as a diluent. The used of limestone consisting mainly of the mineral calcite (calcium oxide, CaO) as calcium based sorbent to absorb CO_2 in the producer gas can make biomass technology more viable. In this paper, the behavior of CaO-sand mixtures in a cold model experiment was studied. The effect of the CaO-sand mixtures, the CaO particle sizes, the volume flow rate and the pressure of air intake were investigated experimentally. The hot model experimental was also conducted to investigate CO_2 absorption at the optimum condition obtained from the cold model experiment. The CaO percentages of 50 and 40 in sand were found to have a good fluidization at all air pressures (2 - 6 bar). In addition to that, the 1000 micron particle size of the CaO–sand mixture and the volume flow rate of air between 15 – 55 $Lmin^{-1}$ were also found to give good fluidization. In the hot model experiment, the best CO_2 absorption occurred at 50% CaO mixture with simulated gas pressure of 3 bar and the volume flow rate of 45 $Lmin^{-1}$ at 650-750°C in a bubbling fluidized bed reactor (BFBR).

Keywords: Biomass, Producer Gas, Fluidization, CaO, CO_2 absorption

1. Introduction

The combustible and non combustible gases in producer gas consist of Carbon monoxide (CO), Hydrogen (H_2), Methane (CH_4), Carbon dioxide (CO_2) and Nitrogen (N_2) (McKendry, 2002b). These gases are resulted from the incomplete combustion and endothermic reaction of the biomass gasification process.

Carbon dioxide, CO_2 in the producer gas reduces its heating value as CO_2 acts as a diluent. The content of CO_2 in the producer gas is about 10-20 % by volume (Munoz et al., 2000, Sridhar et al., 2001, Zainal et al., 2002, Dogru et al., 2002 and Uma et al., 2004) with a heating value about 4-6 MJ/m^3 (Jorapur and Rajvanshi, 1995 and Zainal 1996). Removing the CO_2 from the producer gas will inadvertently increase its heating value.

Recent year, the number of CO_2 sorbents have been intensively investigated. The used of dolomite (Felice et al., 2010, Wu and Williams, 2010, Hassanzadeh and Abbasian, 2010), amines (Sjostrom and Krutka, 2010), lithium Li_4SiO_4 (unpublished work) and potassium carbonate (Zhao et al., 2009, Chen et al., 2009) have been applied in several fields for the purpose of CO_2 absorption. In biomass technology, calcium oxide (CaO) have been intensively studied in the last five years (Guoxin and Hao, 2009, Florin and Harris, 2008, Mahishi and Goswami, 2007, Hanaoka et al. 2005). The CaO can be used as a sorbent via absorption process to absorb CO_2 at about 500-700°C and in a calcination process to release the CO_2 at 800-900°C (Shimizu et al. 1999 and Stefan et al. 2009). The concept of CO_2 absorption based on calcium-based sorbents is usually written as follows

Calcination process

$$CaCO_3(s) \rightarrow CaO(s) + CO_2(g) \quad (1)$$

Absorption process

$$CaO(s) + CO_2(g) \rightarrow CaCO_3(s) \quad (2)$$

CO_2 absorption have been widely studied in the last few decades with the use of CaO as calcium based sorbents in a carbonator, thermal gravimetric analysis, small circulating fluidize bed, particle acceleration tube, carbonator-calciner and pressurize fluidized bed combustor. (Abanades et al. 2005, Grasa and Abanades, 2007, Grasa et al. 2008, Chen et al. 2007, Abanades, 2002 and Salvador et al. 2003). However, so far none of the researchers uses CaO-sand mixture as a bed material for the absorption process in the fluidized bed reactor. The purpose of using the sand is because it has a very good fluidization characteristic as compared to CaO alone. The behavior of CaO-sand mixture in a cold model is presented here. The hot model experiment has also been done to determine the CO_2 absorption using the optimum condition obtained from the cold model. The purpose of this work is to study the fluidization characteristics of various ratios of CaO-sand mixtures and to determine the CO_2 absorption using producer gas. In order to gain more information about the behavior of CaO-sand mixtures ratio, the effect of CaO particle sizes, air volume flow rate, and intake air pressure on the hydrodynamic characteristics were investigated.

2. Experimental set-up

2.1 Cold model

Hydrodynamic study with pressurized air at ambient temperature has been conducted in a bubbling fluidized bed (BFB). Figure 1 shows the schematic diagram of the experimental setup. The fluidized bed is made of transparent perspex with an inner diameter of 74 and 600 mm height. The distributor plate has five nozzles each having four holes of 1.6 mm diameter.

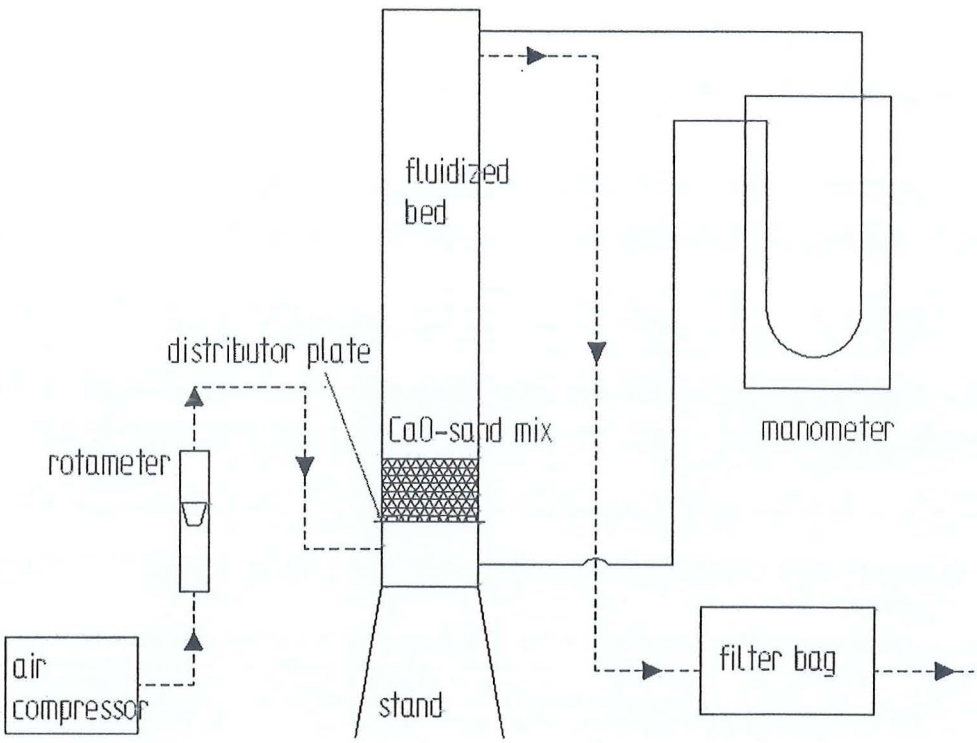

Figure 1: Schematic diagram of a cold model experimental setup.

The BFB is connected to a 1.9 kW air compressor model HD47C to provide compressed air at various pressures and a filter bag to capture any of the bed material entrained from the fluidized bed. A simple U-tube manometer is connected across the fluidized bed to monitor the pressure drop with different bed height and particle size. The CaO mixed with sand was used as the bed material in the fluidized bed. Variables affecting the fluidization height were studied such as CaO-sand mixture percentages (70, 60, 50, 40% CaO), air volume flow rates (5, 15, 25, 35, 45, 55 $Lmin^{-1}$), air intake pressures (2, 3, 4, 5, 6 bar) and different CaO particles sizes (100, 500 and 1000 micron). For each run, 4 cm arbitrary chosen constant height of the CaO was measured (Table 1) and mixed with 1.7, 2.7, 4 and 6 cm of sand where the particle size used were 100, 500 and 350 micron.

Table 1: CaO weight for 4 cm height

CaO particle size (micron)	CaO weight (g)
100	172.30
500	198.65
1000	240.00

The air flow from the air compressor was set to the desired pressure and volume flow rate. During the experiment, the hydrodynamic behaviors such as the bed expansion height and the pressure drop across the fluidized bed were recorded. Fine particles found in the filter bag was weighed and recorded at the end of the experiment. The experiment was repeated 8 times to obtain the average value and to determine the measurement error. The mean value (μ), standard deviation (σ) and the standard error of the mean (σ_μ) samples were calculated using the Equation 3, 4 and 5: (Richard and David, 1998)

$$\mu = \frac{\sum x}{n} \tag{3}$$

$$\sigma = \sqrt{\frac{(x_1 - \mu)^2 + (x_2 - \mu)^2 + ... + (x_n - \mu)^2}{n}} \tag{4}$$

$$\sigma_\mu = \frac{\sigma}{\sqrt{n}} \tag{5}$$

2.2 Hot model

The experiments with simulated gas consisting of 20% CO_2 and 80% N_2 at selected temperatures have been conducted in a bubbling fluidized bed reactor (BFBR). Figure 2 shows the schematic diagram of the experimental setup. The BFBR is made from stainless steel 304. The same distributor plate was used to allow the simulated gas to flow. Figure 3 shows a photo of the bubbling fluidized bed reactor.

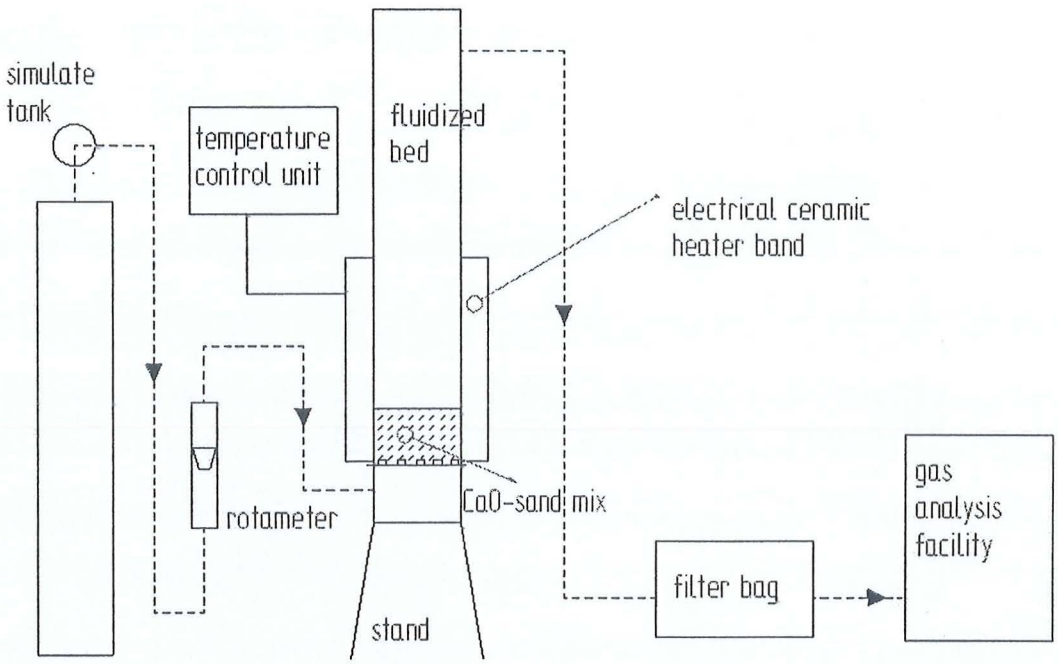

Figure 2: Schematic diagram of a hot model experimental setup

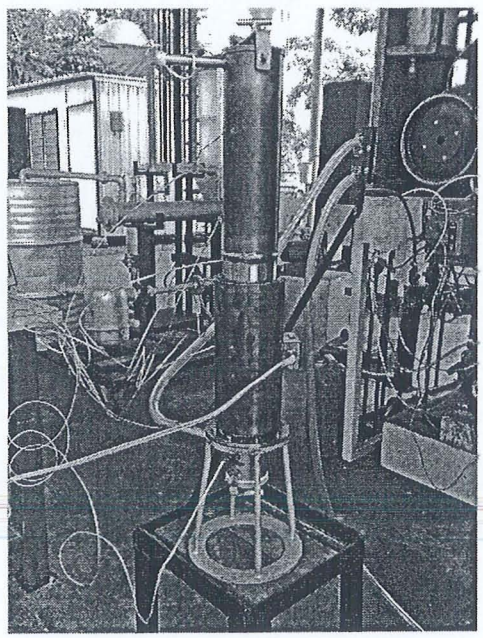

Figure 3: The photo of the bubbling fluidized bed reactor (BFBR)

A 3 kW electrical ceramic heater band was coupled to the fluidized bed for heating the CaO-sand mixture at various temperatures. The selected variables obtained from the cold model experiment were studied in this work such as CaO-sand mixture percentages (50 and 40% CaO), volume flow rates (15, 25 and 45 $Lmin^{-1}$), intake pressures (2, 3 and 4 bar) and the CaO particle size of 1000 micron. For each run, 4 cm constant height of the 1000 micron CaO was used and mixed with 4 and 6 cm of the 350 micron sand. These particles sizes were sieved using an Endecott's multi-layer test sieve shaker.

The controller of the ceramic heater band was set to 900°C. When the temperature inside the fluidized bed reached 650-750°C, the simulated gas was set to 2 bar using a pressure regulator with a gas flow rate of 15 $Lmin^{-1}$ controlled by a rotameter. The simulated gas at the exit of the fluidized bed was collected by gas sampling bags at an interval of 5 minutes for 60 minute experiment. The gas samples were analyzed in a gas chromatograph (Hewlett Packard Module 4890). Some of the fine particles found in the filter bag was weighed and recorded at the end of each experiment. At the end of the absorption experiment the CO_2 is released from the $CaCO_3$ via calcination process at temperature above 850°C.

3. Results and discussion

Table 2 shows the data obtained from the 100 micron cold model experiment. Using these data, the error analysis has been done. The commercial software "SPSS Statistics 17" was used to perform the analysis. Table 3 shows the results obtained from the analysis and Figure 4 is a graph representing the data.

Table 2: Repeated experiment data of the cold model experiment, (time operation: 1 min)

CaO Particle size (micron)	100
CaO mixture (%)	70
Pressure, P (bars)	2
Volume flow rate, Q (Lmin-1)	25
	Bed expansion height (cm)
Run 1	6.0
Run 2	5.8
Run 3	6.0
Run 4	6.0
Run 5	6.2
Run 6	6.0
Run 7	5.8
Run 8	6.0

Table 3: Results analysis "SPSS Statistics 17"

Statistics

cm

N	Valid	8
	Missing	6
Std. Error of Mean		.04532
Std. Deviation		.12817
Variance		.016
Range		.40
Minimum		5.80
Maximum		6.20

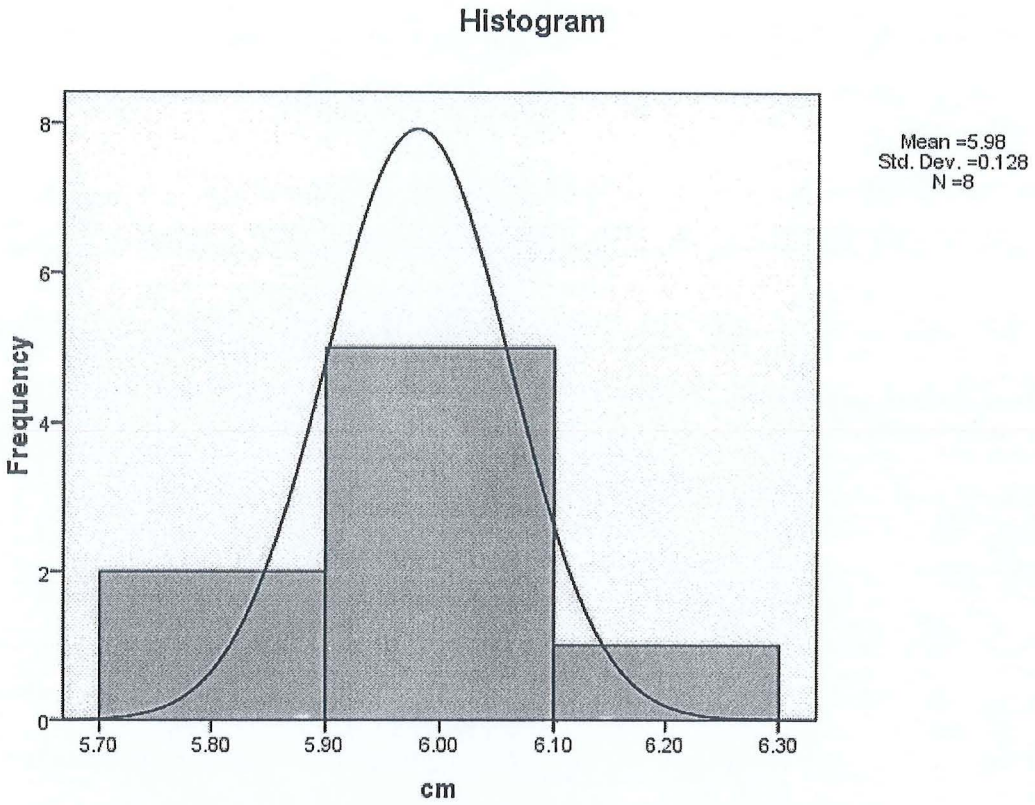

Figure 4: The data based on "SPSS Statistics 17"

From Table 3, the standard error of mean obtained is 0.04532 and the population of the data is in the normal distribution curve (Figure 4). The analysis show the data is in a good accepted value.

3.1 Cold model

3.1.1 Effect of the CaO-sand mixture ratio

The bed expansion heights at constant air pressure are shown in Figures 5-9. The amount of CaO percentages in the mixture has an effect on the bed expansion height at constant pressure and particle size. With the decrease in CaO percentages from 70, 60, 50 to 40%, it was found that the bed expansion height

increased between 0 to 17 cm for all the cases of pressures 2 to 6 bars. This is evidence of adhesive force between CaO particles such as the Van der Waals force, the electronic force and the liquid bridge that exists in the powder as defined by Hiroaki, 2006. The force reduced with the increase of sand % in the mixture. This can be seen in Figure10. Although the fluidization was observed at all pressures however at the early stages of the experiment at 2 and 3 bars for the particle sizes of 100 and 500 micron, there is no bed expansion indicating that there was no fluidization at 70% CaO mixture (Figures 5 and 6). At that percentage, the amount of sand was insufficient to overcome the adhesive forces of the CaO particles which prevented fluidization. The similar trends can be seen where there is no bed expansion for 1000 micron, when the CaO mixture was 70% and 60% at low superficial velocity of 0.02-0.06 m sec^{-1}. These happened at pressures of 2 to 5 bar (Figures 5-8). In Figure 9, no fluidization happened at low superficial velocity of 0.02 m sec^{-1} for all percentages of CaO mixture with 1000 micron particle size. The superficial velocity has not reach the minimum superficial velocity where the upward force exerted by the fluid on the particles is not sufficient to force the weight of CaO-sand mixture of the bed.

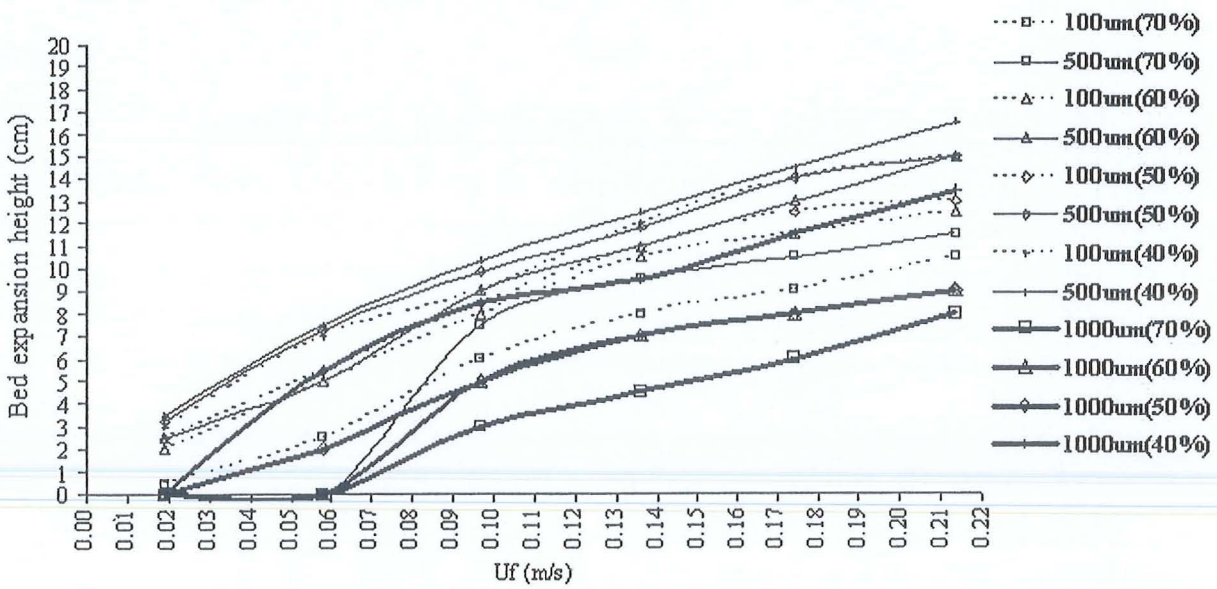

Figure 5: Relation between CaO-sand mixture percentages, air volume flow rate and particles size on the bed expansion height (2 bars)

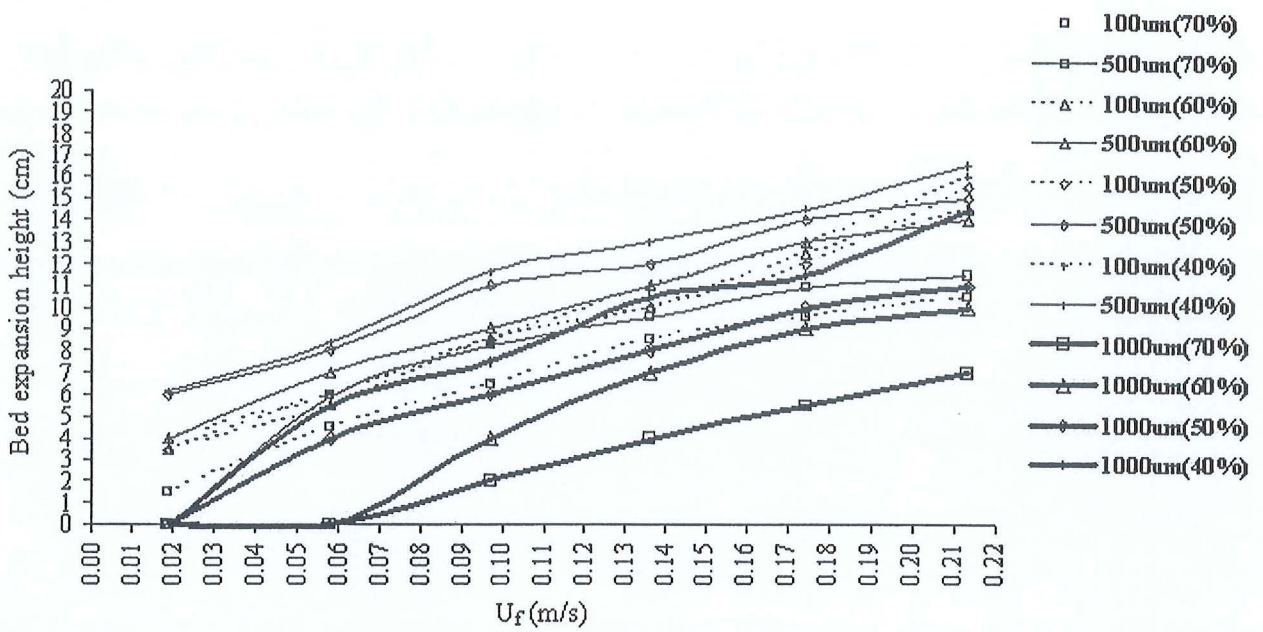

Figure 6: Relation between CaO-sand mixture percentages, air volume flow rate and particles size on the bed expansion height (3 bars)

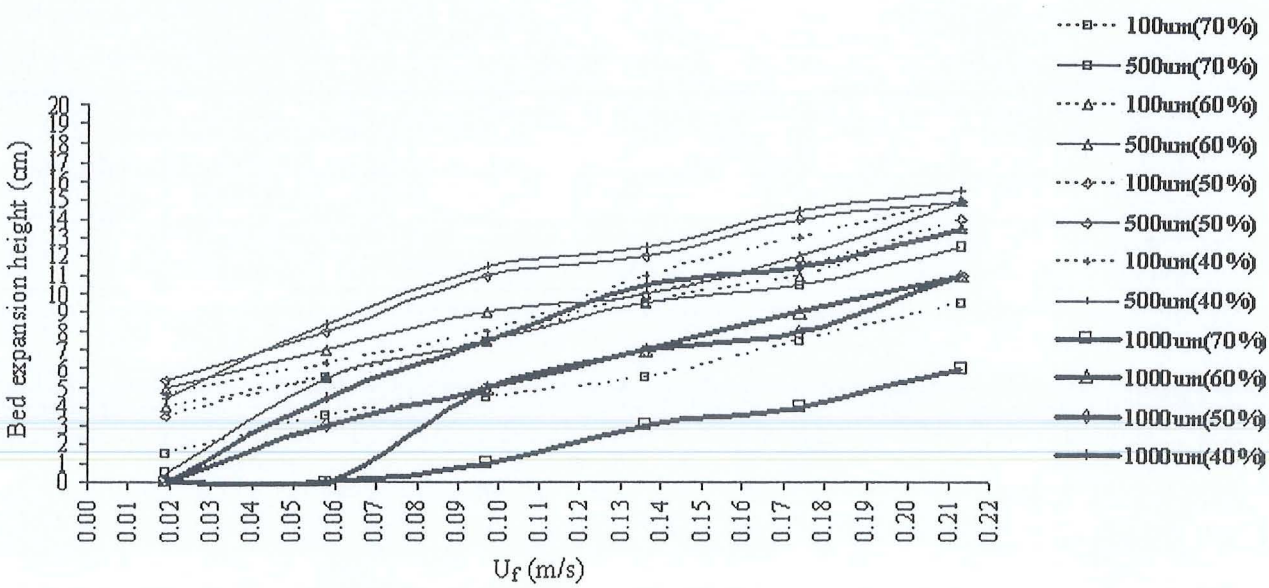

Figure 7: Relation between CaO-sand mixture percentages, air volume flow rate and particles size on the bed expansion height (4 bars)

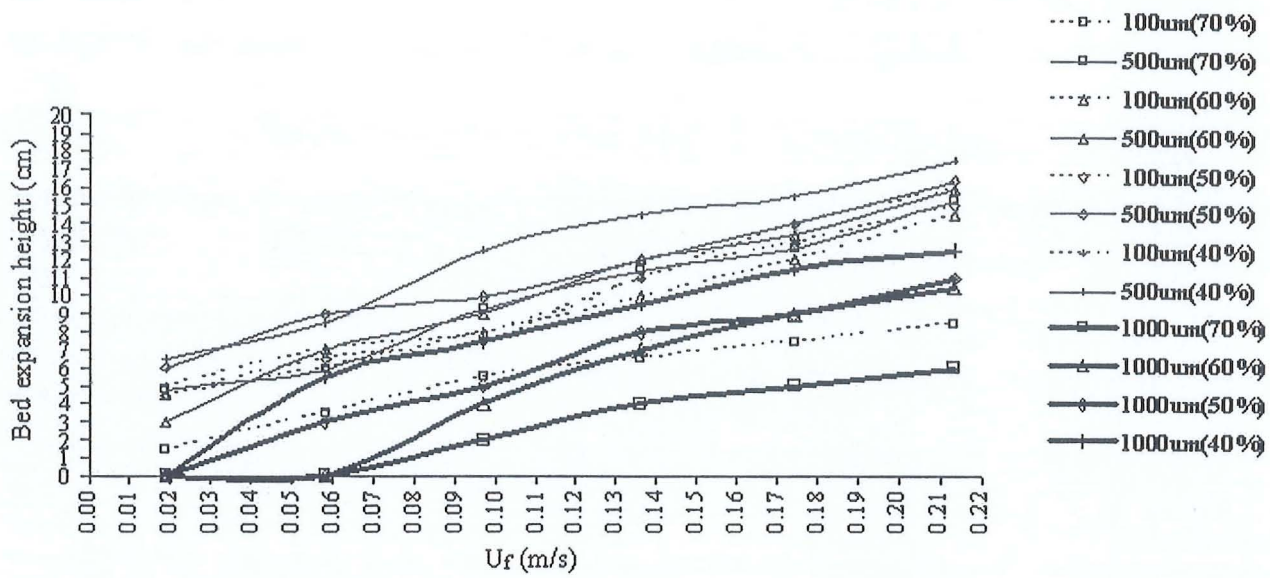

Figure 8: Relation between CaO-sand mixture percentages, air volume flow rate and particles size on the bed expansion height (5 bars)

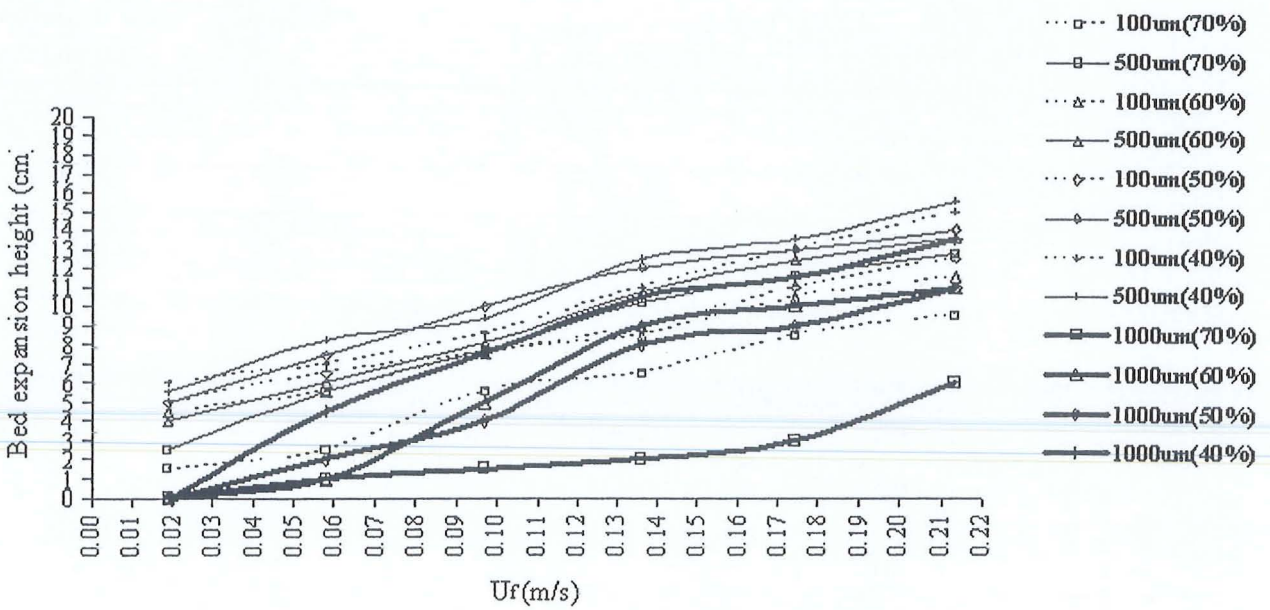

Figure 9: Relation between CaO-sand mixture percentages, air volume flow rate and particles size on the bed expansion height (6 bars)

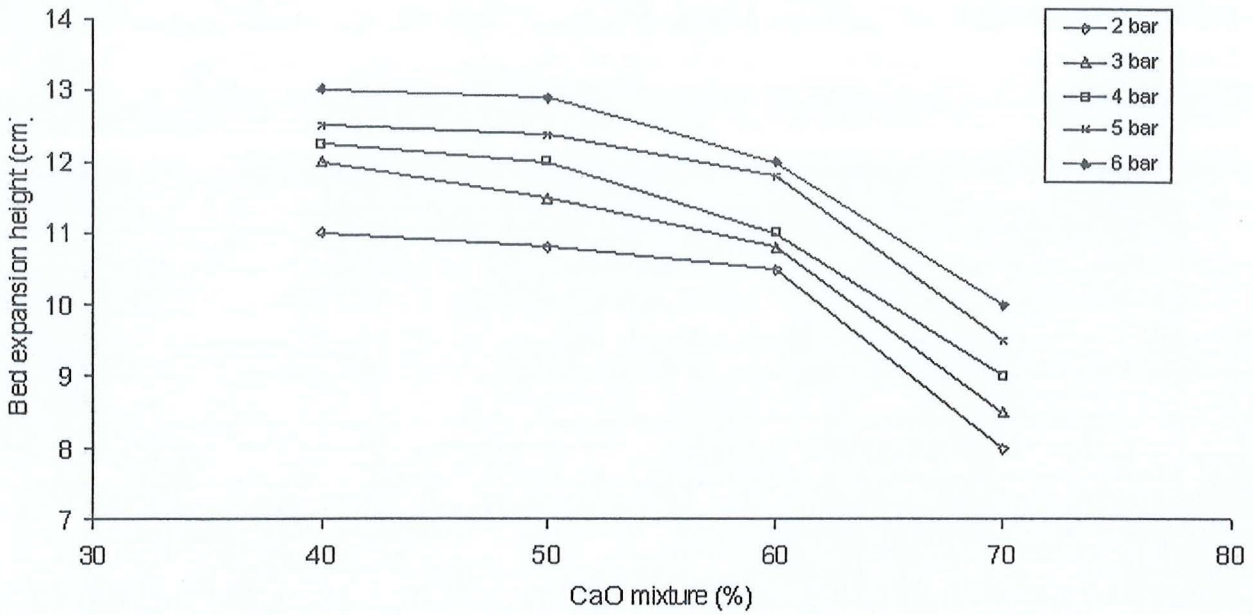

Figure 10: Effect of CaO-sand % mixture on the bed height (constant: 100 micron, 35 $Lmin^{-1}$)

The pressure drop in the chamber increased when the percentage of CaO in the mixture decreased at 2 bar air pressure (Figure 11). Similar observation was found for air pressures of 3, 4, 5 and 6 bars. The increase of pressure drop in the reactor was due to the increase in the amount of mass of the solid particles (CaO-sand) in every mixture.

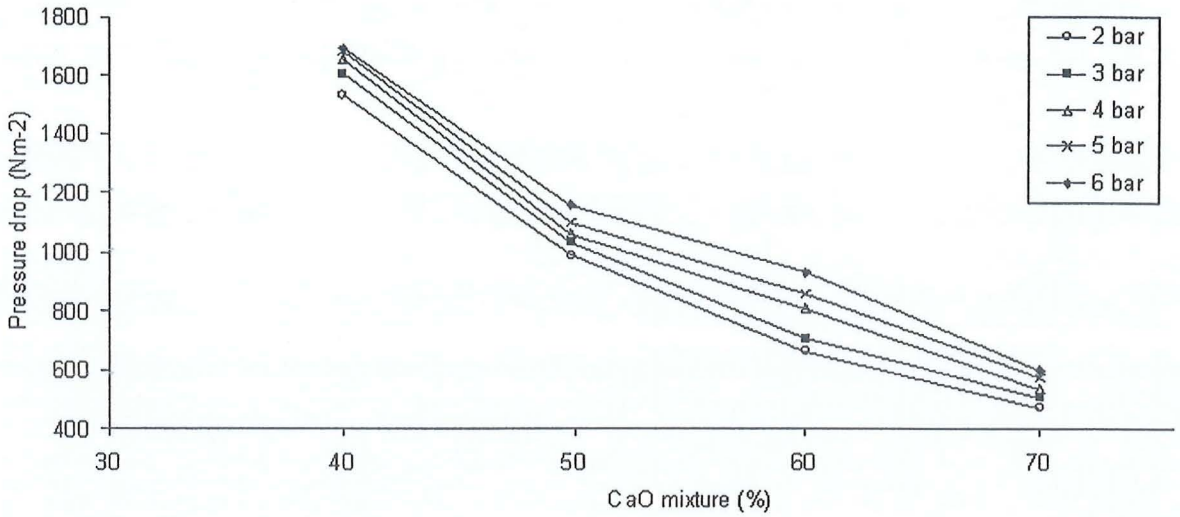

Figure 11: Effect of CaO-sand % mixture on the pressure drop (constant: 100 micron, 35 $Lmin^{-1}$)

3.1.2 Effect of the CaO particle size

To investigate the effect of particle size on the bed expansion height for all air pressures, three particle sizes of 100, 500 and 1000 micron CaO were tested. Previous studies showed that the particle size in the range of 150-500 micron (Geldart Group B) with density of 1500-4000 kgm^{-3} has a better fluidization compared to the 30-150 micron (Geldart Group A) and above 600 micron (Geldart Group D). Relatively in this experiment, as seen in Figure 12, the CaO particle size of 500 micron has better bed expansion height than 100 and 1000 micron. The 500 micron particle size has negligible inter-particle forces compared to 100 micron, which can fluidize well with vigorous bubbling actions. The 1000 micron particle size is large and dense, hence the inter-particle forces between particles are negligible, but the high density of the particle makes it difficult to fluidize and enormous amount of air is needed to overcome the size and weight.

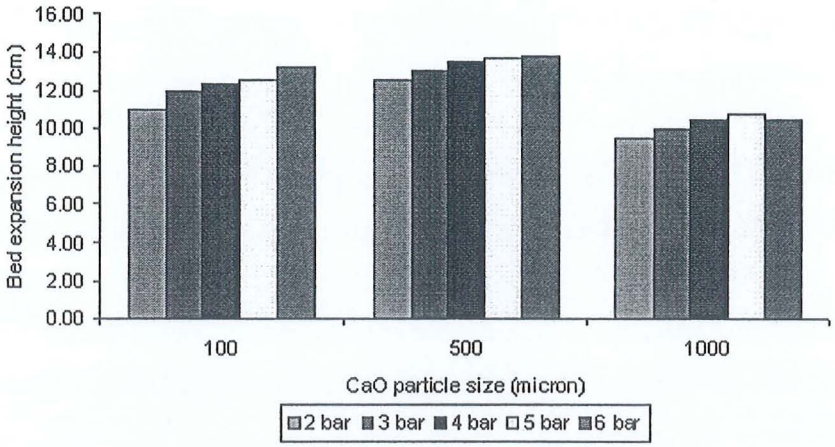

Figure 12: Effect of CaO particle size on the bed height (constant: 40% CaO mixture, 35 $Lmin^{-1}$)

3.1.3 Effect of the air volume flow rate and air pressure

Air volume flow rate and pressure are important operating parameters in fluidized bed. The CaO–sand mixture was tested at 5, 15, 25, 35, 45 and 55 $Lmin^{-1}$ flow rates with different air pressures to determine the hydrodynamic behavior. As seen in Figure 13, when the air volume flow rate increases, the bed expansion height also increased at all air pressures except at the volume flow rate less than 15 $Lmin^{-1}$ at 2 bar and 5 $Lmin^{-1}$ at 3 bar (500 micron and 70% CaO mixture), where no fluidization was found. Only one rat hole was observed for low air pressure. This is due to strong interacting force between the molecules of the 70% CaO particles, even though the minimum fluidization velocity has been reached. Figure 14 shows the picture of this phenomenon.

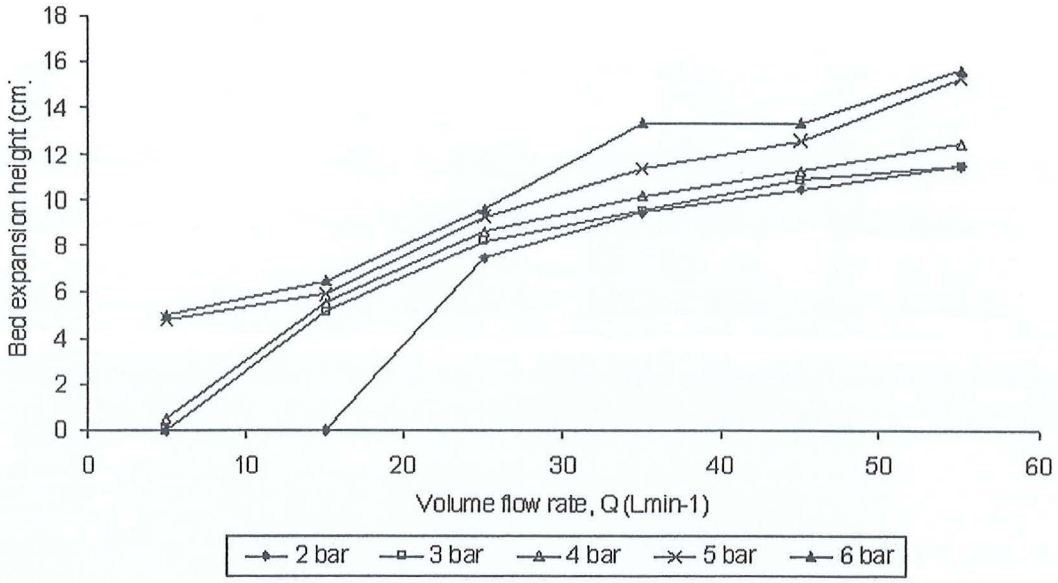

Figure 13: Effect of the air volume flow rate and air pressure on the bed height (constant: 70% CaO mixture, 500 micron particle size)

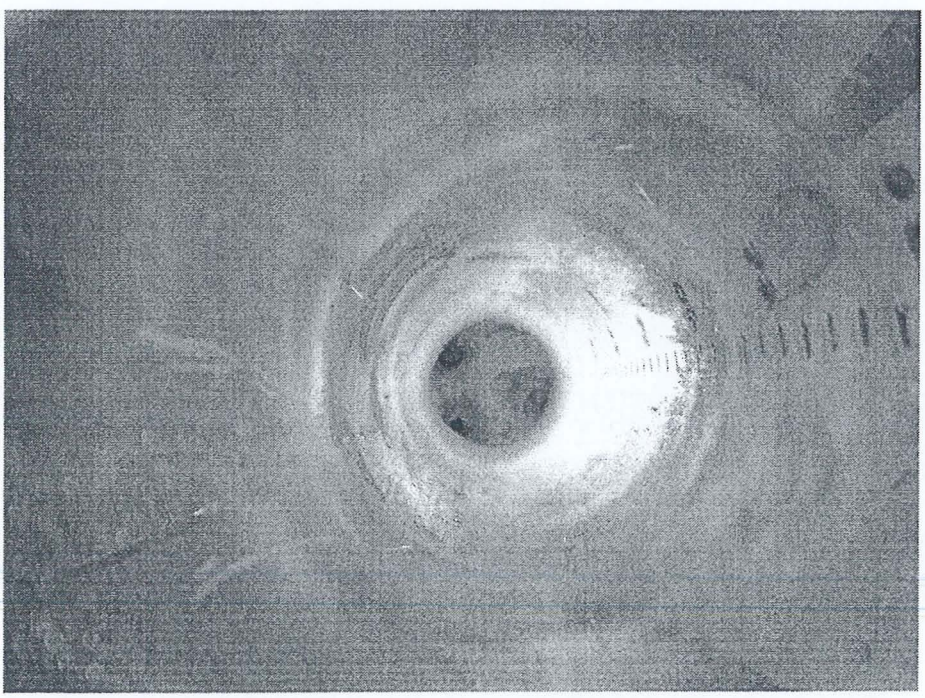

Figure 14: Rat holes formed during operation (15 $Lmin^{-1}$, 500 micron, 70% CaO mixture, 2 bars)

3.1.4 Mass flow rate of CaO entrained

The test results of mass flow rate of CaO entrained from the reactor are shown in Figures 15-19. In Figure 16, its can be observed that with the increase of the air flow rate, the mass flow rate of the CaO entrained increases The minimum and maximum mass flow rates obtained are 0.2 and 1.42 g/min. For 1000 micron particle size, its can be seen that the mass flow rate of CaO entrained was constant at 0-0.6 g/min for all CaO-sand mixture percentages and pressures, although the air flow rate has been increased. The high density of the 1000 micron particle is the factor why the mass flow rate of CaO entrained is less compared to 100 and 500 micron.

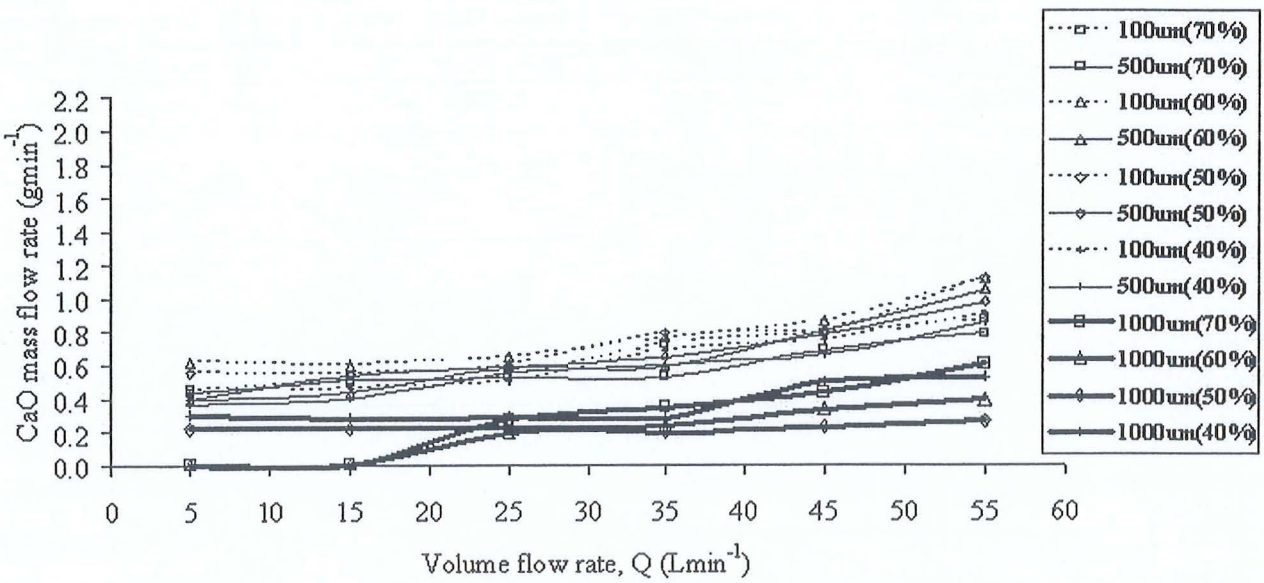

Figure 15: Amount of CaO entrained from reactor (2 bars)

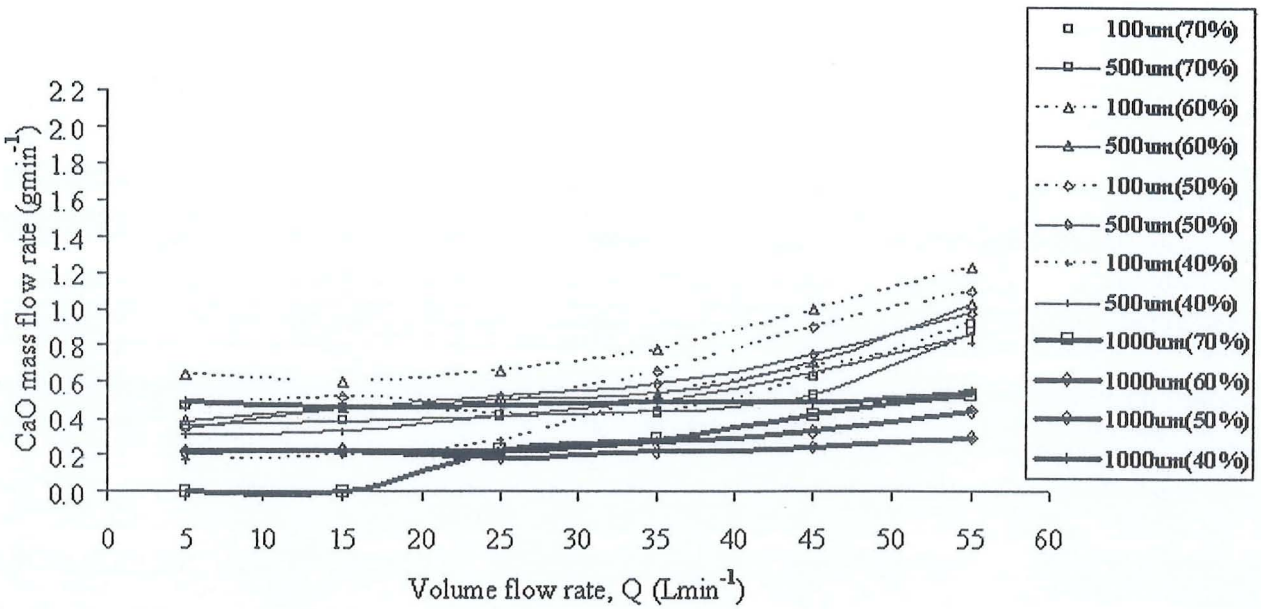

Figure 16: Amount of CaO entrained from reactor (3 bars)

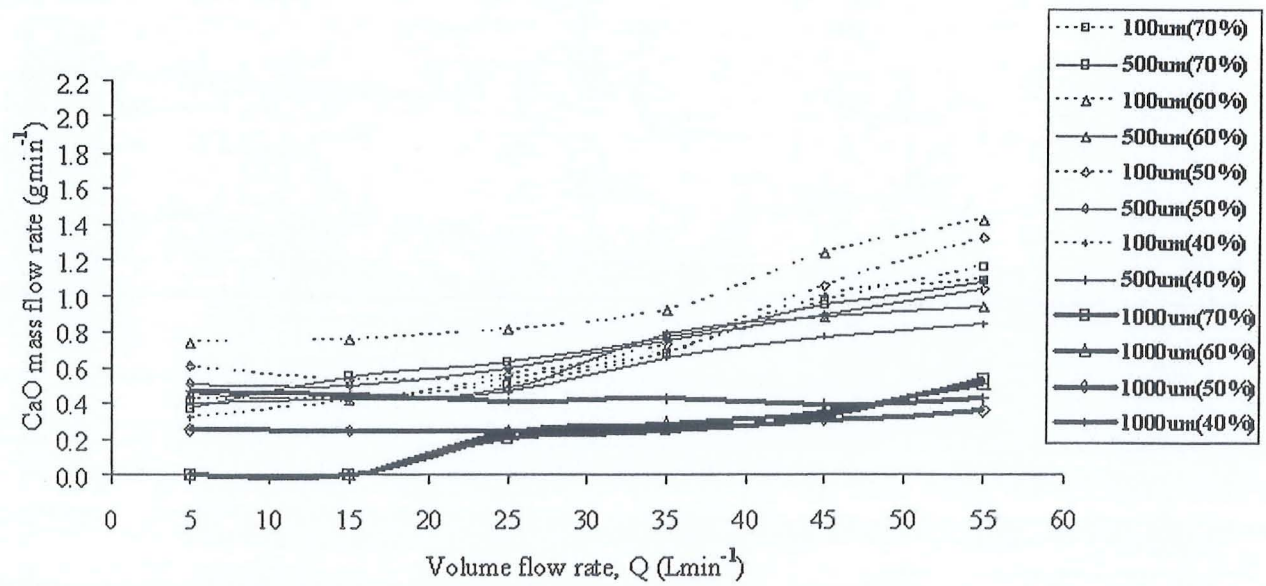

Figure 17: Amount of CaO entrained from reactor (4 bars)

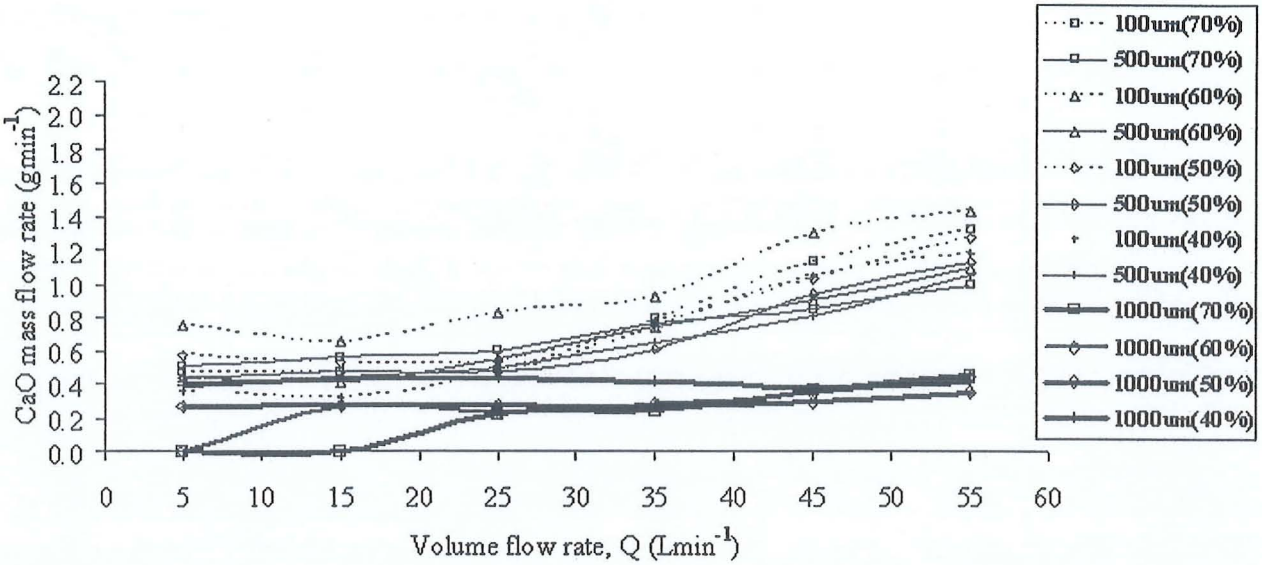

Figure 18: Amount of CaO entrained from reactor (5 bars)

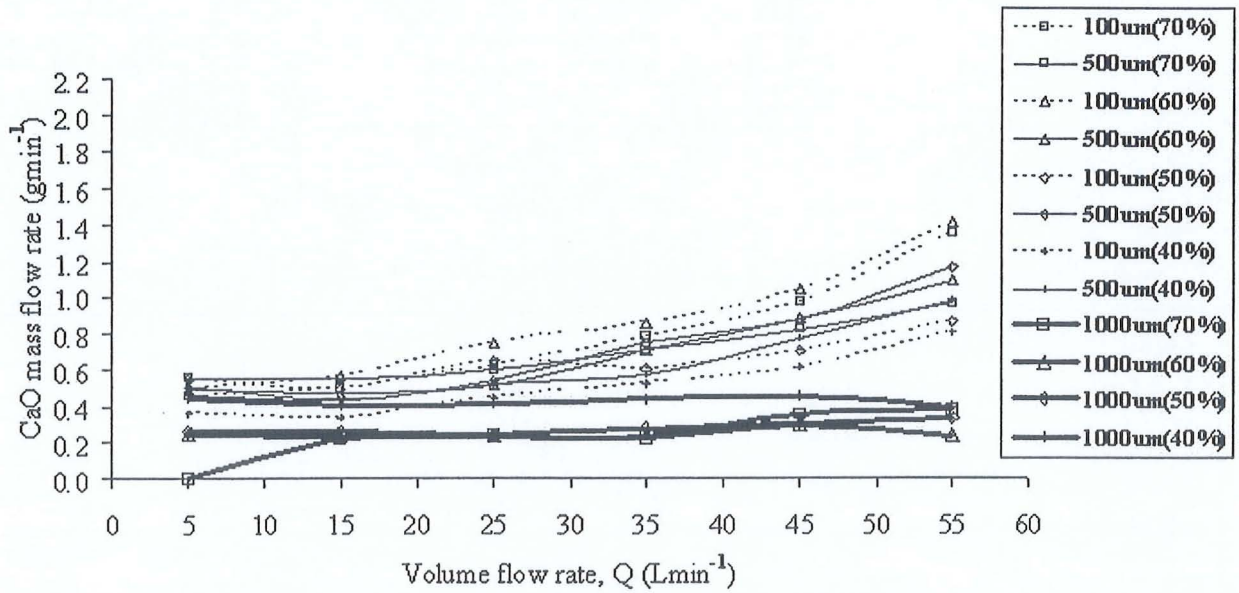

Figure 19: Amount of CaO entrained from reactor (6 bars)

3.2 Hot model

In the hot model experiment, only 1000 micron particle size was used to determine CO_2 absorption. The CaO percentages of 50 and 40 were found to have a good fluidization at all air pressure (2 - 6 bar). In addition to that, the volume flow rate of air between 15 – 55 $Lmin^{-1}$ was also found to give a good fluidization. Using the simulated gas contents (20% CO_2 and 80% N_2) the CO_2 absorption by CaO has been determined experimentally.

3.2.1 Transient effect of CO_2 absorption using simulated gas

The CO_2 detected by gas chromatograph versus time at constant pressure 2, 3 and 4 bars for 50% and 40% CaO-sand mixture are shown in Figures 20-22. The 50% CaO-sand mixture showed low CO_2 composition compared to 40% CaO-sand mixture. The 20% CO_2 absorption only occurred for 15 min at 2 bars then increased to the max 20% vol. CO_2 in 60 min (Figure 20). This similar trend was also found at the pressures of 3 and 4 bars. In 40% CaO-sand mixture, the collision between the CaO and sand particles is higher compared to 50% CaO-sand mixture percentage because of the large amount of sand in the 40% CaO mixture. Some of the 1000 micron particle size became smaller and then entrained from the reactor. The ability of the 40% CaO-sand mixture to absorb 20% CO_2 becomes less.

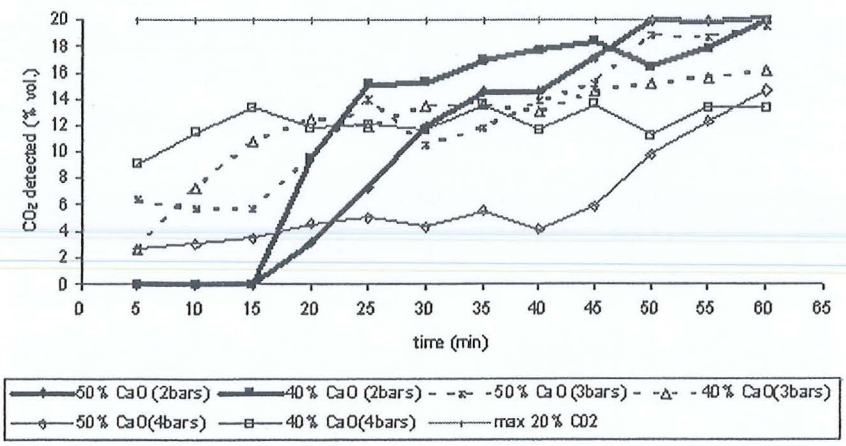

Figure 20: CO_2 absorption of 50% and 40% CaO-sand mixture. (15 $Lmin^{-1}$, 650-750^{O}C, 1000 micron)

The comparison of the CO_2 composition of the simulated gas for volume flow rate 25 and 45 $Lmin^{-1}$ is shown in Figures 21 and 22. The CO_2 gas supplied from the simulated gas tank to the reactor is constantly absorbed for about 60 mins at flow rate 45 $Lmin^{-1}$. It is observed that at 50% and 40% CaO mixture, the best condition for CO_2 absorption is at 3 bar. The CO_2 detected by gas chromatograph shows that only around 4% vol. CO_2 was found in the simulated gas. This is the minimum CO_2 composition obtained compared to the other conditions.

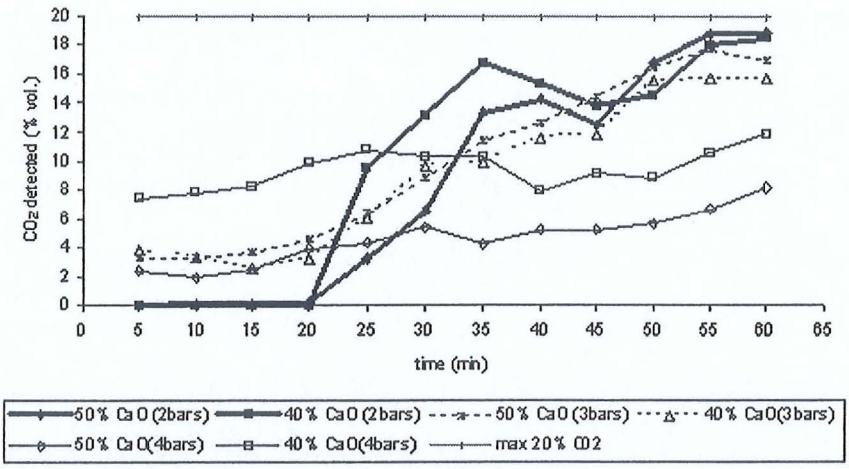

Figure 21: CO_2 absorption of 50% and 40% CaO-sand mixture. (25 $Lmin^{-1}$, 650-750^{O}C, 1000 micron)

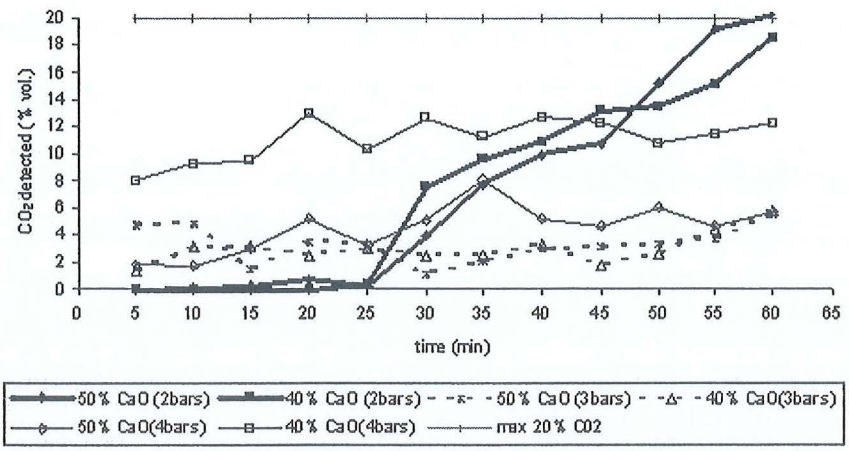

Figure 22: CO_2 absorption of 50% and 40% CaO-sand mixture. (45 $Lmin^{-1}$, 650-750^{O}C, 1000 micron)

3.2.2 CaO entrained from reactor

The test results of CaO entrained from the reactor is shown in Figure 23. With the increase in volume flow rate and pressure, the CaO entrained increases from 32.7 – 82.3 gram for 50 and 40% CaO mixtures. The highest amount of CaO entrained was found at 4 bar and 40% CaO mixture for all volume flow rates. The collision between the CaO and sand particles is higher at 40% CaO-sand mixture compared to 50% CaO-sand mixture because of the large amount of sand. Some of the 1000 micron particle size became smaller and then entrained faster from the reactor because of the high pressure and volume flow rate.

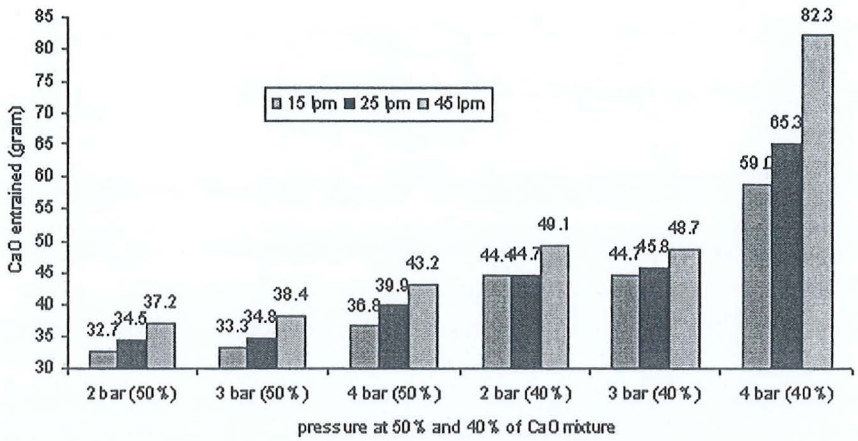

Figure 23: CaO entrained from reactor

4. Conclusion

The characteristic behaviors of CaO-sand mixtures in the cold and hot model experiments (650-750°C) for CO_2 absorption of producer gas using simulated gas were determined. The investigation result is listed as follows:

4.1 Cold model

1. The CaO percentages of 60, 50 and 40 for 100 and 500 micron sizes were found to have good fluidization for all air pressures (2, 3, 4, 5 and 6 bars).
2. The volume flow rates of air between 15 – 55 $Lmin^{-1}$ were found to have a good fluidization for all variables except for 70% CaO – sand mixture at 100 and 500 micron sizes.
3. The 500 micron CaO particle size shows better fluidization characteristics behavior compared to 100 and 1000 micron particles size. However the 1000 micron CaO size is utilized because it gave good fluidization with less CaO entrained compare to 100 and 500 micron sizes.

4. The 50 and 40% CaO mixture for 1000 micron were found to have a good fluidization in the range 15-55 $Lmin^{-1}$ for all air pressures (2, 3, 4, 5 and 6 bars). Only at 5 $Lmin^{-1}$, no fluidization was found.

4.2 Hot model

1. The 50% CaO-sand mixture percentage shows good CO_2 absorption gas compare to 40% CaO-sand mixture percentage at all pressures (2, 3, 4 bars) and volume flow rates (15, 25, 45 $Lmin^{-1}$).
2. At volume flow rate of 45 $Lmin^{-1}$, the CO_2 gas is absorbed constantly for 60 min and has the best CO_2 absorption for 50% and 40% CaO-sand mixture at 3 bar.
3. The highest amount of CaO entrained was at 4 bar and 40% CaO-sand mixture at volume flow rates 15, 25 and 45 $Lmin^{-1}$.

Appendix A: Nomenclature

μ_g	dynamic viscosity of the carrier gas (kg/m.s)
ρ_g	density of the carrier gas (kg/m^3)
d_s	solid particles size (m)
Ar_{numb}	Archimedes number
μm	micron meter
x	data sample
n	number of data sample

References

Abanades, J.C, Anthony, E.J., Wang, J., Oakey, J.E., 2005. Fluidized bed combustion system integrating CO2 capture with CaO. Environmental Science and Technology, 39(8):2861-2866.

Abanades, J.C., 2002. The maximum capture efficiency of CO2 using a arbonation/calcinations cycle of $CaO/CaCO_3$. Chemical Engineering Journal, 90:303-306.

Chen X.P., Zhao C.W. and Zhao C.S. 2009. Characteristics of regeneration reaction of dry potassium-based sorbent for CO_2 capture. Journal of Engineering Thermophysics, 30: 2145-2148

Chen Z., Lim C.J., Grasa J.R., 2007. Study of limestone particle impact attrition. Chemical Engineering Science, 62:867-877.

Dogru M., Howarth C.R., Akay G., Keskinler B. and Malik A.A., 2002. Gasification of hazelnut shells in a downdraft gasifier. Energy, 27: 415-427.

Felice L.D., Courson C., Jand N., Gallucci K., Foscolo P.U. and Kiennemann A, 2010. Catalytic biomass gasification: Simultaneous hydrocarbons steam reforming and CO_2 capture in a fluidised bed reactor. Chemical Engineering Journal, 154: 375-383.

Flamant G., Fatah N., Steinmetz D., Murachman B. and Laquerie C., 1991. High-temperature velocity and porosity at minimum fluidization. Critical analysis of experimental results. International Chemical Engineering, 31: 673-684.

Florin N.H. and Harris A.T., 2008. Enhance hydrogen production from biomass with in situ carbon dioxide capture using calcium oxide sorbents. Chemical Engineering Science, 63: 287-316.

Geldart, D. Types of gas fluidization, 1973. Powder Technology, 7: 285-292.

Grasa G.S. and Abanades J.C., 2007. Narrow fluidized beds arranged to exchange heat between a combustion chamber and a CO2 sorbent regenerator. Chemical Engineering Science, 62:619-626.

Grasa G.S., Abanades J.C., Alonso M., Gonzalez B., 2008. Reactivity of highly cycled particles of CaO in a carbonation/calcination loop. Chemical Engineering Journal, 137(3):561-567.

Guo Q., Yue G., Suda T. and Sato J., 2003. Flow characteristics in a bubbling fluidized bed at elevated temperature. Chemical Engineering and Processing, 42: 439-447.

Guoxin, H. and Hao, H., 2009. Hydrogen rich fuel gas production by gasification of wet biomass using a CO2 sorbent. Biomass and Bioenergy, 8: 91-98.

Hanaoka T., Yoshidaa, Y., Fujimotoa, S.J., Kamei, K., Harada, M., Suzuki, Y. et al., 2005. Hydrogen production from woody biomass by steam gasification using a CO2 sorbent. Biomass and Bioenergy, 28:63-68.

Hassanzadeh A. and Abbasian J. 2010. Regenerable MgO-based sorbents for high-temperature CO_2 removal from syngas: 1. Sorbent development, evaluation, and reaction modeling. Fuel, 89: 1287-1297.

Hiroaki M., Higashitani K., Yoshida H., 2006. Powder Technology Handbook, Third Edition. Taylor & Francis 2006, New York.

Jorapur, R.M. and Rajvanshi, A.K., 1995. Development of sugarcane leaf gasifier for electricity generation. Biomass and Bioenergy, 8: 91-98..

Mahishi M.R. and Goswami D.Y., 2007. An experiment study of hydrogen production by gasification in presence of CO_2 sorbents. International Journal of Hydrogen Energy, 32: 2803-2808.

McCabe W.E., Smith J.C. and Harriott P., 2004. Unit Operations of Chemical Engineering (7th Edition). McGraw Hill, New York.

McKendry, P., 2002a. Energy production from biomass (part 1): overview of biomass. Bioresource Technology, 83: 37-49.

McKendry, P., 2002b. Energy production from biomass (part 3): gasification technologies. Bioresource Technology, 83: 55-63.

Munoz, M., Moreno, F., Morea, R.J., Ruiz, J. and Arauzo, J., 2000. Low heating value gas on spark ignition engines. Biomass and Bioenergy, 18: 431-439.

Richard I.L. and David S., 1998. Statistics for Management (7th Edition). Pearson, India.

Salvador C., Lu D., Anthony E.J., Abanades, J.C., 2003. Enhancement of CaO for CO2 capture in a FBC environment. Chemical Engineering Journal, 96:187-195.

Shimizu T., Hirama, T., Hosoda, H., Kitano, K., Inagaki, M., Tejima, K, 1999. A twin fluid bed reactor for removal of CO2 from combustion process. Trans. IChemE, 77:62-66.

Sjostrom S. and Krutka H. 2010. Evaluation of solid sorbents as a retrofit technology for CO_2 capture.Fuels, 89: 1298-1306.

Sridhar G., Paul P.J. and Mukunda H.S, 2001. Biomass derived producer gas as a reciprocating engine fuel-an experimental analysis. Biomass and Bioenergy, 21: 61-72.

Stefan, K., Christoph, P., Reinhard, R., Hermann, H., Tonja, M.M., Michael, S., 2009. H2 rich product gas by steam gasification of biomass with in situ CO2 ansorption in a dual fluidized bed system of 8 MW fuel input. Fuel Processing Technology, 90:914-921.

Svoboda K. and Hartman M., 1981. Influence of temperature on incipient fluidization of limestone, lime, coal ash and corundum. Industrial Engineering Chemistry Process Design and Development, 20: 319-326.

Uma R, Kandpal T.C and Kishore V.V.N., 2004. Emission characteristics of an electricity generation systems in detail in diesel alone and diesel fuel modes. Biomass and Bioenergy, 27: 195-203.

Wen C.Y., 2003. Handbook of Fluidization and Fluid-Particle Systems. CRC Press, New York.

Wu C. and Williams P.T. 2010. A novel Ni–Mg–Al–CaO catalyst with the dual functions of catalysis and CO_2 sorption for H_2 production from the pyrolysis–gasification of polypropylene. Fuels, 89: 1435-1441.

Yates J.G., 1983. Fundamentals of fluidized-bed chemical processes. Butterworth-Heinemann.

Zainal Z.A., 1996. Performance and characteristics of a biomass gasifier system. Ph.D dissertation, Division of Mechanical Engineering and Energy Studies, School of Engineering, University of Wales, College of Cardiff, United Kingdom.

Zainal Z.A., Rifau A., Quadir G.A. and Seetharamu K.N., 2002. Experimental investigation of a downdraft biomass gasifier. Biomass and Bioenergy, 23: 283-289.

Zhao C.W., Chen X.P. and Zhao C.S. 2009. CO_2 capture using dry potassium-based sorbents in a bubbling fluidized-bed reactor. Proceedings of the 20th International Conference on Fluidized Bed Combustion, 562-568.

Proceedings of the Conference of the International Journal of Arts and Sciences, Feb 16-19, 2009, Vol. 1(8), ISSN: 1943-6114, Orlando, Florida, United State of America.

Review of Producer Gas Quality from Biomass Gasification Technology in University of Science Malaysia (USM), Engineering Campus

Mohammud M. M.*, Zainal Z. A.

School of Mechanical Engineering, Universiti Sains Malaysia Eng. Campus, Pulau Pinang.
Email: madek123@streamyx.com,mezainal@yahoo.com*

Abstract

Biomass gasification is a possible alternative to the direct use of fossil fuel energy. Producer gas, produced from biomass gasification process can be used to generate power and electricity. However, the inefficiencies in the technology make the biomass gasification uneconomical. The power loss called de-rating of the engines fuelled by producer gas-air mixture is found to be around 20% to 40% in SI engine and 15% to 30% in CI engine and this is the major problem why this research is studied. The power de-rating is cause due to lower heating value of the producer gas-air mixture from biomass gasification process. Thus in this paper, a highlights of several years and current works on the producer gas quality from biomass gasification activities is carried out. These works have been done by bio-energy research group in School of Mechanical Engineering, USM. The conclusion has been determined where the new method has to be design to improve the previous producer gas quality. This method is expected to increase the heating value of producer gas from low heating value (4-6 MJ/Nm^3) to medium heating value (10-16 MJ/Nm^3).

Keywords: Biomass, Gasification, Producer Gas, Power loss, Design

1. Introduction

Biomass is a renewable and carbon neutral energy resource. Sources such as wood and other forms including energy crops, agricultural and forestry wastes are some of the main renewable energy resources available. During World War II, wood or biomass gasification is the biomass energy which has been proven reliable and had been extensively used for transportation and also on the farm systems[1,2]. Although the biomass gasification is an old technology, but it still can be used as an alternative way to substitute the conventional energy source. Currently, the interest in such technology is increasing due to the increase of fuel prices and the global warming problem.

Biomass gasification means incomplete combustion of biomass resulting in production of combustible gases consisting of Carbon monoxide (CO), Hydrogen (H_2) and traces of Methane (CH_4). This mixture is called producer gas. Producer gas, produced from biomass gasification process can be used to generate power and electricity. However, the inefficiencies in the technology make the biomass gasification uneconomical. The power loss called de-rating of the engines fuelled by producer gas-air mixture is found to be around 15% to 30% in CI engine and 20%

to 40% in SI engine. The power de-rating is cause due to lower heating value of the producer gas-air mixture from biomass gasification process. Thus in this paper, a highlights of several years and current works on the producer gas quality from biomass gasification activities is carried out. These works have been done by bio-energy research group in School of Mechanical Engineering, USM. The conclusion has been determined where the new method has to be design to improve the previous producer gas quality.

2. Producer Gas

Biomass which can be burnt or gasified will produces a producer gas or dirty raw gas mixture that composed of Hydrogen (H_2), Carbon Monoxide (CO), Carbon Dioxide (CO_2), Water (H_2O), Methane (CH_4) and various light hydrocarbons along with undesirable dust (ash and char), tar, Ammonia (NH_3), alkali (mostly potassium) and some other trace contaminants[3,4]. About 40% of the producer gas is combustible gas and when putting in the internal combustion engine, it can generally operate the engine. Theoretically, the compositions of producer gas-air mixture were contained 15-20% H_2, 10-15% CO, 9-15% CO_2, 3-5% CH_4 and 40-50% N_2 by volume. In table 1 shows the gas composition by percentage volume of the producer gas-air mixture from other researches.

Table 1: Gas compositions in producer gas reported by other researchers.

	~% Vol.				
	H_2	CO	$C0_2$	CH_4	N_2
Munoz et al.[5]	14	22	13	3	48
Sridhar et al.[2]	19	19	12	2	48
Zainal et al.[6], Hoi[7], Hollingdale[8], Walawender et al.[9].	15	24	15	2	44
Dogru et al.[10]	15	19	16	2	48
Uma et al. [11]	14	19	10	2	55

Producer gas must have energy content greater than 4 MJ/Nm^3 for most application to run the Diesel engine. The energy content can be calculated from the energy content of the components using low and high heating values for each gas as show in equation 1.

$$HV_{pg} = \sum (\%vol.)_g (HV)_g \qquad (1)$$

Where HV: heating value (MJ/m^3)
pg : producer gas
g : gas

The energy of producer gas can be classified into three types, low (4-6 MJ/Nm^3), medium (10-16 MJ/Nm^3) and high heating values (40 MJ/Nm^3)[12]. The low heating value used air as agent for gasifying, the medium heating value used steam or oxygen and the high heating value used hydrogen as a gasifying agent. In table 2 shown the comparisons of the heating value of the producer gas obtained from other researches.

Table 2: Comparisons of heating value of producer gas with other researchers.

Researchers	Heating Value (MJ/NM^3)
Graham et. al [13]	6.39
Walawender et. al [9]	5.51
Xu et. al [14]	5.5
Hoi [7]	4.97
Jorapur et. al [15]	5.04
Zainal [16]	5.34
Sridhar et. al [2]	4.67
Dogru et. al [10]	5.15
Uma et. al [11]	4.60

3. Research Activities in USM

3.1 Introduction

Works on biomass renewable energy in USM has been done since 1998, where the main research is on the combustion characteristics of the gasifier and the performance of the IC engine. These works have been done by local and international USM researchers and postgraduate students.

The engine mostly used for the research is diesel engine. It is because diesel engine can be run with producer gas in a 'dual fuel' mode with minor modification.

3.2 Experimental Setup

Overall view of the gasifier and engine test are shown in Figure 1 and Figure 2. The 5 kW single cylinder direct injection, Yanmar diesel engine on dual fuel mode of operation coupled with a 10 kg capacity downdraft gasifier was used. The small blocks of furniture wood were used as biomass fuel. The producer gas flow rate was set to 80 L/min and 100 L/min, and engine was set at 2000 and 2400 rpm with 20%, 40% and 60% load. The engine was coupled to the dynamometer to measure the performance of the engine.

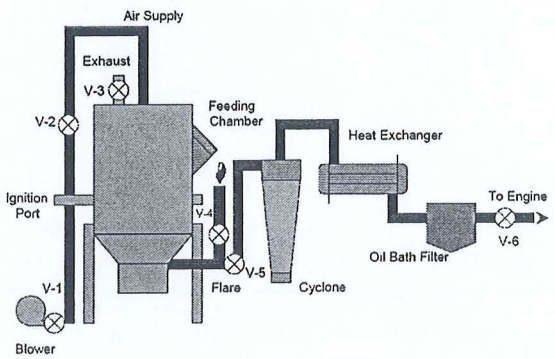

Figure 1: Downdraft Gasifier

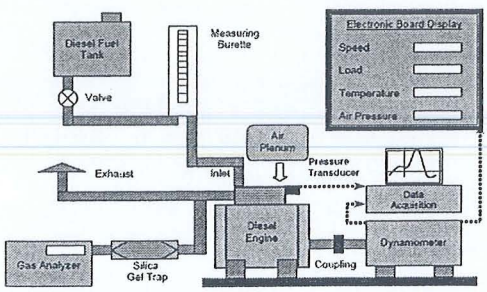

Figure 2: 5 kW Single Cylinder Direct Injection Diesel Engine System

The second research was done using 50 kg capacity downdraft gasifier and 20 kW direct injections Perkins diesel generator engine connected to an electrical load bank in the dual fuel mode operation. The 50-100 mm cubes off cut furniture wood were used as biomass fuel. The various flow rate of producer gas between 40–80 Nm^3/hr was used, and engine was set at constant 1500 rpm with loads of 9, 12, 15 and 18 kW. Figure 3 shows the overall view of the system.

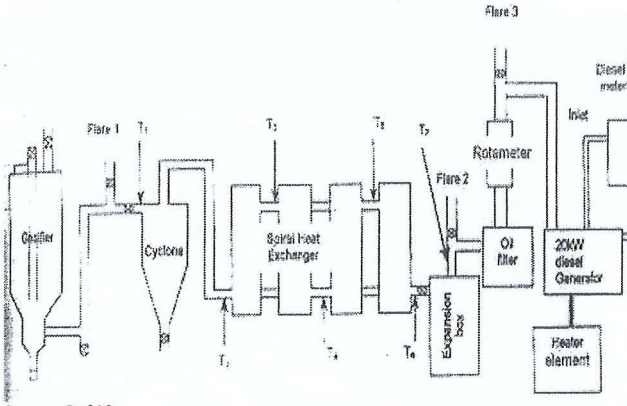

Source: Ref 18

Figure 3: Overall View of 50 kg Capacity Downdraft Gasifier connected to 20kW Diesel Generator

3.3 Results and Discussions

Table 3 shows the data comparison of gas composition and heating value of the producer gas that has been found from experiment in USM. The gas composition of the producer gas has been measured and analyzed using Gas Chromatograph HP module 4890 with helium as a carrier gas.

Table 3: Data comparison of gas composition and heating value of the producer gas

	% Vol.						
Gases	H_2	CO	CO_2	CH_4	N_2	O_2	Heating Values (MJ/NM^3)
Ref.17	10.25	8.9	19.18	6.68	54.99	0	4.67
Ref.18	8.3	8.9	19.2	6.7	54.9	2	4.42

It shows that the heating value of the producer gas is in the range of low heating value about 4-6 MJ/Nm^3. The most possible reason was due to lower percentage volume of combustible gases such as H_2, CO and CH_4 in the producer gas.

In dual fuel mode operation of 10 kg capacity downdraft gasifier, the maximum diesel replacement was recorded as 60%. Figure 4 and 5 show the graphs of the thermal efficiency (BTE) versus the brake mean effective pressure (BMEP) of dual fuel mode. It can be seen that the BTE for diesel fueled producer gas was 36-41% lower than diesel alone at 2000 rpm and 2400 rpm, respectively. A similar trend also found for these two graphs. These phenomenons were due to higher mass of fuel which results of rich mixture, thus lead to incomplete combustion in the engine's cylinder.

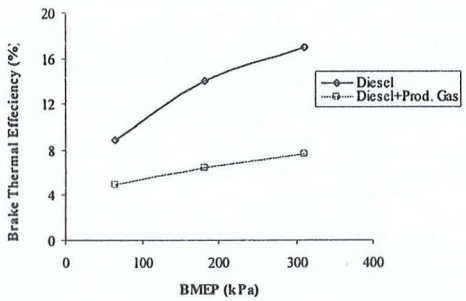

Figure 4: BTE versus BMEP at 2000 rpm

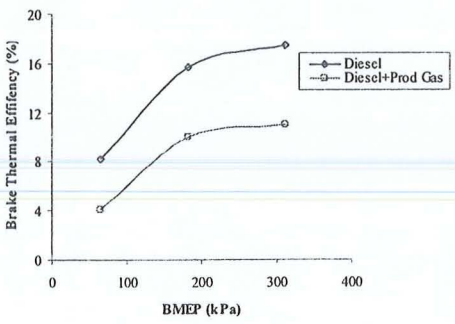

Figure 5: BTE versus BMEP at 2400 rpm

For 50 kg capacity downdraft gasifier experiment, the maximum diesel replacement was recorded as 80% at 12 kW load. Figure 6 shows the graph of the engine efficiency versus electrical load dual fuel mode. The efficiency of engine was dropped in dual fuel mode. It was found that the engine efficiency for various loads with producer gas dropped haft compared to the diesel alone. This phenomenon was due to lower flame speed of the combustion for diesel fueled producer gas compared to diesel alone.

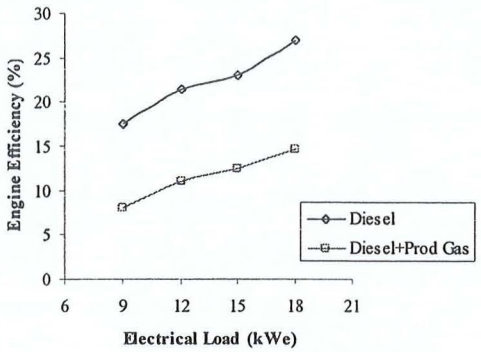

Figure 6: Engine Efficiency versus Electrical Load Dual Fuel Mode.

In terms of combustion analysis, it can be seen the most possible reason why the power de-rating was observed is due to lower heating value of the producer gas-air mixture from biomass gasification process.

4. Design of Reactor

4.1 Introduction

A reactor has been designed by Universiti Sains Malaysia and fabricated by local manufacturing firm. The purpose of the design is to improve the previous producer gas quality. The concept of the reactor is to remove the carbon dioxide by chemical absorption process using calcium oxide

(CaO). The reactor has been name as CO_2 absorption reactor.

4.2 Dimension of CO_2 Absorption Reactor

The construction features of CO_2 absorption reactor consist of main furnace, stand and nozzle distributor plate. The reactor was developed for the laboratory scale purpose. The overall height of the reactor is 877.5 mm. The inner diameter of the reactor is 74 mm and the outer diameter is 88 mm. The main furnace and nozzle distributor plate are made from stainless steel 304 to detain high temperature operation around 1200°C while the stand made from mild steel. The height of the furnace is 600 mm and has 6 holes for the thermocouples. The nozzle distributor plate has five small nozzles that protrude up from the surface of the plate. Each nozzle has four holes of 1.6 mm diameter to allow gas to flow. Figure 7 shows the picture of CO_2 absorption reactor.

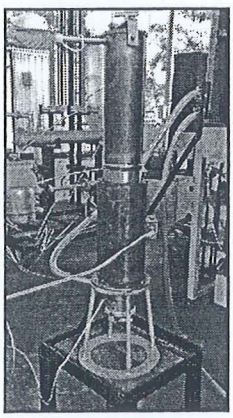

Figure 7: The CO_2 Absorption Reactor.

5. Conclusion

A highlight of several years and current works on the producer gas quality from biomass gasification activities in USM have been carried out. The comparison between other researchers on heating value of the producer gas has been presented. The design and fabricate of the CO_2 absorption reactor has been done due to lower heating value of the producer gas from biomass fuel and the power de-rating of Diesel engine. Therefore, the medium heating value around 10-16 MJ/Nm^3 of producer gas will be expected and decrease the power de-rating of the Diesel engine. The experiment will be start in the next stage of the studies.

References

1. Solar Energy Research Institute (1979). Generator Gas – The Swedish Experience from 1939-1945, SERI, Golden, Colorado. Chap. 1.

2. Sridhar, G.; Paul, P.J.; and Mukunda, H.S. (2001). Biomass derived producer gas as a reciprocating engine fuel-an experimental analysis. Biomass and Bioenergy, **21**, pp 61-72.

3. Zhang, R.; Brown, R.C; Suby, A. and Cummer, K. (2004). Catalytic destruction of tar in biomass derived producer gas. Energy Conversion and Management, **45**, pp 995-1014.

4. Mukunda H.S[2]., Shrinivasa U., Paul P.J., Dasappa S. and Rajan N.K.S (2000). Stand Alone Small Power Level Systems, *Combustion, Gasification and Propulsion Lab, IIS.*

5. Munoz, M.; Moreno, F.; Morea-Roy, J.; Ruiz, J. and Arauzo, J. (2000). Low heating value gas on spark ignition engines. Biomass and Bioenergy, **18**, pp 431-439.

6. Zainal, Z.A.; Ali Rifau; Quadir, G.A. and Seetharamu, K.N. (2002). Experimental

investigation of a downdraft biomass gasifier. Biomass and Bioenergy, **23**, pp 283-289.

7. Hoi, W.K. (1992). Gasification of rubberwood in a downdraft gasifier. Ph.D. dissertation, The University of Aston in Birmingham.

8. Hollingdale (1983). Production gas fuelling of a 20kW output engine by gasification of solid biomass. Oversea Development Natural Resources Institute, ISBN 09528245.

9. Walawender, W.P.; Chern, S.M. and Fan, L.T. (1985). Wood chips gasification in a commercial downdraft gasifier. In: Overend RP, editor. Fundamentals of thermo chemical biomass conversion, Amsterdam: Elsevier Applied Science, pp 911.

10. Dogru, M.; Howarth, C.R.; Akay, G.; Keskinler, B. and Malik, A.A. (2002). Gasification of hazelnut shells in a downdraft gasifier. Energy, **27**, pp 415-427.

11. Uma, R; Kandpal, T.C and Kishore, V.V.N (2004). Emission characteristics of an electricity generation systems in detail in diesel alone and diesel fuel modes. Biomass and Bioenergy, **27**, pp 195-203.

12. McKendry, P. (2002). Energy production from biomass (part 2): conversion technologies. Bioresource Technology, Vol. 83, pp. 47-54.

13. Graham, R.G. and Huffman, D.R. (1981). Gasification of Wood in A Commercial Scale Downdraft Gasifier. In: Energy from Biomass 5, Lake Buena Vista, FL. Jan., pp 633-650.

14. Xu, G.Q and Wang, Y. (1988). Gasification of Agricultural and Forestry Residues. 23rd Proc. Intersociety Energy Conversion Engineering Conference. Denver, U.S.A.

15. Jorapur, R.M. and Rajvanshi, A.K. (1995). Development of Sugarcane Leaf Gasifier for Electricity Generation. Biomass and Bioenergy. Volume 8, No. 2, pp 91-98.

16. Zainal, Z.A. (1996). Performance and Characteristics of A Biomass Gasifier System. Ph.D Dissertation, Division of Mechanical Engineering and Energy Studies, School of Engineering, University of Wales, College of Cardiff, United Kingdom.

17. Andi, M. (2005). Combustion Characteristics of Diesel Engine Fueled with Producer Gas from Downdraft Gasifier System. M.Sc Thesis, School of Mechanical Engineering, Universiti Sains Malaysia, Malaysia.

18. Muharnif. (2005). Performance of Small Scale Downdraft Gasifier Power Plant. M.Sc Thesis, School of Mechanical Engineering, Universiti Sains Malaysia, Malaysia.

The Ability of CaO-Sand Mixture to Absorb CO_2 Composition of the Simulated Gas and Producer Gas using Bubbling Fluidized Bed Reactor

Mahadzir M. M., Faculty of Mechanical Engineering, Universiti Teknologi MARA (UiTM), Penang Branch Campus, Pulau Pinang, Malaysia.
Zainal Z. A., School of Mechanical Engineering, Universiti Sains Malaysia (USM), Eng. Campus, Pulau Pinang, Malaysia.

Abstract: Producer gas, from biomass gasification process can be used to generate power as an alternative to fossil fuel. The producer gas consists of carbon monoxide (CO), hydrogen (H_2), methane (CH_4), carbon dioxide (CO_2) and nitrogen (N_2). It has low calorific value (LCV) around 4-6 MJ/Nm^3 because of CO_2 content is about 10-20 % by volume. The used of calcium oxide, CaO to absorb CO_2 in the producer gas can make biomass technology more viable because its low calorific value can be increase. In this paper, the ability of CaO-sand mixture to absorb CO_2 composition of the simulated gas (consisting of 20% CO_2 and 80% N_2) and the simulated producer gas (consisting 16% CO_2, 24% CO, 12% H_2 and 48% N_2) have been shown. The experiment has been conducted using 1000 micron CaO particle size, 50% CaO mixture with gas pressure of 3 bar and the volume flow rate of 45 $Lmin^{-1}$ at 650-750°C. The result obtained shows the CO_2 composition of the simulated gas was decreased from 20% to 2% for 60 min operated. The same treads of CO_2 absorption also occurred for the simulated producer gas where the CO_2 composition decreased from 16% to 8% average when operated for 60 min.

Keywords: CaO-sand mixture, Simulated Producer Gas, Bubbling Fluidized Bed Reactor, CO_2 Absorption.

Introduction

Biomass is one of the sources of renewable energy where it is derived from living or recently living organism such as wood, waste, and alcohol fuels. Currently, the interest in biomass technology gets a lot of attention due to the increase in fuel prices and issues of global warming (Guoxin and Hao, 2009, Florin and Harris, 2008, Mahishi and Goswami, 2007, Hanaoka et al. 2005). Therefore, people are now considering using biomass gasification to generate electricity and power as an alternative to fossil fuel.

Biomass gasification, means incomplete combustion of biomass resulting in the production of combustible and non combustible gases consisting of Carbon monoxide (CO), Hydrogen (H_2), Methane (CH_4), Carbon dioxide (CO_2) and Nitrogen (N_2) (McKendry, 2002) called producer gas. The content of CO_2 in the producer gas is about 10-20 % by volume (Hollingdale et al., 1983, Walawender et al., 1985, Munoz et al., 2000, Sridhar et al., 2001, Zainal et al., 2002, Dogru et al., 2002 and Uma et al., 2004) causes the low calorific value to be about 4-6 MJ/Nm^3 (Graham and Huffman, 1981, Jorapur and Rajvanshi, 1995 and Zainal 1996). To increase the low calorific value of the

producer gas, the used of the Calcium Oxide, CaO has been studied. The CaO is used to absorb CO_2 in the producer gas. In the present paper, the experiment contained CaO-sand mixture has been conducted in the Bubbling Fluidized Bed Reactor. The purpose of this work is to determine the ability of CO_2 absorption with the simulated gas and producer gas.

Experimental

The experiments with simulated gas consisting of 20% CO_2 and 80% N_2 (simulate tank) at selected temperatures have been conducted in a bubbling fluidized bed reactor (BFBR). Figure 1 shows the schematic diagram of the experimental setup. The BFBR is made from stainless steel 304. The distributor plate was used to allow the simulated gas to flow.

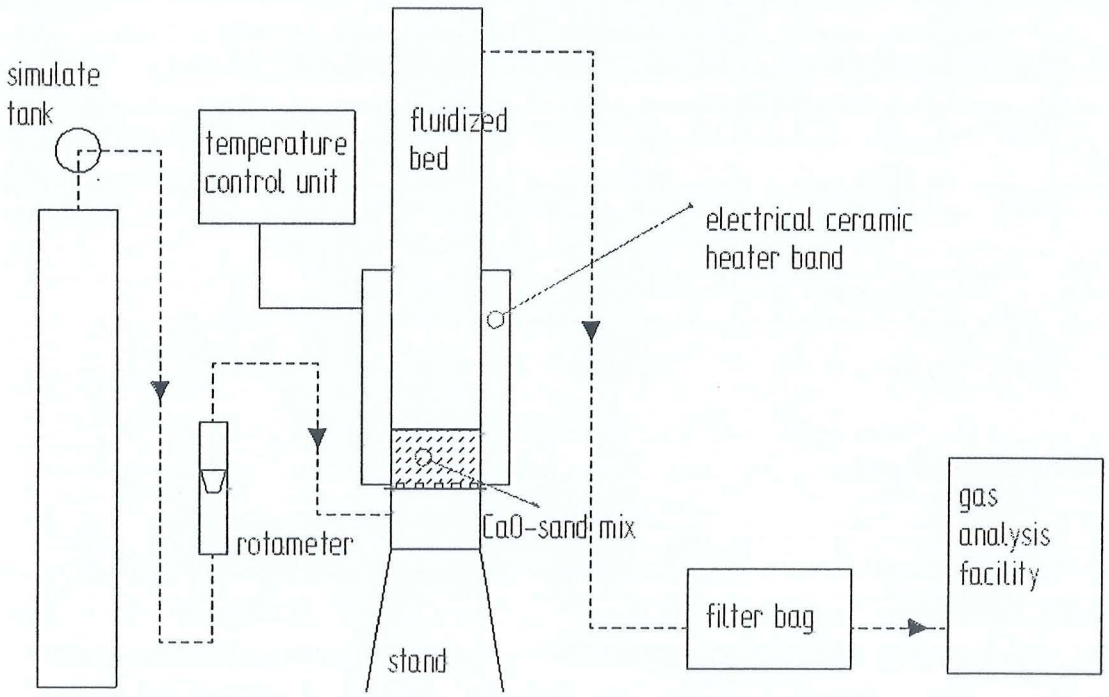

Figure 1: Schematic diagram of a experimental setup

The experiment has been conducted using 1000 micron CaO particle size, 50% CaO mixture with gas pressure of 3 bar and the volume flow rate of 45 $Lmin^{-1}$ at 650-750°C.

A 3 kW electrical ceramic heater band was coupled to the fluidized bed for heating the CaO-sand mixture at various temperatures. First, the controller of the ceramic heater band was set to 900°C. When the temperature inside the fluidized bed reached 650-750°C, the simulated gas was set to 3 bar using a pressure regulator with a gas flow rate of 45 $Lmin^{-1}$

controlled by a rotameter. The simulated gas at the exit of the fluidized bed was collected by gas sampling bags at an interval of 5 minutes for 60 minute experiment. The gas samples were analyzed in a gas chromatograph (Hewlett Packard Module 4890). Some of the fine particles found in the filter bag was weighed and recorded at the end of each experiment. At the end of the absorption experiment the CO_2 is released from the $CaCO_3$ via calcination process at temperature above 850°C for about 90 min. Then the steps were repeated using simulated producer gas contains 16% CO_2, 24% CO, 12% H_2 and 48% N_2 for the next experiment.

Results and Discussion

CO_2 absorption of the simulated gas

The CO_2 detected by gas chromatograph versus time at constant pressure 3 bar for 50% CaO-sand mixture, 1000 micron particle size and 45 $Lmin^{-1}$ at 650-750°C are shown in Figure 2.

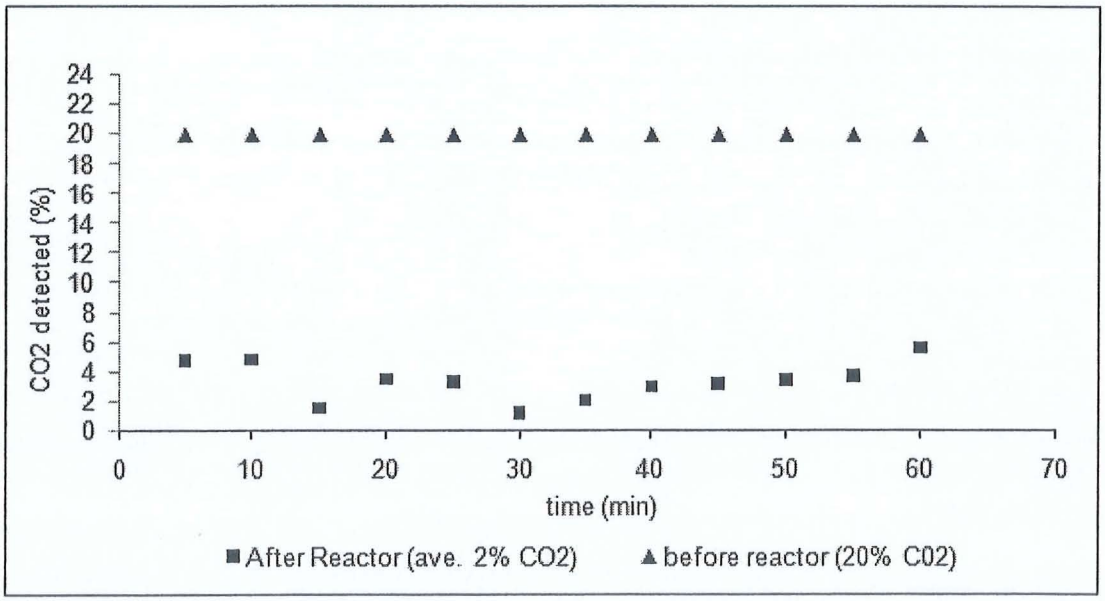

Figure 2: Simulated gas results analysis used gas chromatograph before and after reactor (BFBR) on parameters 50% CaO-sand mixture, 45 $Lmin^{-1}$, 650-750°C and 1000 micron.

The CO_2 gas supplied from the simulated gas tank to the BFBR is constantly absorbed for about 60 min at flow rate 45 $Lmin^{-1}$. It is observed that the 20% CO_2 composition in the simulate gas reduces to the average of 2% CO_2 detected by gas chromatograph and it's occurred for 60 min at 3 bars. The fluidization of the bed material contains CaO and sand help the CO2 gas that passed through the CaO-sand mixture and absorbed the CO2 gas. The purpose of using the sand because it has a very good fluidization characteristic as compared to CaO alone was successful.

CO_2 absorption of the simulated producer gas

In the Figure 3, the result of the CO2 absorption using CaO- sand mixture to absorb CO2 gas composition in the simulated producer gas is shown.

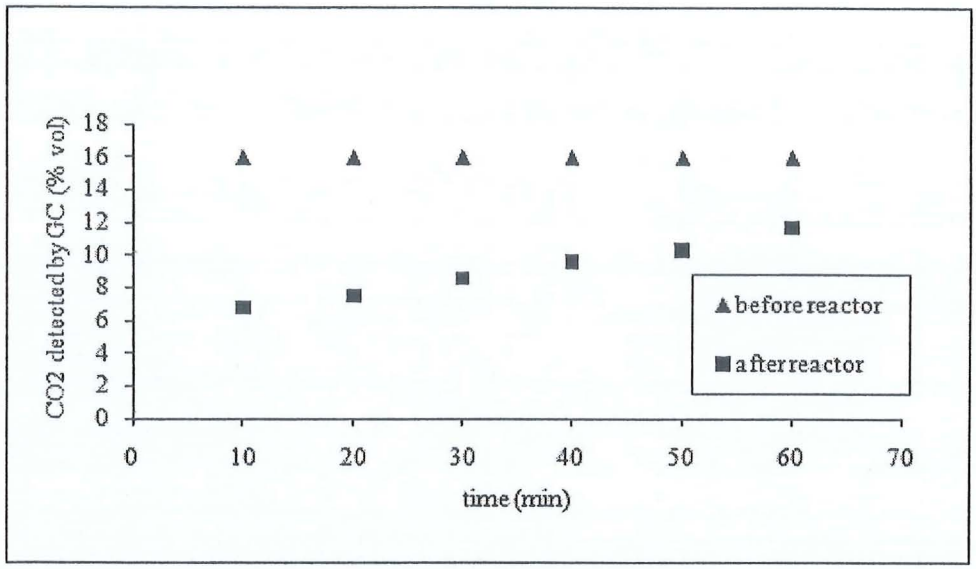

Figure 3: CO_2 composition of the simulated producer gas analysis used gas chromatograph before and after reactor (BFBR) (50% CaO-sand mixture, 45 $Lmin^{-1}$, 650-750^{o}C and 1000 micron)

The CO_2 gas supplied from the simulated producer gas tank contains 16% CO_2, 24% CO, 12% H_2 and 48% N_2 to the BFBR is absorbed for 60 min at the flow rate 45 $Lmin^{-1}$. It is observed that during the first 10 min, the 16% CO_2 composition in the simulate producer gas reduces to 7% CO_2 when it is analyzed by gas chromatograph. Then the percentage of the CO2 composition increase to 11% at end of the experiment for 60 min. Although, the maximum CO2 % is 11% but it still less than 16% CO2 gas supplied from the simulated producer gas tank.

In 50% CaO-sand mixture, the collision between the CaO and sand particles is occurred because of the fluidization phenomena in the bed. Some of the 1000 micron particle size became smaller and then entrained from the reactor. The ability of the 50% CaO-sand mixture to absorb 16% CO_2 composition of the simulated producer gas becomes less at the end of the experiment.

Conclusion

The research study and experiment contained CaO-sand mixture have been carried out in the Bubbling Fluidized Bed Reactor. The parameters used of 1000 micron CaO particle size, 50% CaO mixture with gas pressure of 3 bar and the volume flow rate of 45 $Lmin^{-1}$ at 650-750^{o}C have found the ability to absorb the CO_2 composition in the simulated gas and producer gas have been successfully done. The good absorption of CO_2 composition

percentage was observed for simulated gas and producer gas, where the CO_2 percentage detected by gas chromatograph analysis were less than 5% and 11% CO_2 after exit from the Bubbling Fluidized Bed Reactor.

Acknowledgments

The authors would like to express their appreciation to The Universiti Teknologi MARA (UiTM), Malaysia for giving the opportunity and supporting to do this biomass research study and also to The Universiti Sains Malaysia for The Research University Grant Scheme (Grant No. MEKANIK/811122) for providing financial support for this study.

References

Dogru M., Howarth C.R., Akay G., Keskinler B. and Malik A.A., 2002. Gasification of hazelnut shells in a downdraft gasifier. Energy, 27: 415-427.

Florin N.H. and Harris A.T., 2008. Enhance hydrogen production from biomass with in situ carbon dioxide capture using calcium oxide sorbents. Chemical Engineering Science, 63: 287-316.

Graham, R.G. and Huffman, D.R., 1981. Gasification of Wood in A Commercial Scale Downdraft Gasifier. In: Energy from Biomass 5, Lake Buena Vista, FL. Jan., pp 633-650.

Guoxin, H. and Hao, H., 2009. Hydrogen rich fuel gas production by gasification of wet biomass using a CO2 sorbent. Biomass and Bioenergy, 8: 91-98.

Hanaoka T., Yoshidaa, Y., Fujimotoa, S.J., Kamei, K., Harada, M., Suzuki, Y. et al., 2005. Hydrogen production from woody biomass by steam gasification using a CO2 sorbent. Biomass and Bioenergy, 28:63-68.

Hollingdale, 1983. Production gas fuelling of a 20kW output engine by gasification of solid biomass. Oversea Development Natural Resources Institute, ISBN 09528245.

Jorapur, R.M. and Rajvanshi, A.K., 1995. Development of Sugarcane Leaf Gasifier for Electricity Generation. Biomass and Bioenergy. Volume 8, No. 2, pp 91-98.

Mahishi M.R. and Goswami D.Y., 2007. An experiment study of hydrogen production by gasification in presence of CO_2 sorbents. International Journal of Hydrogen Energy, 32: 2803-2808.

McKendry, P., 2002. Energy production from biomass (part 3): gasification technologies. Bioresource Technology, 83: 55-63.

Munoz, M., Moreno, F., Morea, R.J., Ruiz, J. and Arauzo, J., 2000. Low heating value gas on spark ignition engines. Biomass and Bioenergy, 18: 431-439.

Sridhar G., Paul P.J. and Mukunda H.S, 2001. Biomass derived producer gas as a reciprocating engine fuel-an experimental analysis. Biomass and Bioenergy, 21: 61-72.

Uma R, Kandpal T.C and Kishore V.V.N., 2004. Emission characteristics of an electricity generation systems in detail in diesel alone and diesel fuel modes. Biomass and Bioenergy, 27: 195-203.

Walawender, W.P.; Chern, S.M. and Fan, L.T., 1985. Wood chips gasification in a commercial downdraft gasifier. In: Overend RP, editor. Fundamentals of thermo chemical biomass conversion, Amsterdam: Elsevier Applied Science, pp 911.

Zainal Z.A., 1996. Performance and characteristics of a biomass gasifier system. Ph.D dissertation, Division of Mechanical Engineering and Energy Studies, School of Engineering, University of Wales, College of Cardiff, United Kingdom.

Zainal Z.A., Rifau A., Quadir G.A. and Seetharamu K.N., 2002. Experimental investigation of a downdraft biomass gasifier. Biomass and Bioenergy, 23: 283-289.

Journal of Applied Sciences 10 (9): 745-751, 2010
ISSN 1812-5654

Characteristics on Fluidization Behaviors of 1000 μm Cao-Sand Mixture by Varying the Percentage of CaO, Air Flow Rate and Pressure

M.M. Mahadzir, Z.A. Zainal, M. Iqbal and S.N. Soid
School of Mechanical Engineering, Universiti Sains Malaysia Eng. Campus, Pulau Pinang, Malaysia

Abstract: The interest in biomass technology has got a lot of attention due to the increase in fuel prices and issues like global warming. Producer gas as a alternative fuel, produced from biomass gasification process can be used to generate power and electricity. However, in air blown gasification, the producer gas produced has Low Calorific Value (LCV) about 4-6 MJ Nm^{-3} with CO_2 content around 10-20% by volume. To increase the LCV, the used of calcium oxide, CaO as sorbent to absorb CO_2 in the producer gas can make biomass technology more viable. In the present study, the aim is to study the fluidization of the bed in terms of the bed expansion and the pressure drop of the 1000 μm CaO-sand mixtures at different percentages, the air volume flow rate and pressurize air intake in the cold model experiment. The behaviors of 1000 μm CaO-sand mixtures have been conducted in a Small Bubbling Fluidized Bed (SBFB). The results show that the decrease of the CaO percentages from 70, 60, 50 to 40, will increase the pressure drop (ΔP) in the SBFB under constant pressure of 2, 3, 4, 5 and 6 bars. The bed expansion height also increased under all air pressures except at the low superficial flow velocity less than 0.06 m sec^{-1} at 2, 3, 4, 5 bars (70, 60% CaO mixture), when the air volume flow rate increased (in term of superficial flow velocities 0.020 to 0.215 m sec^{-1}). The conclusion has been determined where the CaO percentages of 50 and 40 were found to have a good fluidization in the range of 15-55 L min^{-1} for all pressurize air compressors supply (2, 3, 4, 5 and 6 bars) when tested in a SBFB.

Key words: Biomass, producer gas, fluidization, CaO, CO_2 absorption

INTRODUCTION

Energy is the most important subject in our life. Currently, the interest in biomass technology has got a lot of attention due to the increase in fuel prices and issues like global warming. Biomass is known as a renewable and carbon neutral energy resource that includes energy crops, agricultural wastes, animal wastes, municipal solid wastes and forestry wastes (McKendry, 2002a). Biomass gasification is technology to produce low to medium gaseous fuel gases. It is defined as the thermal decomposition of biomass in the present of limited oxygen to produce a gas known as producer gas. The producer gas consists of Carbon monoxide (CO), Hydrogen (H_2), Methane (CH_4), Carbon dioxide (CO_2) and Nitrogen (N_2) (McKendry, 2002c). It can be utilized in internal combustion engines or coupled to turbines to generate power.

The producer gas has Low Calorific Value (LCV) of about 4-6 MJ Nm^{-3} (Graham and Huffman, 1981; Jorapur and Rajvanshi, 1995; McKendry, 2002b; Rezaiyan and Nichol, 2005) because CO_2 is diluents as non reactive produce about 10-20% by volume (Hollingdale *et al*., 1988; Walawender *et al*., 1985; Munoz *et al*., 2000; Sridhar *et al*., 2001; Zainal *et al*., 2002; Dogru *et al*., 2002; Uma *et al*., 2004). The LCV of the producer gas is depend on the particles size distribution of the biomass material, biomass fuel composition, moisture content, volatile matter, ash content and heating value (Yusof *et al*., 2008; Miskam *et al*., 2009). Nowadays, the used of the mineral called calcium oxide, CaO as calcium based sorbent to absorb CO_2 in the producer gas can enhance the quality of the producer gas. Therefore in the last five years, the numbers of CO_2 sorbents have been intensively investigated in the biomass technology fields (Guoxin and Hao, 2009; Florin and Harris, 2008; Mahishi and Goswami, 2007; Hanaoka *et al*., 2005) because of their low cost, abundance and availability.

The $CaCO_3$ must first undergo a calcination process to release the CO_2 at a temperature of 800-900°C converting into CaO and than an absorption process to absorb CO_2 at reaction temperature around 600-700°C to reform to $CaCO_3$. The concept is based on the

Corresponding Author: Mohd Mahadzir Mohammud, School of Mechanical Engineering, Engineering Campus, Universiti Sains Malaysia, Seri Ampangan, 14300 Nibong Tebal, Seberang Perai Selatan, Pulau Pinang Malaysia Tel: 6-019-4547002 Fax: 604-3823192

carbonation/calcination loop using the reversible reaction used by Shimizu *et al.* (1999) and Stefan *et al.* (2009):

$$CaO(s) + CO_2(g) \leftrightarrow CaCO_3(s) \quad (1)$$

Although, the researches on the CO_2 absorption have been widely studied in the last few decades, however the focused is only the use of calcium based sorbents either in term of $CaCO_3$ or CaO in a reactor (Abanades *et al.*, 2005; Grasa and Abanades, 2007; Grasa *et al.*, 2008; Chen *et al.*, 2007; Abanedes, 2002; Salvador *et al.*, 2003). The study done by the researchers so far none have used the CaO-sand mixture as a bed material for the carbonation-calcinations process to absorb and release the CO_2. In the present study, the behaviors of 1000 μm CaO-sand mixtures in the cold model experiment have been conducted. The purpose of this work is to study the fluidization of the bed in terms of the bed expansion and the pressure drop of the 1000 μm CaO-sand mixtures at different percentages in the cold model experiment. The use of sand is due to its good fluidization characteristics compared to the calcium based sorbents alone. In order to gain more information about the behaviors of CaO-sand mixtures, the effect of the air volume flow rate and pressurize air intake were investigated experimentally.

MATERIALS AND METHODS

Cold model experiments in a Small Bubbling Fluidized Bed (SBFB) were conducted using compressed air. Figure 1 and 2 show the cold model experimental setup. The SBFB consists of a nozzle distributor plate and was supported on a stand. The main bed was made from transparent perspex. The overall height of the SBFB is 877.5 mm. The main bed has an inner diameter of 74 and 600 mm height. The nozzle distributor plate has five small nozzles that protrude up from the surface of the plate. Each nozzle has four holes of 1.6 mm diameter to allow gas to flow. The distributor plate was made from stainless steel. Figure 3 shows the 3-D diagram of the nozzle distributor plate.

The SBFB is connected to a 2.5 hp air compressor model HD47C to provide a compressed air flow and a bag filter to capture any of the bed material leaving the reactor.

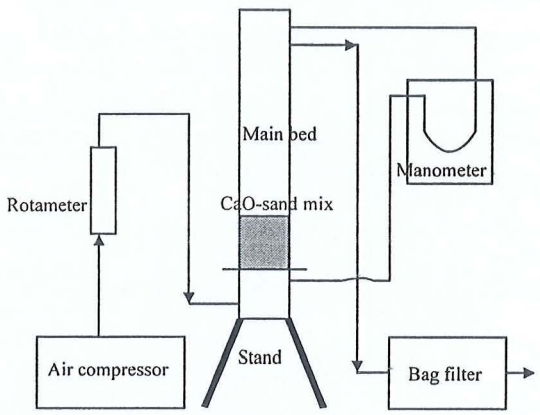

Fig. 1: Schematic diagram of the experimental setup

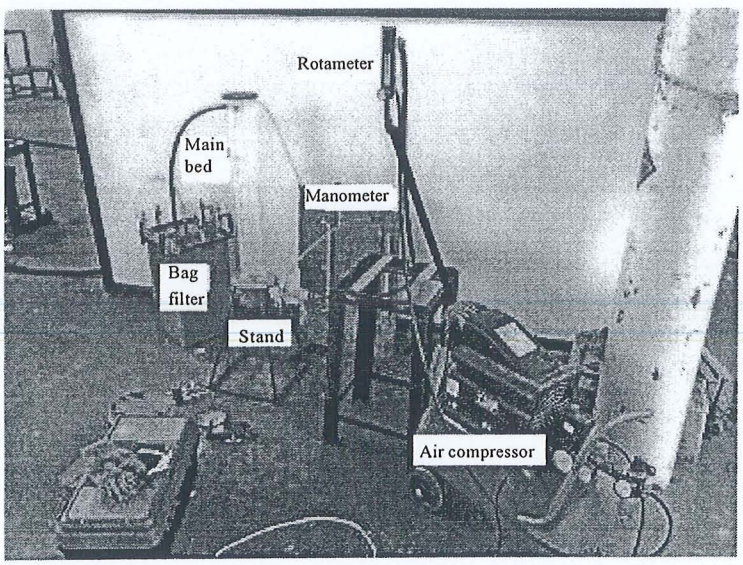

Fig. 2: Photograph of the cold model experimental setup

A simple U-tube manometer was used to determine the pressure drop of the material. Figure 4 shows the 2-D design of the small bubbling fluidized bed.

The 1000 μm of CaO mixed with 350 μm sand was used as the bed material. These particles sizes were sieved using an Endecott's multi-layer test sieve shaker. The 350 μm sand particles size has been selected in this experimental because according to Geldart (1973) and Yates (1983), the particles size of sand in the range of 150-500 μm (the Group B powders) gives well fluidization. In the experiment, for each run, 240 g constant weight of CaO was used and mixed with 226, 421, 496 and 808 g of sand to obtain the CaO-sand mixture percentages. The experiment started when the mixtures of 240 and 226 g were put into the SBFB. Then the air compressor was set to 2 bar using pressure regulator and the air flow in term of the volume flow rate of 5 L min^{-1} was passed to the SBFB controlled by a rotameter. During the experiment the fluidization behaviors in term of bed expansion height and the pressure drop inside the SBFB were recorded. Some of the fine particles found in the bag filter was weighed and recorded at the end of the experiment. The experiment was repeated at different CaO mixture percentages (70, 60, 50, 40%), air volume flow rate (5, 15, 25, 35, 45, 55 L min^{-1}) and air intake pressure (2, 3, 4, 5, 6 bar).

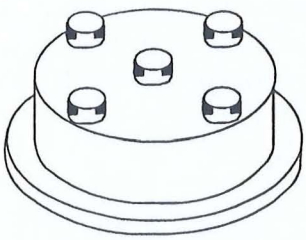

Fig. 3: 3-D diagram of the nozzle distributor plate

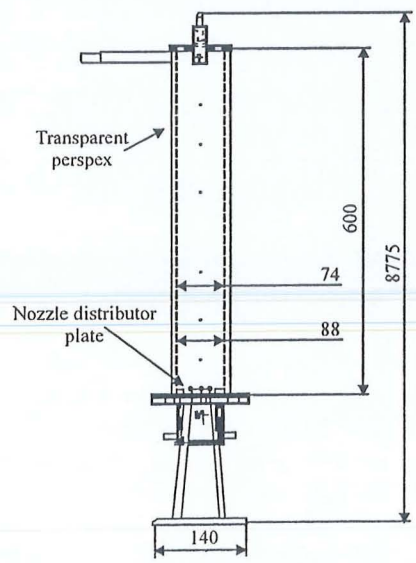

Fig. 4: The design of the SBFB. All dimensions in mm

RESULT AND DISCUSSION

Table 1 shows the expected minimum fluidization velocity (u_{mf}) obtained for every percentage mixture of 1000 μm CaO and air pressure. All the expected minimum fluidization velocity was calculated based on the Ergun Equation (Wen, 2003; McCabe *et al.*, 2004) using:

$$u_{mf} = \frac{\mu_g}{\rho_g d_s}\left[\left(33.7^2 + 0.0408 Ar_{numb}\right)^{\frac{1}{2}} - 33.7\right] \quad (2)$$

where, μ_g is dynamic viscosity of the carrier gas (kg m^{-1} sec), ρ_g is density of the carrier gas (kg m^{-3}), d_s is solid particles size (m) and Ar_{numb} is Archimedes number.

The u_{mf} is needed to separate the particles of CaO and sand from each other and float in the SBFB. As shown in Fig. 5, under the constant air pressure of 2 bars, the bed

Table 1: Expected minimum fluidization velocity

$CaCO_3$ (%)	Air pressure (bars)	Minimum fluidization velocity, u_{mf} (m sec^{-1})	Volume flow rate, Q (L min^{-1})
70	2	0.063	16.19
	3	0.061	15.85
	4	0.060	15.54
	5	0.059	15.25
	6	0.058	14.97
60	2	0.063	16.31
	3	0.062	15.96
	4	0.061	15.64
	5	0.059	15.35
	6	0.056	14.51
50	2	0.054	13.93
	3	0.053	13.73
	4	0.052	13.54
	5	0.052	13.36
	6	0.051	13.19
40	2	0.049	12.57
	3	0.048	12.46
	4	0.048	12.35
	5	0.047	12.24
	6	0.047	12.14

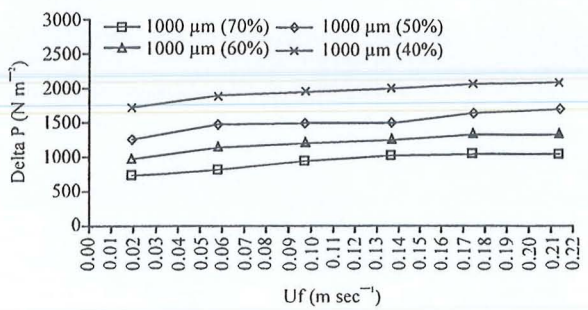

Fig. 5: Effect of 1000 μm $CaCO_3$ mixture percentages, air volume flow rate and air pressure on the pressure drop (2 bars)

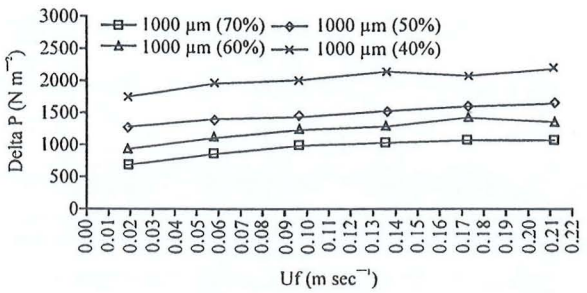

Fig. 6: Effect of 1000 µm $CaCO_3$ mixture percentages, air volume flow rate and air pressure on the pressure drop (3 bars)

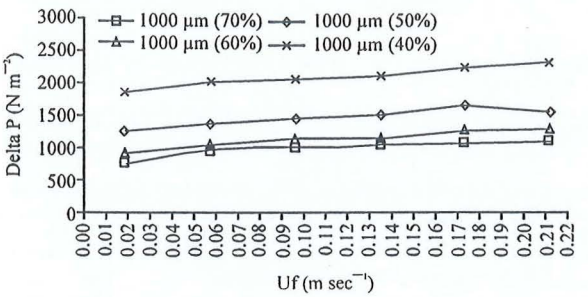

Fig. 7: Effect of 1000 µm $CaCO_3$ mixture percentages, air volume flow rate and air pressure on the pressure drop (4 bars)

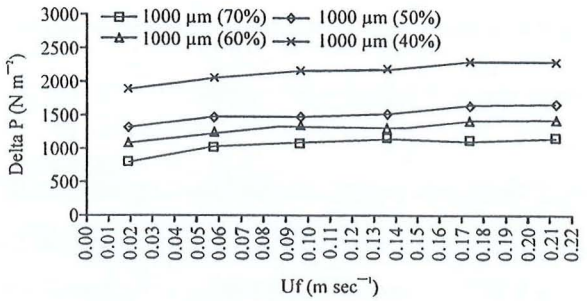

Fig. 8: Effect of 1000 µm $CaCO_3$ mixture percentages, air volume flow rate and air pressure on the pressure drop (5 bars)

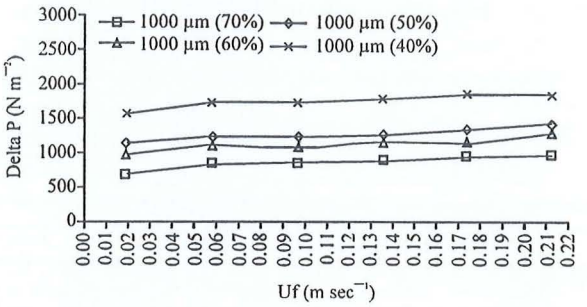

Fig. 9: Effect of 1000 µm $CaCO_3$ mixture percentages, air volume flow rate and air pressure on the pressure drop (6 bars)

pressure drops for different CaO-sand percentages were not similar. However the constant bed pressure drop was obtained when the u_{mf} reached for every CaO-sand percentages (between 0.05-0.08 m sec^{-1}). In Fig. 6, when the u_{mf} reached 0.04-0.06 m sec^{-1}, the constant bed pressure drop was obtained for all percentage mixture of 1000 µm CaO under 3 bars constant air pressure. The similar trends can also be seen in Fig 7-9. When the u_{mf} reached 0.05-0.06 m sec^{-1}, the constant bed pressure drop was obtained for all constant air pressure 4, 5 and 6 bars. The comparison between the expected minimum fluidization velocity (Table 1) using Ergun Equation (Wen, 2003; McCabe *et al.*, 2004) and the experimentally (Fig. 5-9) were approximately same.

When the superficial fluid velocity was gradually increased, the bed pressure drop gradually increased for all percentage mixture of 1000 µm CaO and air pressure. Then the bed pressure drop levels off and no longer increases as the superficial velocity is increased because it has reached the u_{mf}. This due to the upward force exerted by the fluid on the particles was sufficient to balance the net weight of the bed and the particles begin to separate from each other and float in the fluid. As the velocity is increased further, the bed continues to expand in height, but the bed pressure drop stays constant. The similar trends on the bed pressure drops constant level in the bubbling fluidization bed also can be found from experimental results reported by Flamant *et al.* (1991), Svoboda and Hartman (1981), Guo *et al.* (2003) and Yates (1983).

Based on the similar experimental results of the minimum fluidization velocity and the constant bed pressure drop were obtained compared to other researchers, the following variables affecting the fluidization height were investigated:

- Percentage mixture of 1000 µm CaO
- Volume flow rate of the compressed air and
- The air pressure

Effect of the CaO percentages: The amount of CaO percentage in the mixture has an effect on the bed pressure drop and bed expansion height under constant pressure. With the decrease of the CaO percentages from 70, 60, 50 to 40%, the bed pressure drop ΔP in the SBFB increased under constant pressure of 2 bars as shown in Fig. 5. When the air pressure increased to 3 bars (Fig. 6),

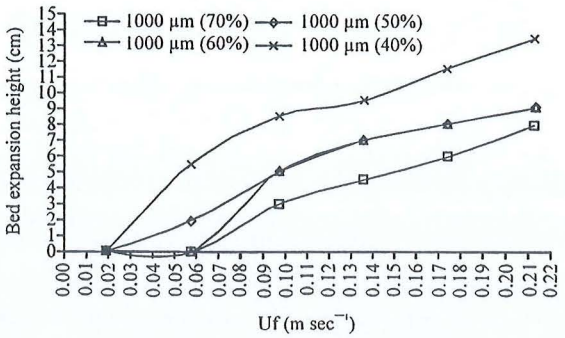

Fig. 10: Bed expansion height results (2 bars)

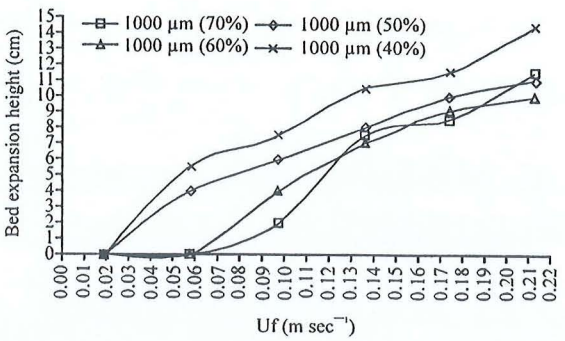

Fig. 11: Bed expansion height results (3 bars)

the similar trend was obtained where the bed pressure drop ΔP increased when the CaO-sand mixtures percentages decreased. These happened because of the increasing in the amount of mass of the solid particles (1000 μm CaO-350 μm sand) in every mixture. These similar trends can also be found in the Fig. 7-9.

In Fig. 10, its can be observed that with the decreased of the CaO percentages by 70, 60, 50 to 40, the bed expansion height increased between 0-14.5 cm when the superficial velocity increased from 0.02-0.215 m sec^{-1} under 2 bars constant air pressure. This can be explained by the adhesive force between CaO particles such as the Van der Waals force, the electronic force and the liquid bridge existing in the powder that has been reduced because of the increased of the 350 μm sand particles in the mixture. Previous studies reported by Geldart (1973) and Yates (1983) showed that the particle size of sand in the range of 150-500 μm (Group B powders) with low density is in the range of 1500-4000 kg m^{-3} has a better fluidization. Similar trends can also be found from the experimental results of Gao *et al.* (2009). However at early stages of the experiments for 70 and 60% CaO mixture, the bed expansion height is 0 cm, which means that these is no fluidization. This is because the superficial flow velocity has not reach the minimum superficial flow velocity where the upward force exerted by the fluid on the particles is not sufficient to force the weight of CaO-sand mixture of the bed. The adhesive force between CaO-sand mixture particles is still strong and the amount of 350 μm of sand is not enough to overcome it.

In Fig. 11-13, the similar trends can also be seen where the bed expansion height was 0 cm when the CaO-sand percentages mixture was 70 and 60% at low superficial velocity of 0.02-0.06 m sec^{-1}. These happened under the constant air pressure of 3, 4 and 5 bars. The superficial flow velocity has not reach the minimum superficial flow velocity where the upward force exerted by the fluid on the particles is not sufficient to force the weight of CaO-sand mixture of the bed.

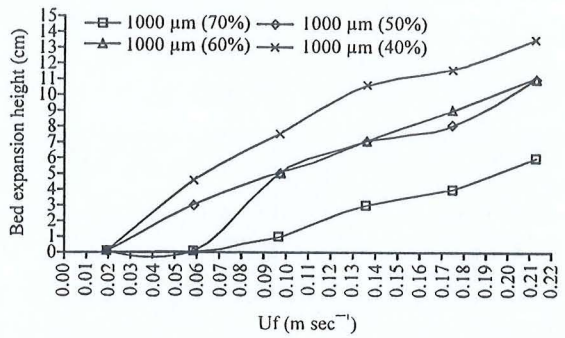

Fig. 12: Bed expansion height results (4 bars)

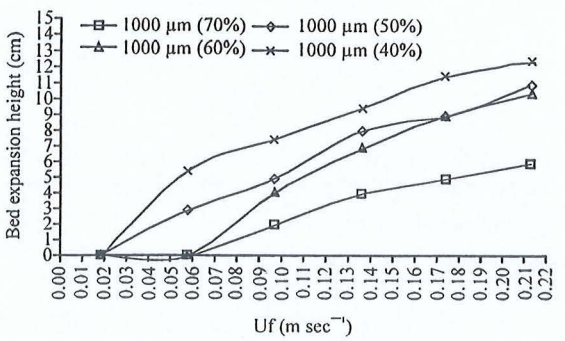

Fig. 13: Bed expansion height results (5 bars)

In Fig. 14, its can be observed that the bed expansion height increased between 0 to 14.5 cm when the superficial velocity increased from 0.02-0.215 m sec^{-1} under 6 bars of the constant air pressure. The increased of the bed expansion height can be seen for all CaO-sand percentages mixture (70, 60, 50 to 40%). The adhesive force between CaO particles existing in the powder has been reduced due to the increased of the air pressure and the amount of sand particles in the mixture. The results obtained were similar with the explanation by Yates (1983).

Effect of the air volume flow rate and air pressure: Air volume flow rate and pressure are important operating

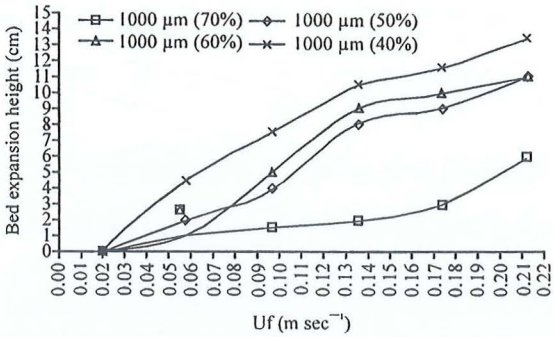

Fig. 14: Bed expansion height results (6 bars)

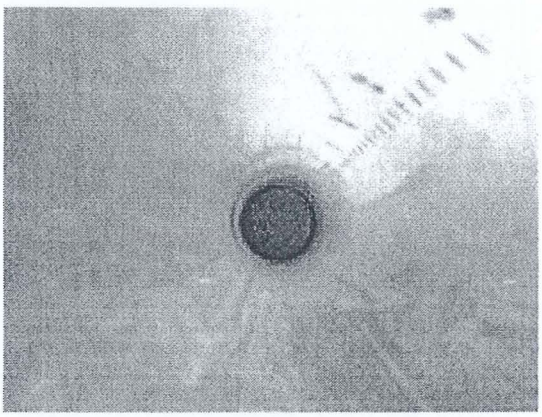

Fig. 15: No rat holes and fluidization formed during operation (15 L min^{-1}, 1000 μm, 70% CaO, 2 bars)

parameters in fluidized bed. The 1000 μm CaO-sand mixture was tested with 5, 15, 25, 35, 45 and 55 L min^{-1} flow rates at different air pressures to determine the fluidization behavior. As shown in Fig. 10-14, when the air volume flow rate increases (in term of superficial flow velocities 0.020 to 0.215 m sec^{-1}), the bed expansion height also increased at all air pressures except at the low superficial flow velocity less than 0.06 m sec^{-1} at 2, 3, 4, 5 bars (70, 60% CaO mixture) and at 5 L min^{-1} (0.02 m sec^{-1}) at all variables. At these conditions, no fluidizations were found. The reason is due to the strong interaction force that acts between two macroscopic bodies such as particle-particle and particle-wall that exist in the bed material. Furthermore the amount percentage of CaO is too much to be overcome by air volume flow rate and pressure. Figure 15 shows the one example of the pictures taken for this phenomenon.

CONCLUSIONS

The characteristics on fluidization behaviors of 1000 μm CaO-sand mixtures in the cold model experiment were determined. The investigations of the fluidization of the bed in term of the bed expansion height and the pressure drop have been listed as follows:

- The CaO percentages of 50 and 40 were found to have a good fluidization in range 15-55 l/min volume flow rates of air for all air pressures (2, 3, 4, 5 and 6 bars)
- At 70 and 60% CaO, the fluidizations only occurred after reach 25 L min^{-1} air flow rate for pressure 2, 3, 4 and 5 bars except at 6 bars, the 1000 μm CaO-sand mixture fluidized in 15-55 L min^{-1} range
- No fluidizations were found at 5 L min^{-1} for all variables

ACKNOWLEDGMENTS

The authors would like to express their appreciation to The Research University Grant Scheme of University Science Malaysia (Grant No. MEKANIK/811122) for providing financial support for this study.

REFERENCES

Abanades, J.C., 2002. The maximum capture efficiency of CO_2 using a carbonation/calcinations cycle of $CaO/CaCO_3$. Chem. Eng. J., 90: 303-306.

Abanades, J.C., E.J. Anthony, J. Wang and J.E. Oakey, 2005. Fluidized bed combustion system integrating CO_2 capture with CaO. Environ. Sci. Technol., 39: 2861-2866.

Chen, Z., C.J. Lim and J.R. Grasa, 2007. Study of limestone particle impact attrition. Chem. Eng. Sci., 62: 867-877.

Dogru, M., C.R. Howrath, G. Akay, B. Keskinler and A.A. Malik, 2002. Gasification of hazelnut shells in a downdraft gasifier. Energy, 27: 415-427.

Flamant, G., N. Fatah, D. Steinmetz, B. Murachman and C. Laquerie, 1991. High-temperature velocity and porosity at minimum fluidization. Critical analysis of experimental results. Int. Chem. Eng., 31: 673-684.

Florin, N.H. and A.T. Harris, 2008. Enhance hydrogen production from biomass with *in situ* carbon dioxide capture using calcium oxide sorbents. Chem. Eng. Sci., 63: 287-316.

Gao J., X. Lan, Y. Fan, J. Chang, G. Wang, C. Lu and C. Xu, 2009. Hydrodynamics of gas-solid fluidized bed of disparately sized binary particles. Chem. Eng. Sci., 64: 4302-4316.

Geldart, D., 1973. Types of gas fluidization. Powder Technol., 7: 285-292.

Graham, R.G. and D.R. Huffman, 1981. Gasification of wood in a commercial scale downdraft gasifier. Proceedings of the Symposium Papers. Energy from Biomass and Wastes V, Lake Buena Vista, Jan. 26-30, Florida, pp: 633-650.

Grasa, G.S. and J.C. Abanades, 2007. Narrow fluidized beds arranged to exchange heat between a combustion chamber and a CO_2 sorbent regenerator. Chem. Eng. Sci., 62: 619-626.

Grasa, G.S., J.C. Abanades, M. Alonso and B. Gonzalez, 2008. Reactivity of highly cycled particles of CaO in a carbonation/calcination loop. Chem. Eng. J., 137: 561-567.

Guo, Q., G. Yue, T. Suda and J. Sato, 2003. Flow characteristics in a bubbling fluidized bed at elevated temperature. Chem. Eng. Proc., 42: 439-447.

Guoxin, H. and H. Hao, 2009. Hydrogen rich fuel gas production by gasification of wet biomass using a CO_2 sorbent. Biomass Bioenergy, 33: 899-906.

Hanaoka, T., Y. Yoshidaa, S. Fujimotoa, K. Kamei and M. Harada *et al.*, 2005. Hydrogen production from woody biomass by steam gasification using a CO_2 sorbent. Biomass Bioenergy, 28: 63-68.

Hollingdale, A.C., G.R. Breag and D. Pearce, 1988. Producer Gas Fuelling of a 20 KW Output Engine b y Gasification of Solid Biomass. Overseas Development Natural Resources Institute, London, UK., ISBN 0-85954-243-2.

Jorapur, R.M. and A.K. Rajvanshi, 1995. Development of sugarcane leaf gasifier for electricity generation. Biomass Bioenergy, 8: 91-98.

Mahishi, M.R. and D.Y. Goswami, 2007. An experiment study of hydrogen production by gasification in presence of CO_2 sorbents. Int. Assoc. Hydrogen Energy, 32: 2803-2808.

McCabe, W.E., J.C. Smith and P. Harriott, 2004. Unit Operations of Chemical Engineering. 7th Edn., McGraw Hill, New York.

McKendry, P., 2002a. Energy production from biomass (part 1): Overview of biomass. Bioresour. Technol., 83: 37-46.

McKendry, P., 2002b. Energy production from biomass (part 2): Conversion technologies. Bioresour. Technol., 83: 47-54.

McKendry, P., 2002c. Energy production from biomass (part 3): Gasification technologies. Bioresour. Technol., 83: 55-63.

Miskam, A., Z.A. Zainal and I.M. Yusof, 2009. Characterization of sawdust residues for cyclone gasifier. J. Applied Sci., 9: 2294-2300.

Munoz, M., F. Moreno, R.J. Morea, J. Ruiz and J. Arauzo, 2000. Low heating value gas on spark ignition engines. Biomass Bioenergy, 18: 431-439.

Rezaiyan, J. and P. Nicholas, 2005. Gasification Technologies: A Primer for Engineers and Scientists. 1st Edn., CRC Press, New York, ISBN-10: 0824722477, pp: 360.

Salvador, C., D. Lu, E.J. Anthony and J.C. Abanades, 2003. Enhancement of CaO for CO_2 capture in a FBC environment. Chem. Eng. J., 96: 187-195.

Shimizu, T., T. Hirama, H. Hosoda, K. Kitano, M. Inagaki and K. Tejima, 1999. A twin fluid bed reactor for removal of CO_2 from combustion process. Chem. Eng. Res. Design, 77: 62-68.

Sridhar, G., P.J. Paul and H.S. Mukunda, 2001. Biomass derived producer gas as a reciprocating engine fuel: An experimental analysis. Biomass Bioenergy, 21: 61-72.

Stefan, K., P. Christoph, R. Reinhard, H. Hermann, M.M. Tonja and S. Michael, 2009. H_2 rich product gas by steam gasification of biomass with *in situ* CO_2 absorption in a dual fluidized bed system of 8 MW fuel input. Fuel Process. Technol., 90: 914-921.

Svoboda, K. and M. Hartman, 1981. Influence of temperature on incipient fluidization of limestone, lime, coal ash and corundum. Ind. Eng. Chem. Process Design Dev., 20: 319-326.

Uma, R., T.C. Kandpal and V.V.N. Kishore, 2004. Emission charteristics of an electricity generation system in diesel alone and dual fuel modes. Biomass Bioenergy, 27: 195-203.

Walawender, W.P., S.M. Chern and L.T. Fan, 1985. Wood Chips Gasification in a Commercial Downdraft Gasifier. In: Fundamentals of Thermochemical Biomass Conversion, Overend, R.P., T.A. Milne and L.K. Mudge (Eds.). Elsevier, UK., pp: 911.

Wen, C.Y., 2003. Handbook of Fluidization and Fluid-Particle Systems. CRC Press, New York, ISBN-10: 082470259X. pp: 1868.

Yates, J.G., 1983. Fundamentals of Fluidized-Bed Chemical Processes. Butterworth-Heinemann, UK., ISBN-10: 040870909X. pp: 240.

Yusof, I.M., N.A. Farid, Z.A. Zainal and M. Azman, 2008. Characterization of rice husk for cyclone gasifier. J. Applied Sci., 8: 622-628.

Zainal, Z.A., A. Rifau, G.A. Quadir and K.N. Seetharamu, 2002. Experimental investigation of a downdraft biomass gasifier. Biomass Bioenergy, 23: 283-289.

CD-ROM. ISSN: 1944-6934.

Investigation of $CaCO_3$- Sand Mixture Fluidization Behaviours in SBFB

Mahadzir M. M., University of Technology MARA, Penang Campus, Pulau Pinang, Malaysia.
Zainal Z. A. and Muhakim M., University of Science Malaysia, Eng. Campus, Pulau Pinang, Malaysia.

Abstract: Alternative source of energy such as biomass gasification can be used to generate power and electricity. Producer gas produced from biomass gasification consists of carbon monoxide (CO), hydrogen (H_2), methane (CH_4), carbon dioxide (CO_2) and nitrogen (N_2). It has low calorific value (LCV) around 4-6 MJ/Nm^3 because of CO_2 content is about 10-20 % by volume. Limestone or specifically calcium carbonate, $CaCO_3$ can be heated up to form calcium oxide, CaO where is used to absorb carbon dioxide (CO_2) of the producer gas to increase its low calorific value. In this paper a cold model experiment in a small bubbling fluidized bed (SBFB) has been conducted to determine the optimum mixing of $CaCO_3$ - sand at certain pressure and flow rate as a first step to design a CO_2 absorption reactor in the School of Mechanical Engineering, University of Science Malaysia. The result obtained shows the $CaCO_3$ percentages of 60, 50 and 40 were found to have a good fluidization in all pressurize air compressors supply (2, 3, 4, 5 and 6 bars). In addition to that, the 500 μm particle size and 15 – 55 l/min flow rate give a good fluidization when experimented.

Keywords: $CaCO_3$-sand mixture, Producer Gas, Limestone, Fluidization behaviors.

Introduction

Biomass is one of the sources of renewable energy where it is derived from living or recently living organism such as wood, waste, and alcohol fuels. It can be converted to other usable forms of energy like methane gas or transportation fuels like ethanol and bio-diesel (McKendry, 2002a). Therefore, people are now considering using alternative source of energy such as biomass gasification due to the increase of fuel prices. Biomass gasification can be defined as incomplete combustion where it produces combustible and non combustible gases which consist of carbon monoxide (CO), hydrogen (H_2), methane (CH_4), carbon dioxide (CO_2) and nitrogen (N_2) (McKendry, 2002c). The combination of these gases is called producer gas. Producer gas can be used to generate electricity and power. It can be applied to power plant, stove, furnace and in a reciprocating engines.

The producer gas produced has low calorific value (LCV) around 4-6 MJ/Nm^3 (Graham and Huffman, 1981; Xu and Wang, 1988; Jorapur and Rajvanshi, 1995; Zainal 1996; McKendry, 2002b; Rezaiyan and Cheremisinoff, 2005) because of CO_2 content is about 10-20 % by volume (Dogru et al. 2002; Uma et al. 2004 and Zainal et al. 2002). Limestone or specifically calcium carbonate, $CaCO_3$ can be heated up to form calcium oxide, CaO where is used to absorb carbon dioxide (CO_2) of the producer gas to increase its low calorific value (Abanades et al. 2005; Grasa and Abanades, 2007; Grasa et al. 2008; Chen et al. 2007; Abanades 2002 and Salvador 2003). In the present paper, the cold model experiment has been conducted, to determine the optimum mixing of $CaCO_3$ - sand at certain pressure and flow rate as a first step to design a CO_2 absorption reactor in the School of Mechanical Engineering, University of Science Malaysia. The purpose of this work is to ensure fluidization occurs inside the chamber. This is a crucial factor because if it does not fluidize then the calcinations-carbonation process will not take place completely. Besides of that, the suitable flow rate is required to make sure that it does not effect in the increment of temperature for the calcinations-carbonation process and at the same time assisting the fluidization in the reactor.

Experimental

Fluidization experiments with pressurized air at room temperature have been conducted as a cold model experiment in a small bubbling fluidized bed (SBFB). The overall height of the SBFB is 877.5 mm. The main bed has an inner diameter of 74 mm and 600 mm height. The nozzle distributor plate has five small nozzles that protrude up from the surface of the plate. Each nozzle has four holes of 1.6 mm diameter to allow gas to flow. Figure 1 shows the schematic diagram of the experimental setup. The bed material used are $CaCO_3$ and sand with different composition. The experiment will be done by using 70%, 60%, 50% and 40% of $CaCO_3$ and the balance material is sand. The flow rate of air going through the nozzle is from 5, 15, 25, 35, 45 to 55 *l*/min. While the pressure used to assist the fluidization is 2, 3, 4, 5 and 6 bar. For the particle size of the material, the size of 100 and 500 micrometers are considered for both $CaCO_3$ and sand.

The mixture of $CaCO_3$-sand is inserted into the fluidized bed reactor. The pressurize air from the 2.5 hp air compressor flow through the nozzle distributor plate inside the transparent perspex chamber. The desired flow of air is controlled by a rotameter whereas the pressure is controlled from the compressor. Small particles of $CaCO_3$ which manage to exit the chamber will directly go to the filter beg. The fluidization of the mixture will be recorded to determine the optimum requirement for the mixture to fluidize.

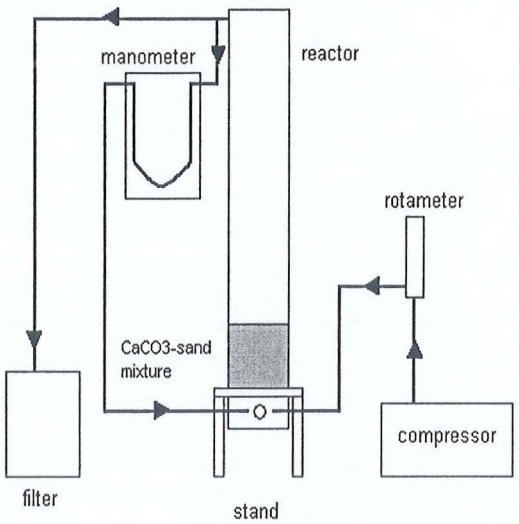

Figure 1: Schematic diagram of experimental setup

Results and discussion

The chart shown in Figures 2 – 9 shows the result of the fluidization of the $CaCO_3$-sand mixture in term of fluidization condition (1 is yes, 0 is no) in the cold model SBFB. The effects of certain parameters on the fluidization are investigated such as the effects of the flow rate, pressure, particle size and also the effects of different composition of bed material.

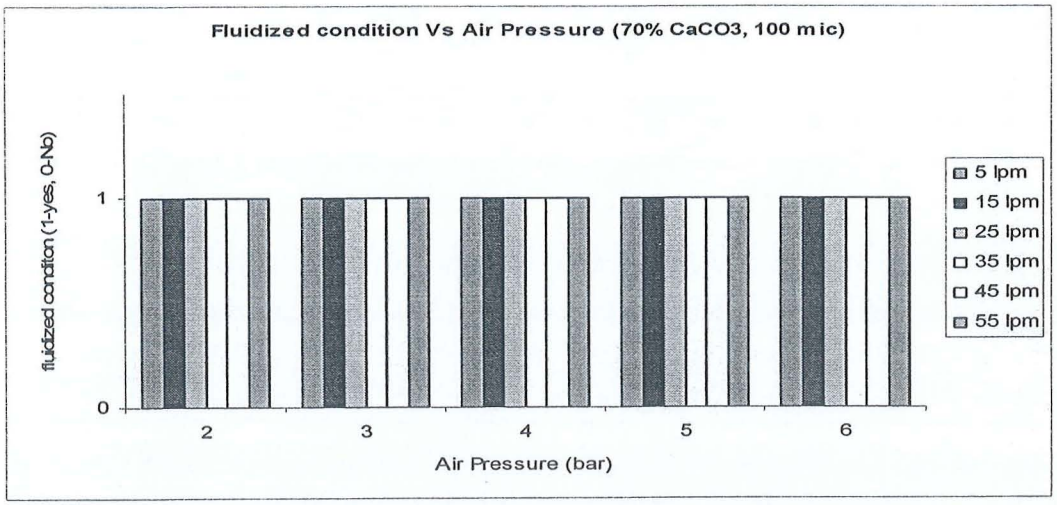

Figure 2: Fluidized condition for 70% $CaCO_3$ (100 micrometer)

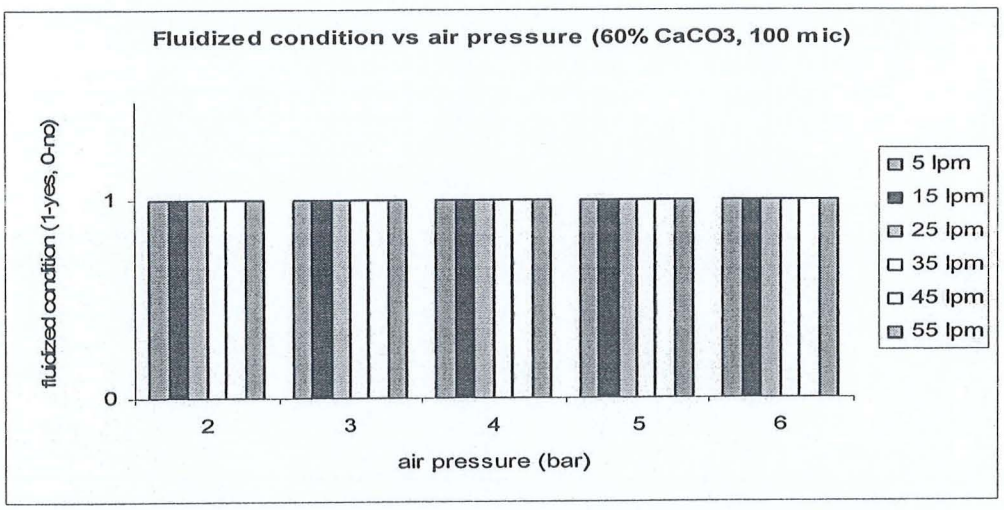

Figure 3: Fluidized condition for 60% $CaCO_3$ (100 micrometer)

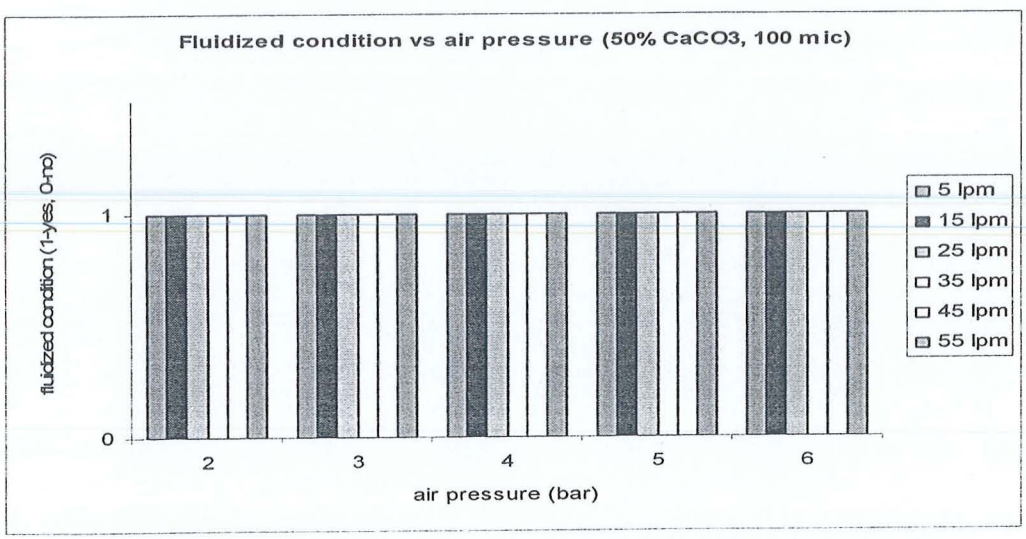

Figure 4: Fluidized condition for 50% $CaCO_3$ (100 micrometer)

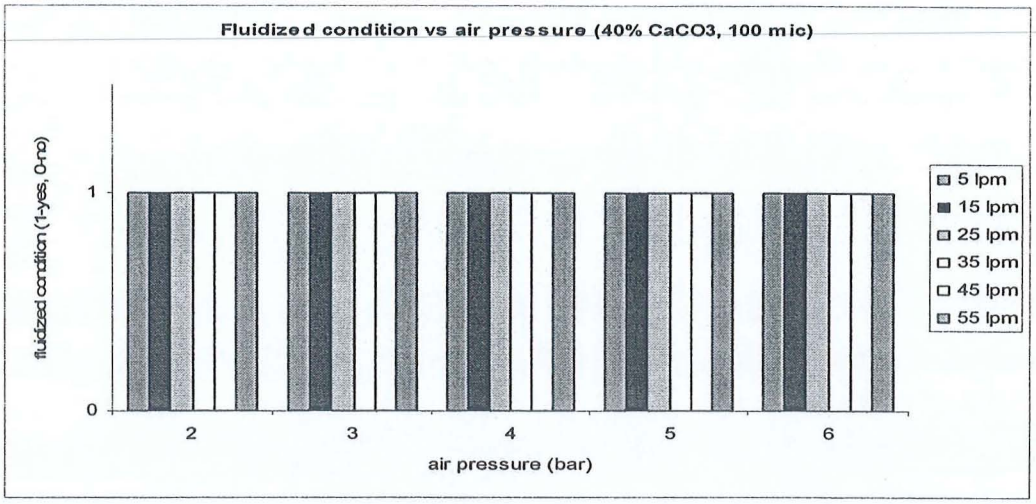

Figure 5: Fluidized condition for 40% $CaCO_3$ (100 micrometer)

From figures 2 - 5, the results show when using $CaCO_3$ with the particle size of 100 micrometers, it can be fluidized at various flow rates, pressures and even with different composition of the mixture. The $CaCO_3$ with size of 100 micrometers is very light (low density) and with the assist of sand, fluidization can occur easily inside the SBFB. Even though it is easily fluidized, the $CaCO_3$ particles will exit the SBFB very fast and this is a problem whereby it will affect the calcinations-carbonation process to run at a short period only.

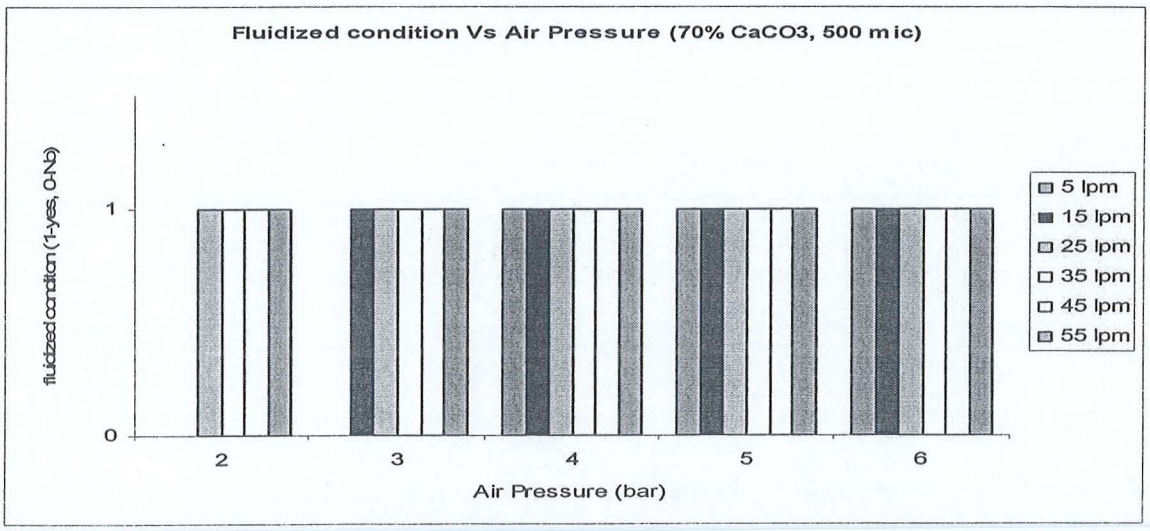

Figure 6: Fluidized condition for 70% $CaCO_3$ (500 micrometer)

In figure 6 for $CaCO_3$ with the particle size of 500 micrometers, fluidization does not occur at low flow rate and low pressure. At the pressure of 2 bars, the $CaCO_3$ can only be fluidized when supplying air with the flow rate of 25 *l*/m. Even when applying 3 bars of pressure, fluidization only starts to take place at the flow rate of 15 *l*/m.

This could be explained by the increase of the particle size and with a high percentage of $CaCO_3$ in the mixture. Increase in the particle size will increase the weight of $CaCO_3$. Therefore, as air with low flow rate is supplied, it does not have enough force to push the heavier mixture to cause fluidization. In addition to that, the percentage of $CaCO_3$ is higher than sand in the mixture. Fluidization does not happen when using $CaCO_3$ alone and sand is used to help fluidization. Despite using sand, using with a small percentage also does not support fluidization in the SBFB.

Results from figures 7 - 9 shows $CaCO_3$ is fluidized at various pressure and flow rate. This is due to the increase percentage of sand in the mixture which helps the fluidization even when it is supplied with low flow rate and pressure.

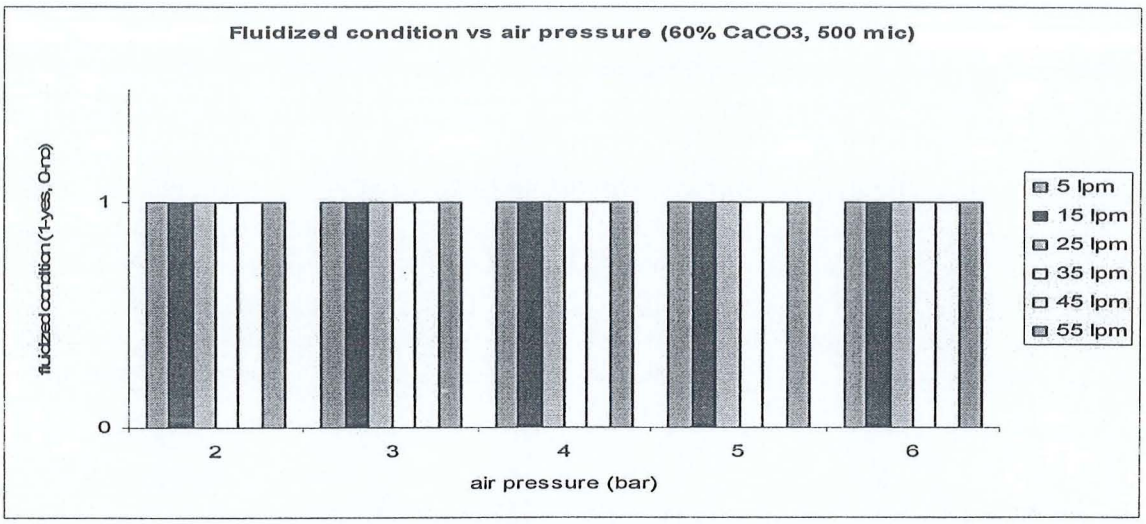

Figure 7: Fluidized condition for 60% $CaCO_3$ (500 micrometer)

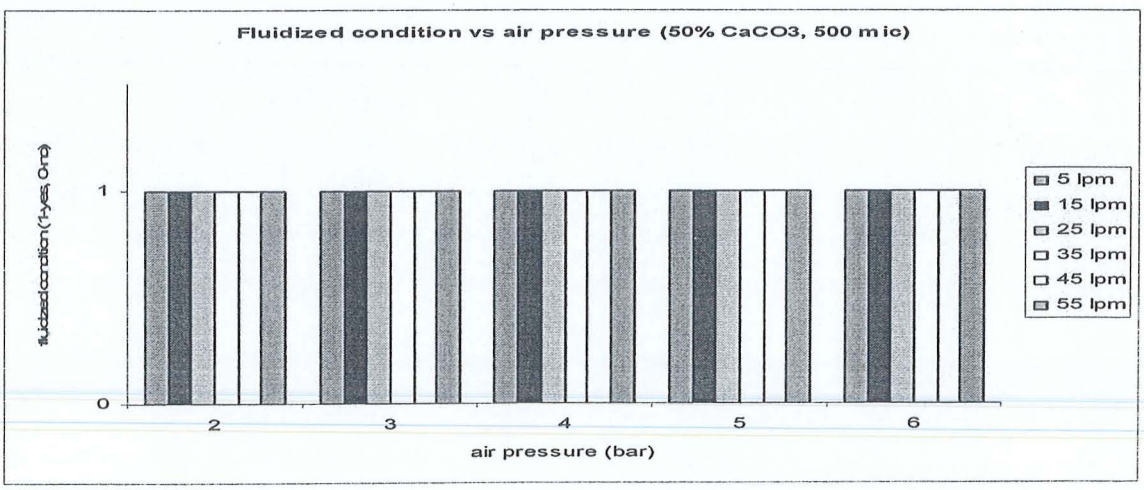

Figure 8: Fluidized condition for 50% $CaCO_3$ (500 micrometer)

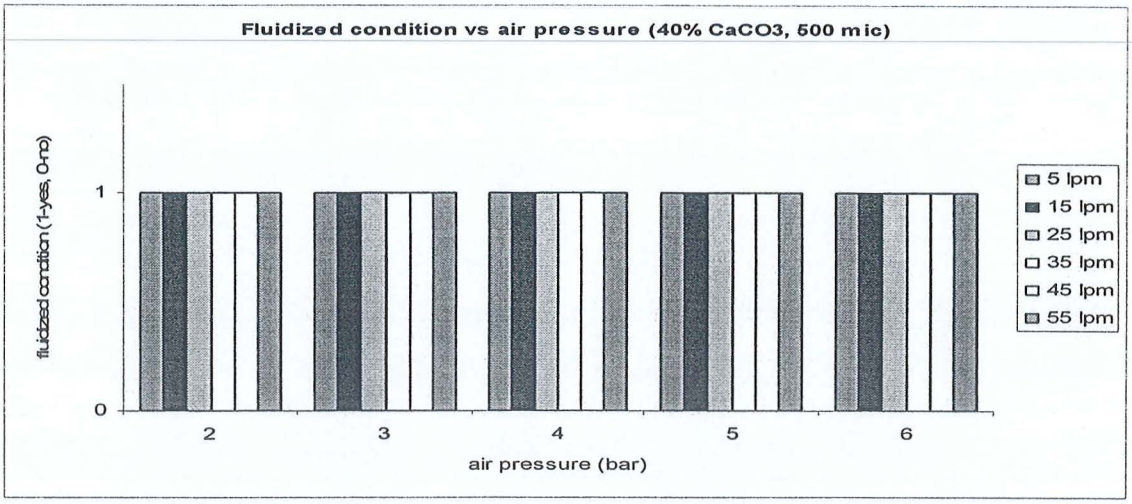

Figure 9: Fluidized condition for 40% $CaCO_3$ (500 micrometer)

Effect of the different percentages of bed material.

As mentioned earlier, the percentage of $CaCO_3$-sand mixture in the SBFB effects the fluidization. As shown in Figure 6, at low pressure and flow rate for 70% $CaCO_3$, fluidization does not occur. This can be explained by the adhesive force between the $CaCO_3$ particles inside the SBFB (Hiroaki et al. 2006). The adhesive force between the particles is strong because of the large amount of $CaCO_3$. By inserting sand, the adhesive force is reduced but it is not sufficient enough to overcome the bond between the particles as a result fluidization does not happen. When the percentage of sand is increased from 40%, 50% to 60%, it can be seen that the fluidization takes place for both particle sizes.

Effect of the particle sizes

From Table 1 and studies according to Geldart (1973) and Yates (1983), they mentioned the particle size which in the range of 150-500 micron meter (Group B powders) which density is in the range of 1500-4000 kg/m^3 has a better fluidization compare to the 30-150 micron meter which has low density less than 1500 kg/m^3 (Group A powders). That is why fluidization for $CaCO_3$ with the size of 500 μm fluidized better than 100 μm.

During the experiment, fluidization for 500 μm only starts to take place when higher flow rate is supplied. Factors such as adhesive force as stated earlier and also increase in particle weight also play its roll in fluidizing the mixture but as the mixture of 500 μm start to fluidized, its bed expansion height shows a better result comparing to the mixture of 100 μm while using the same parameter.

Table 1: The detail of groups for each solid particle

Group	Particle sizes	Fluidizing	Examples	
C	< 30 μm (< 0.03 mm)	difficult	Flour or cement	Finest
A	≈ 30-150 μm (0.03-0.15 mm)	easier	Fine biomass powder	
B	150-500 μm (0.15-0.50 mm)	Fluidize well	Sand	
D	> 500 μm (> 0.5 mm)	difficult	Crushed limestones or coffee beams	Coarsest

Effect of the volume flow rate and pressure.

The air volume flow rate and pressure from the compressor is an important operating parameter to ensure fluidization in the SBFB. Increase in the flow rate of air through the distribution plate at constant pressure will definitely enhance the fluidization of $CaCO_3$-sand mixture. Referring the result from Figure 6, it proves that as the flow rate increased, fluidization occurred. At a constant pressure of 2 and 3 bars, the result proves that at a low flow rate of 5 *l*/m, fluidization does not happen. Once the flow rate increases to 15 and 25 *l*/m, fluidization starts to show in the SBFB.

The pressurized air from the compressor has its effects on the fluidization. As the pressure increases, it enhances the fluidization of the mixture. The purpose is to overcome the adhesive force from the powder and so that fluidization will occur as well as increase the bed height expansion.

Conclusion

The investigation of the fluidization of the $CaCO_3$-sand mixture in a cold model SBFB has been carried out. From the results, it can be concluded as the following:

a) $CaCO_3$-sand mixture with particle size of 100 μm (70%, 60%, 50% and 40% $CaCO_3$), can be fluidized at all flow rates (5, 15, 25, 35, 45 and 55 *l*/m) at constant pressure of 2, 3, 4, 5 and 6 bars.
b) The $CaCO_3$-sand mixture with particle size of 500 μm fluidized at all condition except for 70% $CaCO_3$ where it does not fluidized at low flow rate.
c) Fluidization for $CaCO_3$-sand (500 μm) is better compared to 100 μm in terms of bed height expansion.
d) The increment of the flow rate at constant pressure is directly proportional to the condition of the fluidization of the mixture.

Acknowledgments

The authors would like to express their appreciation to The Research University Grant Scheme (Grant No. MEKANIK/811122) for providing financial support for this study.

References

Abanades, J.C, Anthony, E.J., Wang, J. and Oakey, J.E. (2005). Fluidized bed combustion system integrating CO2 capture with CaO. Environmental Science and Technology, Vol. 39: 2861-2866.

Abanades, J.C., (2002). The maximum capture efficiency of CO_2 using a carbonation/calcinations cycle of $CaO/CaCO_3$. Chemical Engineering Journal, Vol. 90: 303-306.

Chen, Z., Lim, C.J. and Grasa, J.R. (2007). Study of limestone particle impact attrition. Chemical Engineering Science, Vol. 62: 867-877.

Dogru, M., Howrath, C.R., Akay, G., Keskinler, B. and Malik, A.A. (2002). Gasification of hazelnut shells in a downdraft gasifier. Energy, Vol. 27: 415-427.

Geldart, D., 1973. Types of gas fluidization. Powder Technology, Vol. 7: 285-292.

Graham, R.G. and Huffman, D.R. (1981). Gasification of wood in a commercial scale downdraft gasifier. In: Symposium Papers. Energy from biomass and wastes V, Lake Buena Vista, FL. Jan. 1981: 633-650.

Grasa, G.S. and Abanades, J.C. (2007). Narrow fluidized beds arranged to exchange heat between a combustion chamber and a CO2 sorbent regenerator. Chemical Engineering Science, Vol. 62: 619-626.

Grasa, G.S., Abanades, J.C., Alonso, M. and Gonzalez, B. (2008). Reactivity of highly cycled particles of CaO in a carbonation/calcination loop. Chemical Engineering Journal, Vol. 137 (3): 561-567.

Hiroaki M., Higashitani K., Yoshida H. (2006). Powder Technology Handbook, Third Edition. Taylor & Francis, New York.

Jorapur, R.M. and Rajvanshi, A.K. (1995). Development of sugarcane leaf gasifier for electricity generation. Biomass and Bioenergy, Vol. 8: 91-98.

McKendry, P. (2002a). Energy production from biomass (part 1): overview of biomass. Bioresource Technology, Vol. 83: 37-49.

McKendry, P. (2002b). Energy production from biomass (part 2): overview of biomass. Bioresource Technology, Vol. 83: 47-54.

McKendry, P. (2002c). Energy production from biomass (part 3): gasification technologies. Bioresource Technology, Vol. 83: 55-63.

Rezaiyan, J. and Cheremisinoff, N.P. (2005). Gasification technologies: a primer for engineers and scientists. CRC Press.

CD-ROM. ISSN: 1944-0994.

Salvador, C., Lu, D., Anthony, E.J. and Abanades, J.C. (2003). Enhancement of CaO for CO_2 capture in a FBC environment. Chemical Engineering Journal, Vol. 96: 187-195.

Uma, R., Kandpal, T.C. and Kishore, V.V.N. (2004). Emission charteristics of an electricity generation system in diesel alone and dual fuel modes. Biomass and Bioenergy, Vol. 27:195-203.

Xu, G.Q and Wang, Y. (1988). Gasification of agricultural and forestry residues. 23rd Proc. Intersociety Energy Conversion Engineering Conference. Denver, U.S.A.

Yates J.G., 1983. Fundamentals of fluidized-bed chemical processes. Butterworth-Heinemann.

Zainal, Z.A. (1996). Performance and characteristics of a biomass gasifier system. Ph.D dissertation, Division of Mechanical Engineering and Energy Studies, School of Engineering, University of Wales, College of Cardiff, United Kingdom.

Zainal, Z.A., Rifau, A., Quadir, G.A. and Seetharamu, K.A. (2002). Experimental investigation of downdraft biomass gasifier. Biomass and Bioenergy, Vol. 23: 283-289

LAMPIRAN C

PENYATA KEWANGAN

UserCode: DROHANA / USMKCTLIVE / PMEKANIK | Program Code: Votebook9100 | Current Program : Votebook (Header)

Current Date : 04/05/2011 11:18:12 AM | Version: 13.91, Last Updated at 01/03/2011 | DB: 13.00, 9/18/2010 VB: 13.01, 3/14/2011 | Switch Language : English /Malay

Wildcard : eg. Like 100%, Like 10%1, Like %1

Element 1: % Element 2: % Element 4: PMEKANIK

Element 5: 811122 Year: 2011 Search Export to Excel

Detail	Excel	Budget Rule	Budget Control	Account Description	Budget Account Code	Roll over	Budget	Cash Received	Advanced	Commit	Actual	Available	Percentag
Detail	Excel	46	T	Projek Kumpulan Wang Uni Penyelidikan	1001.111.0.PMEKANIK.811122	26,858.58	0.00	0.00	0.00	0.00	13,600.00	13,258.58	0.00
		46	T	SubTotal		26,858.58	0.00	0.00	0.00	0.00	13,600.00	13,258.58	0.00
Detail	Excel	47	T	Projek Kumpulan Wang Uni Penyelidikan	1001.221.0.PMEKANIK.811122	13,000.00	0.00	0.00	0.00	0.00	0.00	13,000.00	0.00
Detail	Excel	47	T	Projek Kumpulan Wang Uni Penyelidikan	1001.224.0.PMEKANIK.811122	4,320.00	0.00	0.00	0.00	0.00	0.00	4,320.00	0.00
Detail	Excel	47	T	Projek Kumpulan Wang Uni Penyelidikan	1001.226.0.PMEKANIK.811122	3,000.00	0.00	0.00	0.00	1,658.00	0.00	1,342.00	0.00
Detail	Excel	47	T	Projek Kumpulan Wang Uni Penyelidikan	1001.227.0.PMEKANIK.811122	-6,095.30	0.00	0.00	0.00	4,305.00	6,227.70	-16,628.00	0.00
Detail	Excel	47	T	Projek Kumpulan Wang Uni Penyelidikan	1001.229.0.PMEKANIK.811122	1,416.40	0.00	0.00	0.00	0.00	0.00	1,416.40	0.00
		47	T	SubTotal		15,641.10	0.00	0.00	0.00	5,963.00	6,227.70	3,450.40	0.00
		9999		GrandTotal		42,499.68	0.00	0.00	0.00	5,963.00	19,827.70	16,708.98	0.00